molecular pharmaceutics

pubs.acs.org/molecularpharmaceutics

Review

Advances in Nanomedicine Design: Multidisciplinary Strategies for Unmet Medical Needs

Taksim Ahmed, Fuh-Ching Franky Liu, Brian Lu, HoYin Lip, Elliya Park, Ibrahim Alradwan, Jackie Fule Liu, Chunsheng He, Abdulmottaleb Zetrini, Tian Zhang, Amin Ghavaminejad, Andrew M. Rauth, Jeffrey T. Henderson, and Xiao Yu Wu*

Cite This: https://doi.org/10.1021/acs.molpharmaceut.2c00038

Read Online

ACCESS | Metrics & More | Article Recommendations

ABSTRACT: Globally, a rising burden of complex diseases takes a heavy toll on human lives and poses substantial clinical and economic challenges. This review covers nanomedicine and nanotechnology-enabled advanced drug delivery systems (DDS) designed to address various unmet medical needs. Key nanomedicine and DDSs, currently employed in the clinic to tackle some of these diseases, are discussed focusing on their versatility in diagnostics, anticancer therapy, and diabetes management. First-hand experiences from our own laboratory and the work of others are presented to provide insights into strategies to design and optimize nanomedicine- and nanotechnology-enabled DDS for enhancing therapeutic outcomes. Computational analysis is also briefly reviewed as a technology for rational design of controlled release DDS. Further explorations of DDS have illuminated the interplay of physiological barriers and their impact on DDS. It is demonstrated how such delivery systems can overcome these barriers for enhanced therapeutic efficacy and how new perspectives of next-generation DDS can be applied clinically.

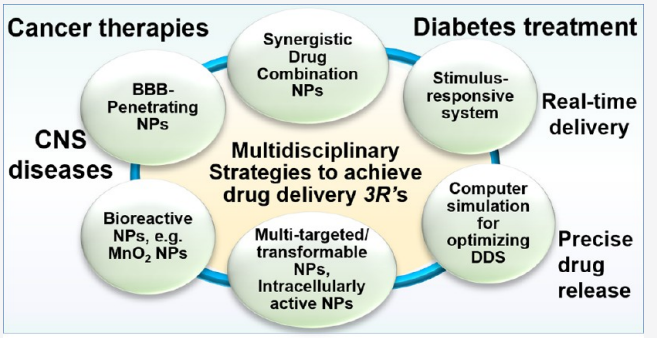

KEYWORDS: *nanomedicine, polymer lipid hybrid nanoparticles (PLN), blood−brain barrier (BBB)-penetrating, synergistic drug combination, multitargeted drug delivery, tumor microenvironment modulation, stimulus-responsive drug release*

1. INTRODUCTION

Numerous diseases continuously affect millions of people and challenge global health care systems, especially those that are chronic in nature, such as cancer, diabetes, and central nervous system (CNS) diseases.[1−6] Currently, worldwide an estimated 233 million people are affected by cancer, 111 million people are affected by neurological disorders, and 422 million are affected by diabetes mellitus.[5,7−11] Global spending on medicines was estimated to surpass $1.1 trillion USD in 2024.[10]

Despite advancement in cancer treatment modalities including new chemotherapy, hormonal therapy, and immunotherapy, aberrant tumor microenvironment (TME), development of multi-drug-resistant (MDR) cells, and toxicity to normal tissue, among other adverse factors, result in unsatisfactory therapeutic outcomes.[12−16] Therefore, enhancing therapeutic effects while minimizing adverse toxicity is the major goal for nanomedicine design. Neurological disorders, including Alzheimer's disease (AD),[17] comprise a global burden accounting for 12% of total deaths.[18] Major challenges of controlling these disorders include early detection, intervention, and effective treatments.[19] The blood−brain barrier (BBB), impermeable to ∼98% of all small-molecule drugs and most macromolecule drugs, represents a key barrier to efficient delivery of therapeutic agents to the brain.[20,21] For effective treatment of neurological disorders, delivering adequate amounts of therapeutics across the BBB and reaching the target region is a critical and challenging task. Diabetes is a chronic hormonal and metabolic disorder that affects over 10% of the adult population globally.[7,8] Although many patients can manage the disease by changing life style, diet, and taking oral medications, daily injection of insulin to regulate blood glucose level is required for all people with type 1 diabetes (T1D) to sustain life and about 30% of people with type 2 diabetes (T2D) to control diabetic complications.[7−9] However, fears of injection and insulin-therapy-associated low blood sugar

Special Issue: Tiny Things, Huge Impact: Nanomedicine in Canada

Received: January 15, 2022
Revised: May 7, 2022
Accepted: May 10, 2022

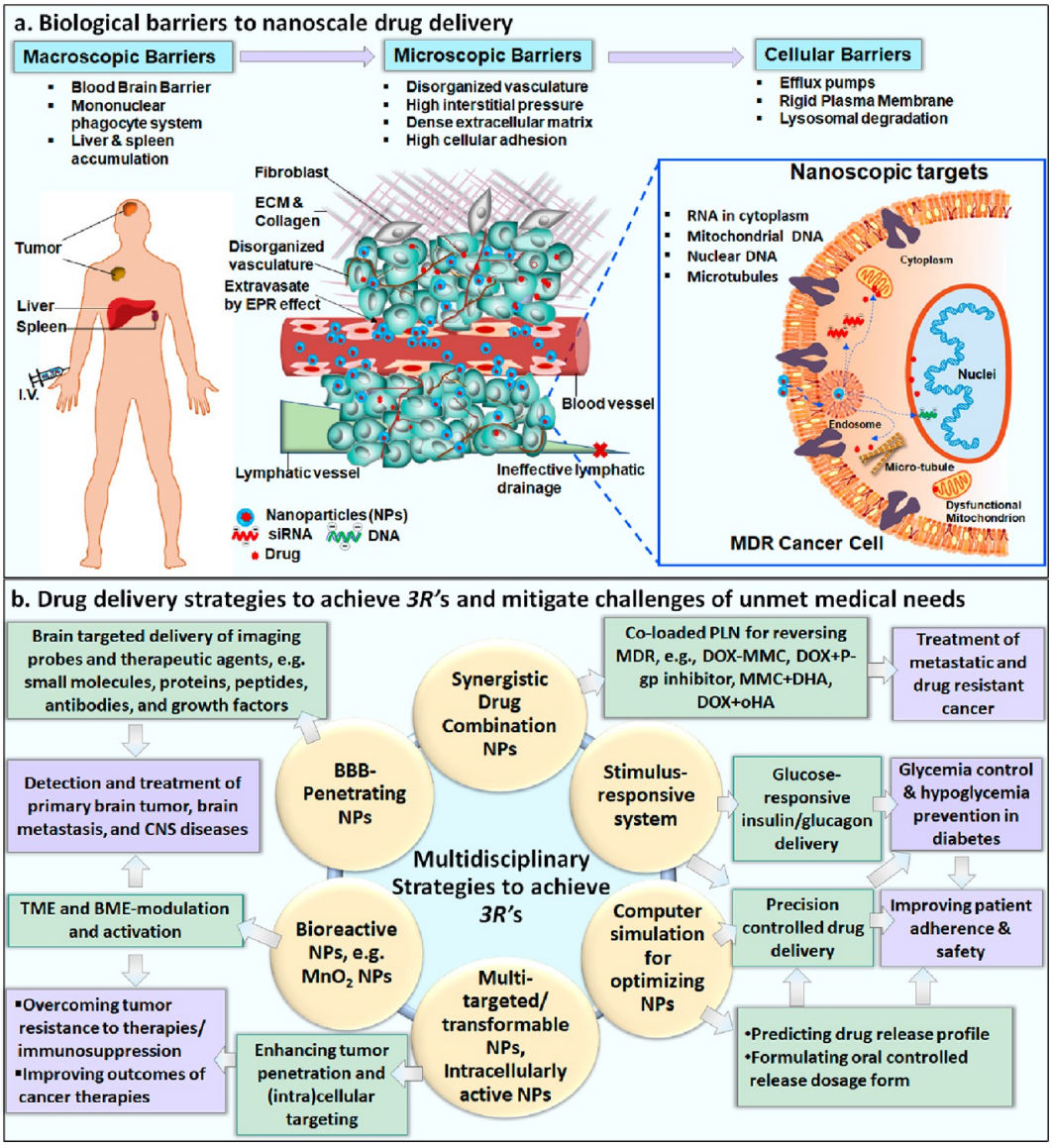

Figure 1. (a) Illustration of the multiple physiological barriers impeding delivery of drugs to nanoscale targets in solid tumors. At macroscopic level (left panel), i.v. administered NPs are removed from the systemic circulation by the MPS, and clearance organs e.g., liver, spleen and kidneys, that results in poor tumor accumulation. At microscopic level (middle panel), low tumor penetration of NP occur at tumor sites owing to complex TME (i.e., disorganized and heterogeneous tumor vasculatures, dense ECM, high cellular adhesion, and dysfunctional lymphatic drainage). At cellular level (right panel), overexpression of efflux pumps, hardened plasma membrane and lysosomal degradation prevents NPs from reaching its nanoscopic targets at various cellular compartments. Figure adapted and reprinted in part with permission from refs 13 and 14. Copyright 2017 The Royal Society of Chemistry and 2018 CPS and SIMM, SpringerNature. (b) Schematic representation of multidisciplinary drug delivery strategies to achieve the 3Rs (to deliver drugs to the *Right* site at the *Right* time with the *Right* level) for unmet medical needs. The text in the circles presents multidisciplinary strategies and technologies developed and exploited to achieve the 3Rs of drug delivery for addressing major unmet medical needs (e.g., cancer, brain tumors and CNS diseases, and diabetes). The green boxes next to the circles (indicated by arrows) represent strategies and examples by which DDS achieve the goals of the 3Rs. The purple boxes represent the ultimate outcomes of such DDS technologies and their therapeutic effects. ECM: extracellular matrix; EPR: enhanced permeation and retention effect; PLN: polymer lipid hybrid NP; TME: tumor microenvironment; BME: brain microenvironment; MDNP: manganese dioxide NPs, LDLR: low density lipoprotein receptor, siRNA: small interfering RNA, CNS: central nervous system, DHA: docosahexaenoic acid; oHA: oligomeric hyaluronic acid.

(hypoglycemia) can often lead to treatment nonadherence and suboptimal insulin dosing.[22−25] Chronic hyperglycemia can result in long-term micro- and macrovascular complications associated with unattained glycemic targets, while hypoglycemia can cause harm and even death to patients. For safe and effective management of diabetes using therapeutic hormones, the timing and dose of hormonal delivery are particularly important, which has been the goal of intelligent drug delivery systems (DDS) for decades.

In the past few decades, many technologies have been developed to design effective DDS for economical, safe, and efficacious drug delivery to address these unmet medical needs. Among these widely investigated DDS, nanoformulations of therapeutics (namely, nanomedicine) and nanotechnology-enabled DDS have gained increasing importance in precise drug delivery to the **R**ight site, at the *Right* time, and at the **R**ight level (the 3Rs).[13,14] For the three major diseases described above, their requirements for DDS to address unmet

https://doi.org/10.1021/acs.molpharmaceut.2c00038
Mol. Pharmaceutics XXXX, XXX, XXX−XXX

Table 1. Selected Examples of Nanoparticles for Single and Co-Loaded Anticancer Drugs for Improved Cancer Therapy[a]

carrier materials	active ingredients	target disease and models	findings	ref
		Microsphere-Based Nanomedicine		
ionic polysaccharide microspheres (MS) derived from dextran	chemo-sensitizers verapamil HCl (VRP) and anticancer drug vinblastine	*in vitro* studies using parent (AUXB1) and MDR (CHRC5) Chinese hamster ovary (CHO) cells	Both drugs showed enhanced loading in the MS. The simultaneous delivery of VRP with vinblastine showed 6−7-fold higher cellular uptake of vinblastine.	Liu et al., 2000[47]
sulfopropyl dextranion-exchange MSs	DOX	*in vitro* cytotoxicity of DOX evaluated in murine EMT6 breast cancer cells using a colony-forming assay	MSs showed enhanced DOX loading. Both free DOX and DOX-MS showed similar cytotoxicity indicating that the bioactivity of drugs was not altered after loading DOX into MSs.	Liu et al., 2001[48]
sulfopropyl dextran MSs	P-gp substrates DOX and MMC	murine breast cancer cells (EMT6 WT) and the DOX-resistant P-gp-overexpressing variant (EMT6/AR1.0)	MS showed sustained release of MMC. The MDR EMT6/AR1.0 cells did not exhibit resistance to both DOX and the DOX-MMC combination. Simultaneous treatment with DOX and MMC showed additive cytotoxic effects on EMT6/WT.	Cheung et al., 2003[232]
MSs made of cross-linked dextran	DOX and VRP (P-gp modulator chemo-sensitizer)	EMT6 murine breast sarcoma cells and MDR phenotype, EMT6/AR1.0 cells-based tumor model; IT injection of MSs used	Around a 34% delay of tumor growth was observed as compared to the nontreatment or blank MSs. The coadministration of VRP and DOX MSs showed a moderate increase in toxicity.	Liu et al.,2003[46]
alginate/chitosan MSs (ACMS)	glucose oxidase (GOX), a reactive oxygen species (ROS) generating enzyme	*in vitro* studies to investigate high drug loading, encapsulation efficiency (EE), and bioactivity	The ACMS showed enhanced GOX loading, and EE. The ACMS also showed sustained generation of H_2O_2 as compared to free GOX. The lyophilized ACMS preserved GOX bioactivity for up to 1 month storage at −20 °C.	Liu et al., 2007[63]
MS made of calcium alginate/chitosan	GOX	loco-regional delivery of MSs in MDR breast cancer cells; *in vitro*/*in vivo* evaluation using murine EMT6/WT and EMT6/AR1.0 cells	GOX-loaded MS showed higher cytotoxicity, significant delay in tumor growth, and less general tissue toxicity than free GOX. It also released H_2O_2 from immobilized GOX.	Liu et al., 2009[64]
alginate/chitosan hydrogel MS	GOX	*in vitro* cytotoxicity evaluated in a murine MDR breast cancer EMT6/AR1.0 cells and wild type EMT6/WT using clonogenic assay	The GOX-MS released ROS *in situ* and showed similar cytotoxicity on both MDR and wild type cells, indicating its superiority in overcoming MDR effects.	Liu et al., 2010[65]
chitosan-alginate MS	GOX	GOX-encapsulated MS prepared with varying sizes; mathematical model generated to predict GOX release kinetics and enzymatic activity; *in vitro* cytotoxicity evaluated on murine breast carcinoma EMT6 cells; computer simulation used to estimate formulation factors on H_2O_2 generation	GOX-MS showed particle-size-dependent H_2O_2 generation and *in vitro* cytotoxicity. At a given dose, a smaller particle showed better effects than the larger ones.	Abdekhodaie et al., 2014[66]
alginate-chitosan MS	GOX	GOX-MS optimized for the use against MDR cells; MS prepared with varied sizes; *in vitro* H_2O_2 generation and cytotoxicity on MDR cancer cells MDR (EMT6/AR1.0) and wild type (EMT6/WT) cells evaluated	Compared to larger particles, the smaller particle size showed higher H_2O_2 generation, uptake, membrane damage, lipid peroxidation and cytotoxicity against MDR cells.	Cheng et al., 2015[67]
biodegradable sulfopropyl dextran MSs	DOX and MMC	*in vivo* therapeutic efficacy and toxicity of drug-loaded MSs evaluated in an EMT6 murine model; intratumoral (IT) administration employed to assess efficacy tumor growth delay (TGD) measured based on the delay time for the tumor to grow up to 1.13 g relative to control	The MMC MS showed around 79% TGD. The coadministration of DOX and MMC MSs exhibited 185% TGD.	Cheung et al., 2005[49]
oxidized sulfopropyl dextran MSs	DOX and MMC	*in vitro* cytotoxicity evaluated against murine breast cancer cell-line EMT6 using a colonogenic assay	MS-loaded MMC and DOX showed sustained release of drugs in physiological buffer (pH 7.4). Free MMC and MMC-MS both showed similar cytotoxicity. Enhanced cytotoxicity was observed when the MMC was administered either simultaneously or after DOX exposure.	Cheung et al., 2006[50]
		Nanoparticle-Based Nanomedicine		
PLN made of stearic acid and anionic polymer hydrolyzed polymer of epoxidized soybean oil (HPESO)	DOX	P-gp-overexpressing breast cancer cell lines (a human cell line, MDA435/LCC6/MDR, and a mouse cell line, EMT6/AR1)	PLNs showed significant cellular uptake and retention of DOX by endocytosis (phagocytosis) and bypassed efflux pumps.	Wong et al., 2006[53]
PLN made of stearic acid and HPESO	DOX	*in vitro* cytotoxicity on MDR breast cancer cell line MDA435/LCC6/MDR and its wild-type cell line	DOX-PLN showed 60−80% EE and showed an over 8-fold increase in cytotoxicity on MDR cells compared to the free DOX solution.	Wong et al., 2006[54]

https://doi.org/10.1021/acs.molpharmaceut.2c00038
Mol. Pharmaceutics XXXX, XXX, XXX−XXX

Table 1. continued

carrier materials	active ingredients	target disease and models	findings	ref
		Nanoparticle-Based Nanomedicine		
SLN based on stearic acid and anionic polymer dextran sulfate	chemosensitizer VRP and DOX	physicochemical properties of PLN evaluated *in vitro*	The charged polymer, e.g., dextran sulfate, helped in enhanced loading of DOX and provided sustained release.	Wong et al., 2004.[51,52]
PLN made of lipids tristearin: stearic acid = 30:70 *w*/*w*) and HPESO	DOX and P-gp inhibitor GG918 (Elacridar)	MDR cancer cells (MDA435/LCC6/MDR1) *in vitro* cytotoxicity using clonogenic assay, drug loading, drug release kinetics, and cellular uptake	DOX and GG918 loaded PLN showed EE up to 89%. Co-encapsulated DOX and GG918 PLN showed the highest DOX uptake and anticancer activity on MDR cells.	Wong et al., 2006[45]
PLN made of stearic acid, tristearin, and HPESO	DOX	*in vitro*/*in vivo* efficacy using murine breast carcinoma cell line EMT6/WT; treatments administered IT	enhanced drug retention increased efficacy and low toxicity The DOX-PLN showed 70 to 100% TGD compared to free DOX and induced significant tumor necrosis.	Wong et al., 2007[55]
PLN	DOX and MMC	*in vitro* studies on MDA435/MDR1 breast cancer cells cytotoxicity results based on clonogenic assay	The co-loaded DOX−MMC−PLN showed enhanced cytotoxicity against murine breast cancer cells. PLNs also showed significant double-stranded DNA breaking based on the TUNNEL assay.	Shuhendler et al,2007[56]
PLN (lipid: myristic acid and HPESO, lipid screening: palmitic, lauric, myristic, or stearic acid)	DOX and MMC at synergistic ratio	MDR human breast cancer cells MDA435/MDR1	The co-encapsulated DOX−MMC−PLN showed enhanced cytotoxicity against MDR cells at around 20−30% lower dose than the free drug. The results were attributed to the synergistic effect between DOX and MM which leads to double-stranded DNA breaks that preceded apoptosis.	Shuhendler et al., 2010.[57]
PLN (lipid: myristic acid, polymer: HPESO)	DOX and MMC at synergistic ratio	*in vitro* studies on multidrug resistance protein 1 (MRP1+) and breast cancer resistance protein (BCRP+) overexpressing human breast cancer cell lines MCF7 VP (MRP1+) and MCF7MX (BCRP+)	Co-loaded DOX-MMC PLN showed 20- to 30-fold more cytotoxicity in MDR cells than free drugs. PLNs loaded with Nile red showed perinuclear localization.	Prasad et al., 2012[58]
stealth PLN based on myristic acid, PEG100SA, PEG40SA and HPESO	DOX and MMC at synergistic ratio	*in vivo* studies on MDA-MB-435/LCC6/WT and the P-gp-overexpressing MDA-MB 435/LCC6/MDR1 cell based human mammary tumor xenografts	The co-loaded DOX−MMC−PLN (DMsPLN) demonstrated superior efficacy (~3-fold increase in survival rate, and 10−20% tumor cure rate). DMsPLNs showed no toxicity in major organs and reduced tumor angiogenesis.	Prasad et al., 2013[59]
stealth PLN based on myristic acid, PEG100SA, PEG40SA and HPESO	DOX and MMC at synergistic ratio	*in vitro* and *in vivo* studies conducted using WT EMT6 breast tumors (WT) EMT6/WT and MDR EMT6/AR1 murine breast cancer cells DOX−MMC−PLN (DMsPLN) compared with liposomal DOX (PLD)	DMsPLNs overcome MDR with enhaced cellular uptake, and intracellular distribution of DOX compared to PLD or free DOX *in vitro*. At higher and repeated doses of DOX and MMC, the DMsPLN did not show any systemic or cardiotoxicity. DMsPLN substantially delayed tumor growth on both WT (~312%) and MDR (28%) models.	Shuhendler et al 2014[60]
stealth PLN based on myristic acid, PEG100SA, PEG40SA and HPESO	DOX and MMC at synergistic ratio	biodistribution and pharmacokinetic evaluations studied on a murine breast cancer model EMT6	The study observed synchronized PK of loaded drugs, ratiometric delivery, superior efficacy, no noticeable cardiotoxicity, sustained release of loaded drugs compared to free drugs or liposomal DOX.	Zhang et al., 2016[61]
PLN based on the lipid: glycerol disterate-type I (ATO5) and polymer polyethylene-glycol (100) stearate (Myrj50)	poly unsaturated fatty acid docosahexaenoic acid (DHA) and MMC; imaging agents: nile red (NR) or 1,1′-dioctadecyl-3,3,3′,3′tetramethylindotricarbocyanine iodide (DiR)	*in vitro* and *in vivo* studies on MDR EMT6/AR1 and its parent cells MDR EMT6/WT	Two-punch mechanism: at first stage DHA-PLN reduces cancer cell membrane rigidity and increases MMC-PLN uptake. At second stage, enzymatic reduction of MMC generates reactive oxygen species (ROS) which then reacts with the adjacent DHA to produce strong mitochondrial lipid peroxidation and damage. Consequently, the DHA−MMC−PLN inhibited tumor growth and had a prolonged survival rate in the MDR breast model.	Zhang et al., 2017[62]
polymeric NPs prepared by complexing anionic ARPI- cationic chitosan (CS) and DOX.	CathB-catalyzed biodegradation of acetylated rapeseed protein isolate (ARPI) and DOX	CathB-hydrolyzed ARPI produces short peptides, and their synergism with DOX evaluated. *in vitro* and *in vivo* studies conducted on CathB-overexpressing MDA−MB−231 and MCF-7 cell lines with low CathB expression	DOX-ARPI/CS NPs showed escape from lysosomal degradation, higher cellular uptake, and intracellular DOX trafficking and cytotoxicity *in vitro*. DOX-ARPI/CS NPs inhibited tumor growth, increased tumor cell apoptosis, and extended host survival in the orthotopic breast cancer mice.	Wang et al. 2018[233]
SLN prepared using the lipid stearic acid and HPESO	DOX	cytotoxicity evaluated against MDR cancer cells (MDA435/LCC6/MDR1)	DOX-SLN showed an enhanced accumulation of drugs inside the cells and exhibited improvement in MDR reversal.	Wong et al., 2005[88]
PLN (various lipids screened for optimum formulation: stearic acid, palmitic acid, myristic acid, dodecanoic acid (DA) and tribehenin; anionic polymer dextran sulfate	model drug VRP	solubility parameters, thermodynamics of binding, and solid-state properties of VRP and DA evaluated using different analytical tools	DA was the best lipid carrier among all those tested, based on their solubility parameters and partition coefficients. DA−VRP−PLN showed highest drug loading capacity.	Li et al., 2006[85]

https://doi.org/10.1021/acs.molpharmaceut.2c00038
Mol. Pharmaceutics XXXX, XXX, XXX−XXX

Table 1. continued

carrier materials	active ingredients	target disease and models	findings	ref
		Nanoparticle-Based Nanomedicine		
sodium (DS) used as a counterionic polymer)				
PLN consisting of dodecanoic acid (DA)	VRP	PLN rationally designed by studying the molecular interactions of ingredients and their internal nanostructure in relation to drug loading and release kinetics	The drug loading and EE of VRP-PLN was around 36 and 99%, respectively. VRP-PLN showed sustained drug release. The molecular mechanism study revealed the presence of strong hydrogen bonding between the drug, polymer and lipids, which helped VRP to uniformly distribute in solid lipid matrix.	Li et al., 2008[86]
PLN made of myristic acid, ethyl arachidate ester and polymer polyvinyl alcohol (PVA)	diruthenium(II,III) metallodrugs of ibuprofen (HIbp), [$Ru_2(Ibp)_4Cl$] or RuIbp, and naproxen (HNpx), [$Ru_2(Npx)_4Cl$] or RuNpx. and indocyanine green (ICG)	*in vitro* studies on breast cancer cells EMT6 and MDA−MB-231 and prostate cancer cells DU145; *in vivo* biodistribution on orthotopic EMT6 breast tumor model	Ru_2(NSAID)-PLNs showed enhanced colloidal properties, cellular uptake, enhanced cytotoxicity *in vitro* as compared to the parent ibuprogen and naproxen drugs. PLNs also showed high biodistributions and tumor accumulation in EMT6 tumor bearing mice.	Alves Rico et al., 2017[234]
PLN based on different lipids (stearic acid, myristic acid, and ethyl arachidate), and polymer HPESO	DOX	different lipids screened for obtaining transformable PLN; cellular uptake and intracellular trafficking PLN investigated *in vitro* on breast cancer cells EMT6 and MDA−MB-231; PLN penetration assessed *ex vivo* on a murine EMT6 tumor bearing mice	The MA-PLN underwent time-dependent size reduction and shape changes from spherical to spiky shape. DOX-PLN showed faster drug release at lower pH in the TME and lysosome. PLN entered breast cancer cells through clathrin-dependent endocytosis and delivered DOX preferentially to mitochondria by fatty acid binding protein-7 reduced mitochondrial transport. MA-PLN also facilitated intratumoral penetration and extravasation of DOX compared to nontransformable liposomal DOX.	Amini, Ahmed, and Liu et al., 2021[33]
pH-responsive polymeric NP made of terpolymer	DOX	interaction between DOX and terpolymer characterized by FTIR, ^{1}H NMR, TEM, DLS, and potentiometric titration	NPs exhibited higher DOX loading and pH-dependent swelling in a physiological pH range and showed pH-dependent drug release with a higher release in pH 5 than pH 7.4 buffers.	Shalviri et al., 2013[99]
polymeric NP, namely, Gd-loaded terpolymer (PolyGd) and Gd-DOX co-loaded NPs (PolyGd-DOX)	DOX and MRI contrast agent gadolinium (Gd)	diethylenetriaminepentaacetic acid (DTPA) chemically linked to terpolymer for chelating Gd *in vitro* binding assay and MRI studies conducted along with *in vivo* biodistribution on a murine EMT6 breast tumor model	Gd loaded NPs showed strong MR signal enhancement compared to commercially available Gd (Omniscan) in both *in vitro* and *in vivo*. Both NPs showed higher accumulation in the periphery and core of tumor up to 48 h. The NPs did not show any major toxicities in major organs at 7 days postinjection.	Shalviri et al., 2012[235]
		Integrin-Targeted NPs		
cRGD-SLN (lipids: Myrj 52 or 56)	pyrene and PbSe QD	mice bearing orthotopic MDA−MB-435 tumors	The cRGD−SLN increased the specificity and accumulation in tumor neovasculature and tumor residence time. However, targeted SLNs showed enhanced distribution in the liver, spleen, and kidneys compared to the nontargeted SLN.	Shuhendler et al., 2012[131]
cRGD-conjugated SLN		different concentrations of RGD used to reduce liver uptake and enhance tumor accumulation *in vitro* binding to $\alpha v\beta 3$ integrin receptor and cellular uptake evaluated in MDA−MB-231 cells with comparison to nonexpressing ($\alpha v\beta 3$ integrin) negative control MCF-7 cells	The cRGD−SLN showed strong binding to $\alpha v\beta 3$ integrin receptor and enhanced cellular uptake. It also inhibited cell invasion (through Matrigel) and adhesion to fibronectin.	Shan et al., 2013[236]
cRGD−SLN prepared with Myrj59 (polyoxyethylene (100) stearate)	pyrene and near-infrared radiation (NIR)-emitting lead selenide quantum dots (PbSe QD)	*in vitro* and *in vivo* studies on triple-negative breast cancer (TNBC) orthotopic MDA−MB-231/EGFP breast tumor model; SLN with different concentrations of cRGD on the surface also investigated	cRGD-conjugates inhibited *in vitro* tumor cell adhesion and invasion of $\alpha v\beta 3$-integrin-overexpressing breast cancer cells. A biodistribution study revealed enhanced accumulation and retention in tumor using the 1% cRGD−PLNs.	Shan et al., 2015[237]
cRGD−PLN based on the Myrj59	DOX and MMC, ICG	lung metastasis of TNBC using human TNBC MDA−MB-231 cells	Dual-targeted hybrid PLN inhibited the progression of lung metastases of TNBC and prolonged the host survival rate. cRGD−DMPLN showed a 31-fold reduction of lung metastases and about 35% prolonged survival rate.	Zhang et al., 2017,[135]
iRGD−PLN made of	oligomeric hyaluronic acid (oHA) and DOX	TNBC	The study showed *in vitro* inhibition of cancer cell migration and invasion. The synergistic effect helped in inhibiting tumor growth of primary TNBC tumors and prevention of spontaneous metastasis to the lungs and lymph nodes.	Zhang et al., 2021[137]

https://doi.org/10.1021/acs.molpharmaceut.2c00038
Mol. Pharmaceutics XXXX, XXX, XXX−XXX

Table 1. continued

carrier materials	active ingredients	target disease and models	findings	ref
		MnO_2-Based NP		
multifunctional albumin-MnO_2 NP	MnO_2	reactivity to modulation of the TME, such as hypoxia, acidic pH, and higher level of reactive oxygen species (ROS, e.g., H_2O_2 and MnO_2) evaluated *in vitro* *in vivo* studies conducted using IT treatment of NPs to a murine breast tumor model based on EMT6 cells	MnO_2NPs showed enhanced oxygen generation and increased TME pH by reacting with H_2O_2 *in vitro* and *in vivo*. The IT administration of NPs downregulated tumor progression factors (e.g., hypoxia-inducible factor-1 alpha (HIF-1α) and vascular endothelial growth factor (VGEF)). Compared to radiation therapy alone, the combination therapy of radiation and MnO_2 NPs substantially reduced tumor growth and induced DNA double strand breaks and cellular deaths.	Prasad et al., 2014[145]
hybrid MnO_2-PLN, created by embedding polyelectrolyte-MnO_2 (PMD) in hydrophilic terpolymer/protein-MnO_2 (TMD) hydrophobic polymer/lipid-MnO_2 (LMD) matrices	MnO_2	Intravenous (i.v.) injectable PLNs were developed, and various *in vitro* and *in vivo* studies were carried out in murine breast cancer cell EMT-6 and TNBC cells MDA−MB-231. LMD showed highest tumor accumulation and retention upon i.v. injection in mice and reduced tumor hypoxia by 45%.	first study designed for i.v. administration of MnO_2 NPs PLNs showed improved colloidal properties. They also showed oxygen generation both *in vitro* an *in vivo*, with LMD being the most effective. On i.v. administration, LMD showed the highest tumor accumulation and reduction in hypoxia of TME.	Gordijo et al., 2015[157,238]
polymeric theranostic NPs (PTNPs) made of polyoxyethylene (100) stearate (Myrj59)	DTX + MnO + NIR fluorophore HyliteFluor 750	dual functional imaging and chemotherapy investigated with both *in vitro* and *in vivo* assays using MDR breast cancer cells of MDA−MB-231 human breast cancer cells	Higher cytotoxicity, significant tumor accumulation, and prolonged retention were observed for the dual NPs. Quantitative MRI revealed that MnO NPs had a 2.7-fold increase in T1 relaxivity over that of free-MnO NPs *in vivo*.	Abbasi et al., 2015[239]
hybrid manganese dioxide (MnO_2) NPs (lipids: myristic acid and polyoxyethylene (40) stearate, NP compositions like those of Gordijo et al.)[157,238]	MnO_2 hydrophilic terpolymer−protein-MnO_2 or hydrophobic polymer−lipid-MnO_2 made of oleic acid	MnO_2 nanoparticles (MDNP) used to modulate TME and enhance radiation therapy in highly hypoxic murine EMT6 or human MDA−MB-231 xenograft breast tumor models	MDNP administration prior to radiation therapy significantly increased radiotherapy efficacy, prolonged median survival of mice (3- to 5-fold), and decreased tumor growth, VEGF expression, and vascular density.	Abbasi et al. 2016,[147]
bioreactive multifunctional hybrid polymer−lipid encapsulated manganese dioxide NP (PLMD NP)	MnO_2, DOX	PLMDs effect on modulating TME, immunosuppression and chemotherapy efficacy evaluated on an orthotopic breast tumor model based on murine EMT6 or 4T1 cells	PLMD NPs showed enhanced cellular cytotoxicity, deep tumor penetration, and therapeutic efficacy and reduced the expression of tumor specific biomarkers. PLMD and DOX combination therapy significantly enhanced tumor infiltrated CD8 T cells and tumor regression and reduced immunosuppression.	Amini et al., 2017 and 2018[34,240]

[a]SLN: solid lipid nanoparticle; PLN: polymer lipid hybrid nanoparticle; VRP: verapamil HCl; GG918: P-gp inhibitor, known as Elacridar; QD(PbSe): quantum dots; Gd: gadolinium; RGD: tripeptide Arg−Gly−Asp; ApoE−LDLR: Due to the presence of PS 80 on the terpolymer, the NPs take the advantage of physiology in which PS 80 recruits apolipoprotein E (ApoE) from plasma and crosses the BBB endothelial cells through low-density lipoprotein receptor (LDLR)-mediated transcytosis; triple-negative breast cancer (TNBC).

https://doi.org/10.1021/acs.molpharmaceut.2c00038
Mol. Pharmaceutics XXXX, XXX, XXX−XXX

Table 2. List of Nanocarriers Used for Drug Delivery to the Brain[a]

carrier type	BBB-penetrating mechanism	drug(s) delivered	major findings and comments	ref
iRGD TPLN (made of the lipid ethyl arachidate and terpolymer)	LDLR-mediated transcytosis	DOX and MMC at synergistic ratio	iRGD−DOX−MMC TPLN PLNs enhanced cellular uptake, cytotoxicity, and accumulation of drugs in tumor site. iRGD−DOX−MMC TPLN showed a higher efficacy to reduce metastatic tumor burden (6- to 19-fold) and tumor associated macrophages (TAM) and prolonged the survival rate of mice (1.3- to 1.6-fold) as compared to those of nontargeted TPLNs and free DOX/MMC.	29
TPLNs made of the lipid: ethyl arachidate and terpolymer	LDLR-mediated transcytosis	diruthenium (II,III)-NSAID (nonsteroidal anti-inflammatory drug) metallodrugs ibuprofenate (RuIbp) and naproxenate (RuNpx) abbreviated as $[Ru_2(NSAID)_4]$-TPLNs	$[Ru_2(NSAID)_4]$-TPLNs showed enhanced cellular uptake, cytotoxicity, and anticancer activity compared to the ibuprofen-TPLNs.	113
polymeric micelles made of poly(methacrylic acid)−polysorbate 80-grafted-starch (terpolymer)	LDLR-mediated transcytosis	DOX	Stable NPs were formed with enhanced drug loading (49.7 ± 0.3%) and EE (99.9 ± 0.1%). DOX release was higher at acidic pH. DOX NPs showed superior cellular uptake and cytotoxicity (20-fold lower IC_{50}) compared to free DOX *in vitro*.	100
polymeric NPs: preformed NPs (PF NPs) and self-assembled NPs (SA NPs)	LDLR-mediated transcytosis	DOX and NIR fluorescent probe HiLyte Fluor 750	SA NPs showed superior blood circulation, tumor uptake and penetration and tumor growth inhibition compared to PF NPs.	102
multifunctional nanotheranostic system based on terpolymer (terpolymeric NP)	LDLR-mediated transcytosis	DOX, Gd, HiLyte Fluor 750, and Hoechst 33342 (DAPI)	The NPs showed extravasation of Gd and DAPI from intact brain microvessels on an intact BBB of healthy mice. The whole body and ex vivo fluorescence imaging showed enhanced accumulation of DOX into the brain metastatic lesions. The DOX NPs significantly reduced brain tumor growth and induced apoptosis in cancer cells as compared to free DOX.	103
amphiphilic polymer−lipid nanoparticle. The amphiphilic polymer was made by covalently linking dodecylamine to the terpolymer.	LDLR-mediated transcytosis	antimitotic drug DTX	TPLNs showed extravasation of BBB impermeable dye across intact BBB of a healthy mice and accumulation into the micrometastasis lesions at the tumor site. PK study revealed that TPLNs enhanced plasma 5.5-fold higher plasma circulation in tumor-bearing mice. The study also showed synchronized DTX kinetics. The DTX PLN prolonged mean survival rate of tumor-bearing mice by 94% as compared to Taxotere.	104,114
TPLN consisting of the polymer (terpolymer) and lipid (ethyl arachidate)	LDLR-mediated transcytosis	therapeutic antibody trastuzumab (TRA) (~150 kDa) antibody was conjugated into the terpolymer.	TPLN successfully delivered therapeutic antibody trastuzumab in the brain, with a 50-fold increase compared to the free TRA in a two-step targeting manner. TRA TPLN significantly inhibited tumor growth (43-fold) and prolonged median survival time (1.3-fold) compared to an equivalent dose of free trastuzumab.	105
anti-Aβ antibody (aAβ)-conjugated, terpolymer (BT), and ROS-activatable (RA) MnO_2 NP (MnO_2 NPs)-containing nanoconstruct (NC) (aAβ-BTRA-NC) [lipids: ethyl arachidate; polymer: terpolymer and PVA]	LDLR-mediated transcytosis	MnO_2, anti-Aβ antibody 4G8	*In situ* synthesis of aAβ-BTRA-NC showed excellent colloidal properties, exhibited superior BBB crossing ability and targeting of amyloid-β and ROS-affected AD brain regions. The NCs also enabled noninvasive detection of early events of cerebrospinal fluid pathology and progression of AD by MRI with high sensitivity and accuracy. The aAβ-BTRA-NC facilitated *in situ* oxygenation, reduced oxidative stress and pro-inflammatory cytokines, and increases neuronal survival.	19
TPLN made of ethyl arachidate (EA) and terpolymer; lipids screened included myristic acid, stearic acid, ethyl myristate, and glycerol monostearate	LDLR-mediated transcytosis	DOX	EA TPLN showed the best colloidal properties (size, polydispersity index (PDI), zeta potential, EE, drug loading, and colloidal stability). DOX TPLNs showed enhanced cytotoxicity, cellular uptake, and deep 3D tumor spheroid penetration *in vitro* compared to free DOX. DOX TPLN also showed enhanced biodistribution at the brain tumor site in an orthotopic GBM brain tumor bearing mice.	109
albumin NP	LDLR-mediated transcytosis	loperamide	A coating of ApoE improved BBB penetration by the NP; antinociceptive effects were induced in CNS by NP only.	241
micelle: pluronic	LDLR-mediated transcytosis	haloperidol	α2-Glycoprotein antibody conjugated nanocarriers increased permeability to the mice brain.	242
nanogel NVP/NIPAM	LDLR-mediated transcytosis	5-fluorouracil (hydrophobic derivative)	The polysorbate coating of nanogel increased brain accumulation from 0.18% of the injected dose to 0.52%.	243
nanosuspension of atovaquone crystal	LDLR-mediated transcytosis	atovaquone	The polysorbate coating of nanosuspension enhanced atovaquone activity in mice with toxoplasmic encephalitis without requirement of apolipoproteins.	244
polymeric NP: poly(lactic-*co*-glycolic acid) (PLGA); surface coating with polysorbate 80 (PS 80), DSPE−PEG−glutathione (GSH), or DSPE−PEG−transferrin (Tf)	multiple BBB crossing mechanism based on the surface coating of NPs; LDLR-mediated transcytosis	small interfering RNA (siRNA)	The surface coating density and surface chemistry enabled higher transport of NPs across BBB. The siRNA-loaded PLGA NPs exhibited higher brain accumulation and 50% gene silencing in traumatic brain injury (TBI) *in vivo*.	245
polymeric NP: PBCA	LDLR-mediated transcytosis	methotrexate	Drug levels in brain and cerebrospinal fluid increased, especially with smaller NPs (<100 nm)	246

https://doi.org/10.1021/acs.molpharmaceut.2c00038
Mol. Pharmaceutics XXXX, XXX, XXX−XXX
pubs.acs.org/molecularpharmaceutics

Table 2. continued

carrier type	BBB-penetrating mechanism	drug(s) delivered	major findings and comments	ref
polymeric NP: MMA−SPM; PCBA	passive diffusion, LDLR-mediated transcytosis	lamivudine, zidovudine	PCBA NPs enhanced the BBB permeability of 3TC and AZT by 10- to 18- and 8- to 20- fold, respectively.	247
transferrin-functionalized chimeric polymersome	transferrin-receptor-mediated transcytosis	siRNA against polo-like kinase 1 (siPLK1)	The polymersome showed effective BBB crossing and silenced the specific gene of the tumor cells, thus enabling inhibition of tumor growth and prolonging survival time in brain metastatic MDA−MB-231 TNBC xenografts mice.	248
ferritin nanocages	transferrin receptor 1 (TfR1)	paclitaxel	The nanocates entered the BBB via transferrin-receptor-mediated endocytosis and showed antitumor effect in mice glioma model.	249
polymersomes: MPEG−PCL and maleimide−PEG−PCL	transferrin receptor	DOX	NPs conjugated with transferrin showed antitumor effects in glioma rats by increased apoptosis of tumor cells and survival time.	250
dendrimer: PEG−poly(amidoamine)	transferrin receptor	DOX	BBB transport of doxorubicin to brain tumor increased from 5 to 13.5% in the dendrimer group.	251
lipid nanocapsule: triglycerides of capric acid and caprylic acids, soy bean lecithin, and solutol	transferrin receptor	ferrociphenol	OX26 antibody conjugated nanocarriers increased permeability and increased the survival time in mice brain tumor model.	252
liposomes-decorated with monoclonal antibody to transferrin receptor	transferrin-receptor-mediated transcytosis	GDNF-expressing plasmid DNA	The treatment enhanced striatal tyrosine hydroxylase (TH) promoter activity (77%) and improvement in neurobehavior in rats.	253
protein nanocapsule: 2-methacryloyloxyethyl phosphorylcholine (MPC)−poly(lactide)-*b*-poly(ethylene glycol)-*b*-poly(lactide)−diacrylate triblock copolymer (PLA-based cross-linker)	nicotinic acetylcholine receptors and choline transporters	therapeutic proteins	The delivery platform was capable of delivering therapeutic proteins across BBB of mice and nonhuman primates.	254
sequential targeting in cross-linking (STICK): NP (micelles)−maltobionic acid (MA)−4-carboxyphenylboronic acid (CBA)	glucose-transporter-mediated transcytosis	hydrophilic (Gd-DTPA, indocyanine green (ICG), DOX hydrochloride (DOX·HCl)) and hydrophobic (Cy7.5, DiD, vincristine (VCR), and paclitaxel (PTX)) agents	This approach overcomes various biological barriers of the blood, BBB/BBTB, and tumor cell penetration by three-step targeting. STICK NPs significantly inhibited tumor growth and prolonged the survival rate in mice with aggressive and chemoresistant diffuse intrinsic pontine glioma.	255
dendrimer: polyether−copolyester	glucose transporter (GLUT-1)	methotrexate	The dendrimer significantly enhanced intratumoral drug transport in gliomas.	256
nanogel: PEG−PEI	endocytosis	oligonucleotides	Accumulation of a ODN in the brain increases by over 15-fold while in liver and spleen decreases by 2-fold compared to the free ODN.	257
nanosuspension of indinavir crystal	use of bone marrow macrophages (BMM)	indinavir	Indinavir nanocrystals were successfully loaded into bone marrow macrophages, released drug for 14 days and reduced HIV-1 in HIV encephalitis areas.	258
gold nanosphere	surface coating of NP with BBB-permeable transactivator of transcription (TAT) peptide	DOX, gadolinium (Gd)	The nanospheres significantly increased survival time and a prolonged retention time of Gd in mice glioma model.	259
gold nanorods	nicotinic acetylcholine receptor (AchR)	diagnostic	The surface of the carriers modified with rabies virus glycoprotein (RVG29) to enter BBB increased the localized signal in response to near-infrared (NIR) light for photothermal therapy.	260

[a]DTPA: diethylenetriamine pentaacetic acid, LRP1: low density lipoprotein receptor-related protein 1; DSPE: 1,2-distearoyl-*sn*-glycero-3-phosphorylethanolamine.

https://doi.org/10.1021/acs.molpharmaceut.2c00038
Mol. Pharmaceutics XXXX, XXX, XXX−XXX

Table 3. Partial Examples of Targeting Different Cancer Types Using Targeted NPs

cancer type	examples of common ligands and their receptors	example of delivered cargo and the biomaterials used	comments
brain	folate to folate receptors, transferrin to transferrin receptors, RGD peptides to integrins, interleukin peptides to IL-4,-13 receptors	IL-13 peptide targeting for IL-13R α2 for docetaxel−PEG−PCL[261]	higher tumor growth inhibition rate and 1.73-fold higher U87 glioblastoma targeting compared to nontargeted treatment[261]
		α βv 3 paclitaxel−PEG−PTMC	∼40% higher cellular uptake, cytotoxicity, and apoptosis in U87 cells
lung	epidermal growth factor EGF to EGFR, interleukin peptides to IL-4,-11 receptors. RGD peptides to integrins, HER2	RGD−(PLGA)−chitosan nanoparticle (CSNP) for integrin $\alpha v\beta 3$ receptor targeted paclitaxel (PTX)[262]	increased uptake enhanced apoptosis and cytotoxicity than its nontargeted counterpart in cancer cells.[262]
		DOX folate-targeted liposomes[263]	higher drug concentrations in whole cells and nuclei compared with exposure to free DOX and significantly more tumor inhibitory than free DOX *in vivo*[263]
breast	androgen, HER2, estrogen, integrins, tumor necrosis factor, folate, chemokine CXCR4, IL-4,-6	AP-1 peptide targeting IL-4 receptor for paclitaxel-cyclodextrin[264]	higher tumor targeting and growth inhibition rate in MDA−MB-231 xenograft model[264]
		angiopep-2 targeting lipoprotein-receptor related protein (LRP) for DOX-dendritic poly-L-lysine-gelatin NP[265]	higher accumulation of NP in tumor; higher tumor growth inhibition rate[265]
		hyaluronic acid targeting CD44 receptor DOX hyaluronic acid-LysLA10[266]	lower relative tumor volume; higher median survival time in MCF-7/ADR xenograft model[266]
liver	vascular endothelial growth factor, epidermal growth factor	DOX-loaded glycyrrhetinic acid-modified alginate NPs[267]	lower cardiotoxicity than mice treated with DOX with liver tumor growth inhibition rate of about 53%[267]
		DOX and galactosylate to asialoglycoprotein receptor[268]	In an orthotopic xenograft model, NPs reduced proliferation, invasion, migration, and angiogenesis.[268]
pancreatic	tumor necrosis factor, IGF1, CXCR4 chemokine	gold NPs (AuNP) with anti-EGFR antibody cetuximab (C225) as a targeting agent for gemcitabine[269]	The quantitation of gold both *in vitro* and *in vivo* confirmed the inhibition of tumor growth by the targeted delivery.[269]
		anti-CD47 mAb receptor Gemcitabine−MIONP	higher cellular uptake but with higher cytotoxicity
prostate	androgen, prostate-specific membrane antigen (PSMA)	testosterone-conjugated lipid (T-DSPE) liposome encapsulated 5-FU to androgen receptors[270]	Testosterone was effective for site-specific delivery of 5-FU to various ARs positive organs shown by biodistribution.[270]
		cisplatin Pt(IV)-encapsulated PSMA-targeted NPs of poly(D,L-lactic-*co*-glycolic acid) (PLGA)-poly(ethylene glycol) (PEG)[271]	The aptamer-derivatized Pt(IV)-encapsulated NPs are significantly superior to cisplatin or nontargeted NPs against the LNCaP cells.[271]
ovarian	folate, HER2, CXCR4 chemokine	polymeric NPs conjugate heptapeptide	higher cellular uptake and 2.6-Fold higher tumor accumulation.[272]
		NR7 targeting EGFR for DOX[272]	
		folate-functionalized gemcitabine-loaded bovine serum albumin NPs (Fa-Gem-BSANPs)[273]	2-fold higher uptake and toxicity in Ovcar-5 cell lines[273]

https://doi.org/10.1021/acs.molpharmaceut.2c00338
Mol. Pharmaceutics XXXX, XXX, XXX−XXX

needs vary, which may or may not need all 3Rs. For example, insulin and glucagon are normally administered via the subcutaneous/transdermal route, and the *right* time and *right* level of their delivery are more crucial. Nevertheless, most of DDS are required to provide the 3Rs.

To achieve the goal of the 3Rs, intravenously (i.v.) injected drug-loaded nanoparticles (NPs) must overcome physiological barriers at the macroscopic, microscopic, and cellular levels before releasing the drug at the intracellular site of drug action (Figure 1a).[6,13,14] Macroscopic barriers usually involve various pathways that remove NPs from the systemic circulation, including hepatic and splenic uptake, rapid renal clearance, and/or uptake by the mononuclear phagocyte system (MPS) (Figure 1a, left panel).[13,14] Furthermore, the BBB, held together by multiple tight junctions, acts as a substantial barrier to CNS drug delivery. The microscopic barriers, in the case of solid tumors, are within the TME, characterized by high interstitial pressure, disorganized and heterogeneous tumor vasculature, dense extracellular matrix (ECM), and high cellular-matrix adhesion (Figure 1a, middle panel). Therefore, drug molecules and NPs cannot penetrate far from the blood vessels to the distal regions of the tumor mass.[13,14] Drug molecules arriving at the target cells still encounter cellular barriers that reduce intracellular drug accumulation and efficacy, including efflux transporters (e.g., P-glycoprotein, P-gp), lysosomal degradation, and other antioxidant, detoxification, and antiapoptosis mechanisms (Figure 1a, right panel).[13,14] Moreover, the thickened and rigid plasma membranes of MDR cancer cells further obstruct endocytic uptake of NPs, while lysosomal entrapment restricts NP escape and drug release to intracellular targets (e.g., the mitochondria and nucleus).[26,27]

Most nanocarriers are designed to overcome macroscopic barriers by reducing uptake by the liver and the spleen and to increase tumor accumulation via enhanced permeability and retention (EPR) effects and/or active targeting;[6] however, their penetration into the deep tumor tissue is not guaranteed due to the microscopic barrier. Recent studies suggest that receptor-mediated transcytosis across the endothelial cells may play an important role in promoting tumor uptake and tissue penetration of NPs.[28−31] NPs with TME-responsive changes in size, shape, and drug release can also facilitate tumor tissue penetration.[32−34] Even though some NPs can reach the cancer cell surface, their cellular uptake and efficient drug release to the site of drug action are often unrealized, which is largely attributable to cell membrane rigidity in MDR cells, lysosomal entrapment, and undesirable drug release profiles.[6,13,14,26] As a result, the efficacy of NP-based cancer therapeutics frequently suffer from poor target penetration (<5% of administered dose),[35] and exhibit subtherapeutic drug levels within cancer cells.[12,13,36]

Over the past two decades, our group has designed nanotechnology-based DDS for overcoming major biological barriers including the formidable BBB, aberrant TME, multiple efflux pumps and rigid plasma membrane in MDR cells, and other resistance mechanisms such as hypoxia and deoxyribonucleic acid (DNA) damage repair mechanisms (Figure 1b). In this review, we provide a comprehensive overview to illustrate how multidisciplinary technologies can be exploited to achieve the goal of the 3Rs with firsthand examples to mitigate the challenges of unmet medical needs with a focus on the treatment of cancer, CNS diseases, and diabetes.

To achieve the goals of the 3Rs, NPs with synergistic drug combinations are designed to overcome cellular mechanisms of MDR (Figure 1b). Polymer−lipid hybrid NPs (PLN) were formulated to accommodate multiple drugs with different properties and pharmacological actions, including P-gp inhibition with doxorubicin (DOX), DOX with mitomycin C (MMC), docosahexaenoic acid (DHA) with MMC, and oligomeric hyaluronic acid (oHA) with DOX. Terpolymer-based NPs were fabricated to deliver imaging and therapeutic agents to cross the BBB for diagnosis and therapy of brain tumors, brain metastasis, and CNS diseases. Bioreactive NPs (e.g., MnO_2-containing PLN) were devised to modulate the TME and enhance the effects of radiotherapy and chemotherapy. Multitargeted NPs were engineered to target tumor neovasculature, cancer cells, and tumor-associated macrophages (TAM). TME and cancer cell enzyme activatable and mitochondria-targeted NPs were formulated to overcome MDR mechanisms and produce anticancer compounds *in situ*. Intratumoral and intracellular transformable PLNs were designed to enhance tumor penetration and active targeting to intracellular organelles. All these NPs were demonstrated to deliver the payload to the desired disease site or drug target (*right* site) and release the drug(s) or generate active compounds at an optimal rate and ratio (*right* time and *right* level). Moreover, stimulus-responsive nano- and microgels were synthesized and used in implantable insulin devices or microneedle (MN) patches to provide glucose-responsive hormone delivery or for pH-responsive drug delivery (Figure 1b). Computer simulation and numerical analyses using various mathematical tools such as the finite element method, artificial neural networks (ANN), and design of experiment (DOE), were carried out to optimize the NP design to achieve precisely controlled drug release kinetics (*right* time and *right* level), cellular uptake and cytotoxicity (*right* site and *right* level). More detailed descriptions of these examples are summarized in Table 1−3 and presented in the main text. We hope that this review will provide insights into multidisciplinary strategies to design innovative nanomedicine and nanotechnology-enabled DDS for improving therapeutic outcomes and patient adherence to meet unmet medical needs.

2. SYNERGISTIC DRUG COMBINATION NANOMEDICINE FOR ENHANCING CHEMOTHERAPY OF MULTI-DRUG-RESISTANT AND METASTATIC CANCER

Cancer is one of the most devastating diseases, accounting for 1 in 6 deaths worldwide.[37,38] In Canada, about 1 out of 4 people is expected to die from different forms of cancers.[39] The socioeconomic burden of oncology drug expenditures in the United States of America (USA) is estimated to be $158 billion USD as of 2020.[40] Currently, extensive research is actively being pursued to develop effective and safe NP-based anticancer therapies in both preclinical and clinical setups.[1,6]

Chemotherapy represents a mainstay in the treatment of primary and metastatic cancers. However, inherent and acquired MDR properties limit the effectiveness of chemotherapy in the clinic, which involves many mechanisms including overexpression of plasma membrane efflux transporters that pump small-molecule drugs out of the cells.[15,41,42] Among various efflux transporters (namely, the adenosine triphosphate (ATP)-binding cassette (ABC) family of transmembrane proteins), multidrug resistance protein 1 (MDR1

https://doi.org/10.1021/acs.molpharmaceut.2c00038
Mol. Pharmaceutics XXXX, XXX, XXX−XXX

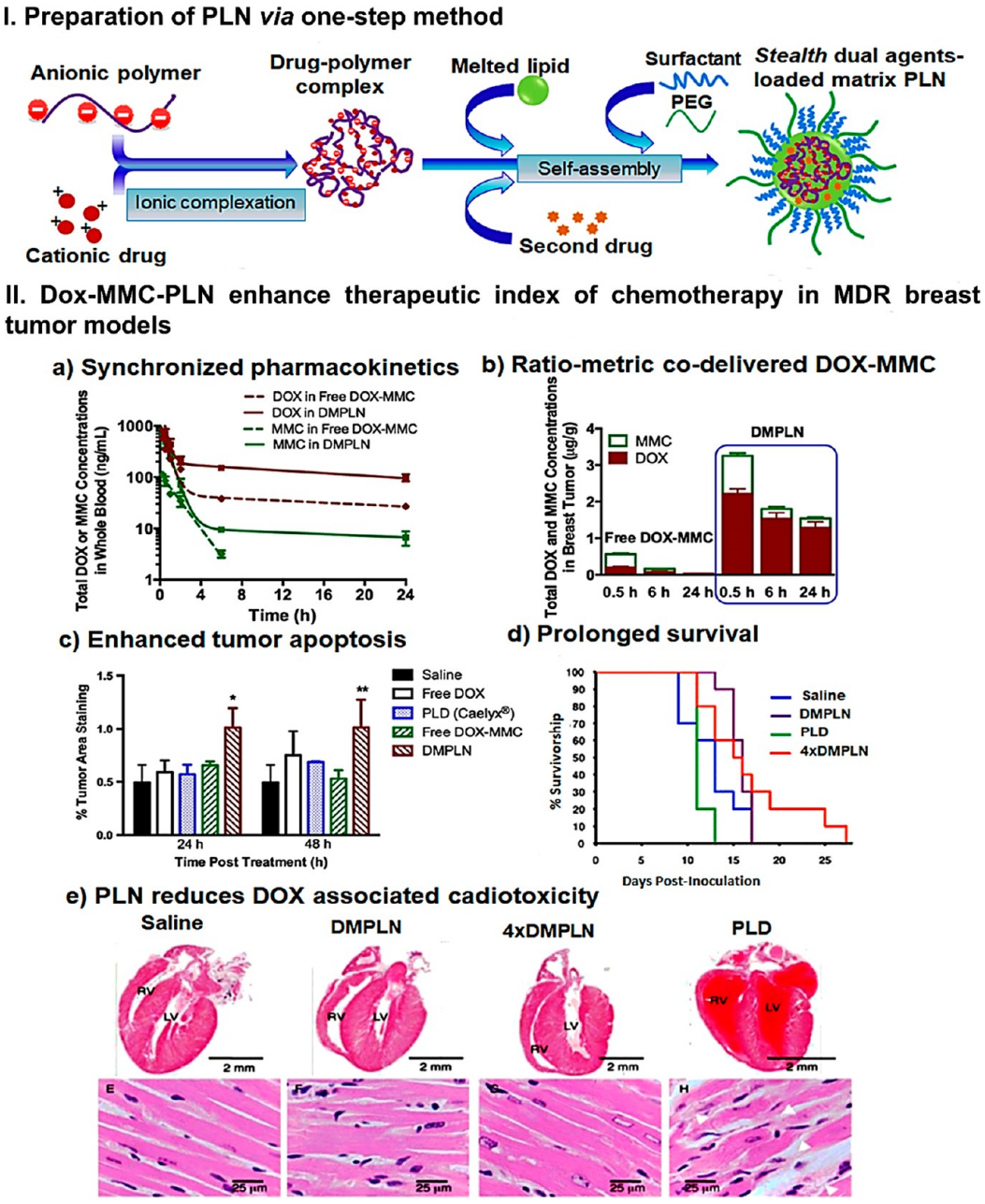

Figure 2. (I) One-step preparation method of PLN. Adapted and reprinted in part with permission from ref 13. Copyright 2017 The Royal Society of Chemistry. (II) Synergistic drug combination loaded PLN for enhanced therapeutic efficacy and improved therapeutic index. Compared to free DOX−MMC, DMPLN (a) extended the blood circulation of DOX and MMC; and (b) facilitated DOX−MMC accumulation and ratiometric codelivery of DOX−MMC combination at breast tumors. (c) DMPLN caused more tumor cell apoptosis than free DOX−MMC and PLD (Caelyx) did. Panels (a−c) are adapted and reprinted in part with permission from ref 61. Copyright 2016 Elsevier Inc. (d) DMPLN extended survival in breast-tumor-bearing mice compared to PLD (Caelyx). (e) H&E stained sections of whole organ morphology (1.2× magnification) (first row), and longitudinal [second row, (E−H)] views (40× magnification). DMPLN (1 and 4 doses) did not show detectable cardiotoxicity compared to saline treatment, whereas only 1 dose of PLD caused myocardial damages in mice. Panels d and e are adapted and reprinted in part with permission from ref 60. Copyright 2014 American Chemical Society.

commonly known as P-gp), MDR-associated protein 1 (MRP1), and breast cancer resistance protein (BCRP) are most commonly linked to the development of MDR.[41,43] Since the discovery of P-gp association with multidrug resistance in 1970s, numerous efforts have been made to identify chemosensitizers and P-gp inhibitors to overcome multidrug resistance in chemotherapy.[44] Since then, three generations of P-gp inhibitors have been identified or designed with increasing potency and specificity. Nevertheless, clinical trials of using these compounds and some FDA-approved P-gp inhibitory drugs with chemotherapy resulted in disappointing outcomes, which either increased neurotoxicity or showed no significant benefit.[44] The major fault in these clinical trials is the unrationalized drug delivery approach. The P-gp inhibitors/sensitizers and anticancer drugs were systemically administered in separate formulations; as such, they may not arrive at the same MDR cancer cells at the same time because of their different pharmacokinetics (PK) and tissue disposition.

https://doi.org/10.1021/acs.molpharmaceut.2c00038
Mol. Pharmaceutics XXXX, XXX, XXX−XXX

In other words, they were spatiotemporally mismatched once administered. Having realized this substantial problem in drug delivery, Wu and co-workers hypothesized that the P-gp inhibitors and cancer drugs must appear at the nanoscale vicinity of the same cell to reach the maximal effect; they thus pioneered co-loading a P-gp inhibitor/sensitizer with an anticancer drug in the same microparticles or NPs to achieve therapeutic synergy.[45] This early example and other examples of synergistic drug combination nano-/microparticles to achieve the 3Rs are presented in Table 1 and elaborated below.

2.1. Nano- and Microparticle-Based Combinatorial Therapy to Overcome MDR. Clinical benefits of chemotherapy with single agents (also known as monotherapy) are limited due to the inability of such therapy to overcome MDR and other drug resistance mechanisms.[15] Thus, combination therapy using two or more anticancer drugs or an anticancer drug with a chemosensitizing agent is extensively exploited. In clinical settings, the sequential administration of drug combination with no overlapping drug resistance mechanisms is recommended rather than simultaneous administration to avoid additive toxicity.[15] In contrast, NP-based drug combination therapy can offer more advantages because NPs can alter the PK, PD, and toxicity profiles of the drugs minimizing normal tissue toxicity compared to free drug combinations. Combination therapies using NPs can be accomplished by several means including (1) free drug mixed with drug loaded NPs, (2) drug loading into two separate NPs, and (3) co-encapsulation of both drugs into a single NP carrier.[13,15] Co-encapsulation of drugs in NPs can be more advantageous from a formulation viewpoint and because it can deliver drugs at synergistic ratios to the cellular and intracellular targets (i.e., more tightly controlled 3Rs).

Co-loading two or more drugs in the same carrier with a synergistic ratio and desirable release kinetics is a challenging task, especially for those with different physicochemical properties. In early proof-of-concept studies, Liu et al. loaded the anticancer drug, DOX, and a chemosensitizer of P-gp, verapamil HCl, into anionic microspheres (MS).[46−48] The drug-loaded MS showed substantially increased cytotoxicity in MDR cells *in vitro* and inhibition of tumor growth in an MDR murine model. Likewise, MS,[49,50] solid lipid NP (SLN),[51,52] and PLN[45,53−62] formulations co-encapsulating DOX and chemosensitizers, or with another cytotoxic drug such as MMC, exhibited superior therapeutic benefit compared to administering free drug solutions, individually or together, in various MDR breast cancer models (Table 1). Similarly, *in situ* ROS-producing glucose oxidase (GOX)-based MS demonstrated substantial bioactivity against MDR breast cancer both *in vitro* and *in vivo*.[63−67] In addition, synergistic ratios of loaded drugs can be tuned to optimize their efficacy against MDR cancer cells through concurrent delivery at the optimal place and time.

For co-loading of hydrophobic and hydrophilic anticancer drugs,[15] Wu and co-workers pioneered PLNs in the early 2000s,[13] which is sometimes called lipid polymer NP (LPN) by some groups later. PLN capitalizes on the properties of a SLN, owing to their solid form at physiological temperature unlike prior lipid bilayer systems (e.g., liposomes and polymeric NPs) (Figure 2I). With both a hydrophobic lipid and more hydrophilic polymer, PLNs are capable of loading both hydrophobic and hydrophilic therapeutic agents, a variety of diagnostic agents, imaging probes, genes, and proteins. The carrier composition can also be tailored to afford desirable drug release profile, improve drug uptake, and enhance intracellular drug transport. Because of its versatility over other NP systems such as conventional SLNs and nanostructured lipid carriers (NLC), PLNs can be designed to circumvent membrane efflux transporters in cancer cells (Figure 2IIb, Table 1).[13,68,69] While PLNs are stratified into two broad categories (i.e., type I (monolithic matrix) and type II (core−shell)),[13,68] this review focuses mainly on Type I.

Similarly, multifunctional poly(ethylene oxide)-*block*-poly(ε-caprolactone) (PEO-*b*-PCL) block copolymers-based polymeric micelles were developed to codeliver a P-gp-silencing siRNA and DOX, to overcome MDR.[70] Upon entering into the MDR cells, the siRNA downregulated the P-gp expression on the plasma and nuclear membranes and increased cellular accumulation of DOX and its toxicity against MDR cells.[70] In a recent study, a chitosan-multilayered NPs (Ch-MLNPs) was developed with a poly(lactic-*co*-glycolic acid) (PLGA) core (loaded with DOX), a liposome-based second layer (hydrophobic drug paclitaxel), and a chitosan-based third layer (loaded with silybin).[71] The chitosan layer helped in targeting cluster of differentiation 44 (CD44)-overexpressing receptors at the MDR breast cancer cells. Silybin inhibited the P-gp efflux pump, enabling synergistic action of DOX−paclitaxel to kill the MDR cells.[71] A PEGylated carboxymethylcellulose conjugate of docetaxel (DTX) (Cellax) was developed to overcome MDR in breast cancer.[72] Compared to free DTX, the NPs reduced P-gp expression in breast cancer cells and enhanced antitumor efficacy compared to DTX in a taxane-resistant breast tumor model. Additionally, polymeric NPs loaded with podophyllotoxin (PPT) (a potent drug against MDR tumors with poor solubility and high system toxicity) showed increased activity against MDR tumors due to the inhibition of P-gp mediated MDR mechanism.[73]

2.2. Rational Selection of Synergistic Drug Combinations to Overcome Multidrug Resistance. Infusion of nanoparticulate drug combinations at synergistic ratios has gained increasing importance for mitigating various resistance mechanisms associated with TME and amplifying anticancer efficacy.[13,15,58,60,61] Hypoxia and chronic oxidative stress are known hallmarks of TME that contribute to tumor resistance to chemotherapy.[74] To mitigate tumor-hypoxia-induced resistance to DOX, MMC was co-encapsulated with DOX for its bioactivation under hypoxic condition (Table 1). The two drugs possess different mechanisms of action to damage DNA. DOX poisons topoisomerase IIα, responsible for catalyzing DNA unwinding during transcription and DNA replication; the inhibition of which causes DNA double strand breaks (DSBs).[75,76] MMC induces DNA alkylation and promotes intra- and interstrand DNA cross-links, disrupting cell repair and replication.[77] This effect, together with glutathione depletion by MMC and formaldehyde formation from MMC enhanced DOX-induced DNA DSBs, demonstrating the synergistic interactions of DOX−MMC combination.[56] However, severe cardiotoxicity has limited the clinical translation of DOX and MMC (DOX−MMC) combinations to cancer patients.[78,79] To maximize the benefit of such drug combinations, nanocarrier systems were designed that circumvented off-target toxicity through tumor-specific release of drugs.[49,50,56,57,80] The synergistic anticancer effect of DOX−MMC combination therapy has been investigated in multiple murine and human breast cancer cell lines and tumor models.[49,50] A DOX to MMC molar ratio of 2:1 was used in a PLN (DMPLN) formulation. DMPLN prolonged plasma

https://doi.org/10.1021/acs.molpharmaceut.2c00038
Mol. Pharmaceutics XXXX, XXX, XXX−XXX

circulation of both DOX and MMC (Figure 2a) and enabled ratio-metric codelivery of DOX and MMC in breast tumors (Figure 2b).[57,61] The DMPLN also exhibited enhanced tumor apoptosis and extended host-survival in both human and murine MDR tumor models compared to free DOX−MMC solution and liposomal DOX (DOXIL) (Figure 2c,d).[59,60] Importantly, DMPLN formulations did not cause detectable cardiotoxicity in the animals, in contrast to free DOX−MMC (Figure 2e). Co-encapsulation of an anticancer drug with an MDR inhibitor/sensitizer at the cellular level presents another promising strategy. A combination of DOX and the P-gp inhibitor GG918 loaded into a monolithic PLN of tristearin/stearic acid = 30:70 *w*/*w* to enhance toxicity in an MDR model of breast cancer *in vitro*.[54] A similar composition was used to prepare and evaluate DOX−PLN for *in vivo* efficacy, off-target toxicity, and distribution of DOX in murine breast cancer models.[55,69] DOX co-loading with different cationic chemosensitizers such as quinidine HCl or verapamil HCl, was achieved using anionic dextran sulfate MS.[51] These formulations exhibited enhanced DOX uptake and cytotoxicity in MDR cells.

To overcome MDR mediated by P-gp overexpression and membrane rigidity, Zhang et al. utilized ω-3 polyunsaturated fatty acid DHA and MMC co-loaded in a PLN system.[62] The presence of DHA reduced membrane rigidity and enhanced MMC uptake in an MDR breast cancer cell line. The intracellularly released MMC was then bioactivated inducing a chain lipid peroxidation facilitated by DHA and causing oxidative damage to mitochondria and apoptosis.[14,32,62] A complete description of all such examples is beyond the scope of this review. The readers are referred to detailed presentations of the PLN carrier systems in previous publications.[13,68,81]

To date there are a plethora of nanomedicines under investigation for treating MDR cancer types, which are extensively summarized in recent review articles.[82,83] Major strategies to overcome MDR include development of inhibitors for ABC transporters, modification of formulation to increase dose of therapeutic agents, and silencing MDR genes to inhibit posttranscriptional process.[83] To address such challenges, various NPs are developed including polymeric NPs (e.g., PLGA, polycaprolactone (PCL), polylactic acid (PLA), polyethyleneimine (PEI), hyaluronic acid (HA)), cyclodextrin, polysaccharides and polypeptides, SLN, liposomes, micelles, mesoporous silica NPs, dendrimers, and NLC.[83] Unfortunately, their clinical translation is limited because multidrug resistance is a complex phenomenon involving multiple pathways associated with not only efflux transporter proteins but also lipid rafts that support P-gp function and membrane rigidity. In this context, combination therapy with nanocarriers to codeliver multidrug-resistance-mitigating agents and anticancer drugs spatiotemporally to the same cancer cell would exhibit superiority.[36,62]

2.3. Rational Design of NPs with Special Properties for Effective Delivery and Therapeutic outcome. Careful design consideration of NPs is required for effective delivery of therapeutic agents to its site of action in order to enhance therapeutic efficacy on MDR tumors.[15] NP formulation typically involves choosing an optimal combination of building blocks (polymer and lipid) to obtain a particle of the desired size, shape, and surface charge.[6] For synergistic drug combinations, the molecular mechanism and physicochemical interactions between NP components (polymer and drugs) need to be carefully considered on a case-by-case basis.[15] Such rational design strategies provide several advantages over conventional nanocarriers. For example, extensive studies have been conducted to investigate lipid composition properties and their interaction(s) with both polymer and drug to optimize NPs for both high drug loading and controlled drug release characteristics.[33,45,54,55,57,68,84−87] The initial PLN prototype utilized a charged polymer (dextran sulfate) incorporated into a SLN to obtain higher drug loading and sustained release of water-soluble drugs (verapamil HCl or DOX).[51,52] In order to achieve a higher drug loading of water-soluble, ionic drugs (e.g., DOX) into a lipid matrix and release them at a desired drug release rate, an anionic polymer (e.g., hydrolyzed polymer of epoxidized soybean oil (HPESO)) was used with stearic acid to effectively load DOX in a PLN. The PLN enhanced the cellular uptake and retention of DOX, bypassing the efflux pumps and providing increased cytotoxicity against human MDR cancer cells.[53,54,69,88]

To further improve intratumoral distribution and cell uptake, a size−shape transformable PLN was developed.[33] By screening a series of lipids for their physicochemical interactions with designed polymers, myristic acid was selected to prepare PLN that gradually changed size and shape (from larger to smaller, and spherical to spiky) over time under physiological conditions (pH 7.4). The transformability of PLN enhanced tumor penetration, cellular uptake, and fatty acid mediated intracellular trafficking of DOX, as demonstrated in an orthotopic breast tumor mouse model.[33]

Overall, the challenges and limitations of drug combination therapy are extensively reviewed in recent review articles.[15,89] Nontargeted combination nanomedicines rely on the EPR effect for passive targeting and tumor accumulation. However, tumor heterogeneity, hypovascularity, changes in tumor angiogenesis and inflammation at different stages of tumorigenesis, and poor lymphatic drainage may substantially impact tumor accumulation of NPs by the EPR effect.[15] Second, the drug release kinetics, PK, and PD, as well as the toxicity profiles of single and combination drugs, should be carefully evaluated.[15] Premature drug release, extremely slow release, and differential release rates of different drugs in the combination NPs may result in poor therapeutic outcomes. Also, the toxicity of a single agent along with combination drugs should be carefully investigated to minimize the overall adverse effects. Using targeted NPs could be a great alternative strategy to mitigate an unpredictable EPR effect, which will be discussed in the later sections. The synergistic ratio between the combination drugs should be thoroughly investigated *in vitro* and optimal ratio should be selected prior to formulate the NPs.[15] For effective encapsulation of multiple drugs and maintaining the synergistic ratio during the course of drug release, the affinity of nanocarrier materials and compatibility of payloads should be carefully considered and drug release mechanisms and release kinetics should be well-controlled. To achieve this aim, a thorough investigation is required to understand the interactions between the building blocks of NPs (e.g., polymers, lipids, surfactants, and other excipients) and the drugs/biologics being delivered, as well as the fate of the drug in physiological conditions and their interplay with biology.[33]

3. BBB-CROSSING NANOMEDICINE

CNS cancers account for millions of deaths globally.[90] In 2020, approximately 308 000 new cases of brain and CNS cancers

https://doi.org/10.1021/acs.molpharmaceut.2c00038
Mol. Pharmaceutics XXXX, XXX, XXX−XXX

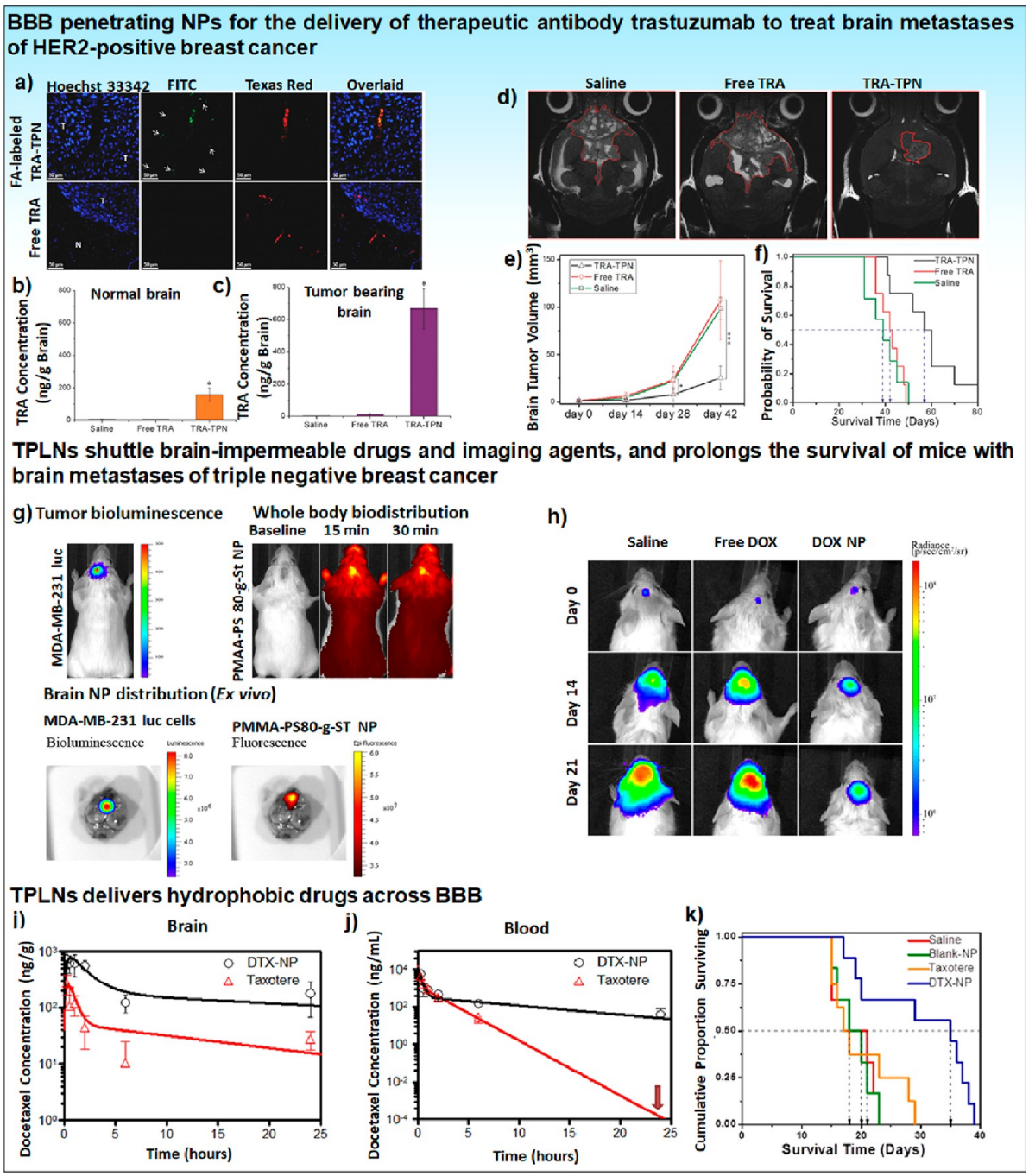

Figure 3. BBB-penetrating NPs for delivery of therapeutic antibody (TRA), small-molecule drugs (e.g., DOX) DTX across BBB. Design of terpolymer NPs or terpolymer−lipid hybrid NPs (TPLN) for drug delivery to the brain. (a) Confocal microscopic images of SCID mouse brain tissue sections 2 h after i.v. injection of FA (HF 750)-labeled TRA−TPN (top panels) or free FA-labeled TRA (bottom panels). Green represents FA-labeled TRA. Blood vessels are shown in red (Texas red dextran). Texas red dextran was administered i.v. to the mice 15 min prior to euthanasia. Cellular nuclei were stained blue using Hoechst 33342. T: brain tumor area; N: normal area without tumor; arrows: FA-labeled TRA TPN. Scale bar = 50 μm for all images. ELISA-based quantification of TRA in healthy SCID mouse brains (b) and HER2 positive tumor-bearing SCID brains (c) at 2 h after i.v. injection. Mice were treated with saline, free TRA or TRA TPN (40 mg/kg, n = 3). (d) MRI images of brain tumor 42 days post-treatment (4×10 mg kg^{-1} TRA, 4×10 mg kg^{-1} TRA TPN, or 4×200 μL saline over a 4 week period). The extent of tumor spread is outlined by the red lines in the panel. (e) Normalized increase in the total tumor volume. Up to day 28, all mice survived. On day 42, the number of mice that survived was 5 and 6 for free TRA and TRA-TPN, respectively. All data are presented as mean ± standard deviation. (f) Kaplan−Meier survival curve of tumor-bearing mice after treatment with saline, free TRA and TRA TPN. Panels (a−f) are adapted and reprinted with permission from ref 105. Copyright 2018 WILEY-VCH Verlag GmbH & Co. KGaA. (g) *In vivo* bioluminescent images of brain tumors, whole body biodistribution and *ex vivo* images of brain accumulation of HF-750 labeled NP in brain metastases of MDA−MB-231−Luc−D3H2LN cells intracranially inoculated in NRG-SCID mice. The panel depicts the bioluminescence of luciferase-expressing tumor cells in the inoculated brain tumors at 10 min post intraperitoneal (i.p.) injection of luciferin solution; bioluminescent image of brain tumor; and fluorescence image of NPs in an excised mouse brain. (h) *In vivo* images of brain tumor bioluminescence demonstrating tumor growth inhibition in NRG-SCID mice. The brain metastases of MDA−MB-231−Luc−D3H2LN cells in NRG-SCID mice were established by intracranial injection. The bioluminescence of

https://doi.org/10.1021/acs.molpharmaceut.2c00038
Mol. Pharmaceutics XXXX, XXX, XXX−XXX

Figure 3. continued

luciferase expressing tumor cells in the inoculated brain tumors were measured 10 min following i.p. injection of luciferin solution and used to monitor tumor growth inhibition. Panels (g,h) are adapted and reprinted in part with permission from ref 103. Copyright 2014 American Chemical Society. Delivery of hydrophobic agents into the brain metastases of brain tumor bearing mice (i,j). Concentration of DTX NP and free DTX in solution (Taxotere) in brain (i) and blood (j). The line represents the fitted data from PK modeling, and symbols represent measured values. (k) Kaplan−Meier survival curve of tumor-bearing mice following the treatment of saline, blank NP, Taxotere (free DTX in solution) (20 mg/kg DTX), or DTX NP (20 mg/kg DTX). Panels (i−k) are adapted and reprinted in part with permission from ref 104. Copyright 2016 Elsevier B.V.

were diagnosed worldwide with an estimated mortality of ∼251 300.[91] It is not surprising that around 55 000 Canadians currently live with a brain tumor, while another 27 Canadians are diagnosed with brain tumor every day.[90] Moreover approximately 20−40% of people with primary tumors at other sites, such as the skin, breast, colon, lungs, and prostate, ultimately experience secondary metastases to the brain.[90] Breast cancer metastases to the brain are the second leading isotype after lung cancer, and about 10−15% of breast cancer patients were clinically diagnosed with such metastases.[92−94] The patients having human epidermal growth factor receptor 2 (HER2)-positive and triple-negative (HER2, estrogen receptor (ER), and progesterone receptor (PR) negative) breast cancer have a higher incidence of CNS metastases.[93] Brain metastases are one of the most difficult malignancies to treat being associated not only with a poor prognosis but also with severe neurological impairment.[93] For patients with multiple brain metastasis lesions, whole brain radiotherapy (WBRT) is recommended to reduce the risk of surgical complications. However, owing to the substantial neurotoxicity induced by WBRT, alternative noninvasive methods including chemotherapy are preferred to treat brain tumors and metastases.[94] Unfortunately, most therapeutic agents are incapable of efficiently penetrating the BBB, leading to subtherapeutic drug accumulation in the CNS.

3.1. Physiological Barriers to Nanoscale Delivery. The unique nature of BBB arises from the presence of transmembrane proteins such as claudins (claudin-1, -3, -12, and particularly -5) in brain endothelial cells forming tight junctions with occludins and junctional adhesion molecules that regulate tight junction formation.[21,95,96] Such proteins connect to the actin cytoskeleton via Zonula occludens-1 (ZO-1). Together they form a tight cellular junction, which acts as a highly selective permeability barrier between blood in the general circulation and the brain and spinal cord. In addition, existence of efflux pumps such as P-gp that are overexpressed in brain microvessel endothelial cells which prevent substrate drugs from entering the brain.[21] Similarly, the blood−cerebrospinal fluid (BCSF) barrier consisting of choroid plexus epithelial cells containing tight-junction proteins regulate the entrance of substances to cerebrospinal fluid (CSF) within the brain.[21] Together, the BBB and BCSF barrier prevent entry of approximately 98% of small molecule therapeutics >400 Da.[20,21,95,96] Notably, several receptors (insulin, transferrin, angiopep-2, and low-density lipoprotein receptors (LDLR)) together with ion channels and influx transport proteins, can facilitate active transport of corresponding compounds. Thus, there exist four primary routes for drugs to enter the brain: (1) paracellular pathways, (2) transcellular diffusion, (3) transcellular transcytosis, and (4) leukocyte mediated transmigration.[95] To overcome the BBB, NPs often utilize receptor/carrier mediated transcytosis (e.g., insulin, transferrin, folate, glucose, glutathione, and LDLR) to deliver a plethora of drugs across the BBB and into the brain.[21,95,97] Table 2 presents representative examples of nanocarriers with various BBB-penetrating mechanisms for CNS drug delivery, using NPs made of organic or inorganic materials. Organic materials have been widely employed for drug delivery due to their good biocompatibility and versatility of composition choices; while inorganic NPs are normally used for diagnostic or theranostic purposes.[98] In addition to incorporation of ligands for receptor-mediated BBB penetration, other types of targeting moieties can be conjugated to nanocarriers for more specific drug delivery in the brain parenchyma. Such NPs are designed to deliver the therapeutics to the disease-affected regions and cells upon crossing the BBB (*right* site) with a proper release rate that can generate therapeutic effect (*right* time and *right* level).

3.2. BBB-Penetrating NP for Treating CNS Tumors. As shown in Table 2, LDLR-mediated BBB-crossing mechanism has been extensively exploited to design NPs for drug delivery and imaging. Wu and co-workers have developed a BBB-penetrating NP platform based on the terpolymer, poly(methacrylic acid)−polysorbate 80-grafted starch (PMAA−PS 80−St).[99−104] In this NP system, the covalently bound PS 80 on the NP surface recruits apolipoprotein E (ApoE) in the blood circulation promoting NP entry into the brain parenchyma via LDLR-mediated transcytosis.[105] The NP systems exhibit a great ability to cross the BBB in both healthy brain and inflammatory brain tissue via the EPR effect and to effectively deliver brain-impermeable imaging agents (gadolinium, Gd-based contrast agent) and a variety of anticancer drugs (DOX, DTX, and the antibody trastuzumab (TRA)) to brain metastases in murine breast cancer models (Table 2).[99−105]

Delivering therapeutic biomolecules to the diseased site in the brain requires special considerations: (1) protecting the biomolecules from degradation, (2) shuttling them across the BBB, and (3) releasing them to the cellular target. On the basis of a terpolymer-antibody conjugate platform, a novel two-step targeted nanoconstruct (NC) system was developed for shuttling the therapeutic antibody TRA into HER2+ breast cancer cells within the brain (Figure 3a−f).[105] The sequential targeting process involved (1) PS 80-enabled LDLR-mediated transcytosis across the BBB followed by (2) dissociation of the NCs that exposed TRA polymer within the brain parenchyma, allowing local bioavailability and extracellular binding of TRA to HER2+ breast cancer cells to produce its targeted therapeutic effect. TRA−terpolymer lipid NP (TPN) extravasated from the blood vessels and accumulated in brain tumor lesions compared to free TRA (Figure 3a) and delivered 40- and 50-fold TRA compared to free TRA into the brain of healthy and tumor bearing mice, respectively (Figure 3b,c). The TRA TPN also inhibited tumor growth as determined by magnetic resonance imaging (MRI) signals (Figure 3d) and tumor volume measured by MRI (Figure 3e) by 43-fold and prolonged the mean survival rate >1.3-fold in a brain metastasis model (Figure 3f).

https://doi.org/10.1021/acs.molpharmaceut.2c00038
Mol. Pharmaceutics XXXX, XXX, XXX−XXX

Many potent anticancer drugs (e.g., DOX and DTX) are ineffective for brain cancer due to poor BBB permeability. A DOX-loaded BBB-penetrating NP system was thus developed which enhanced accumulation within brain metastasis approximately 30 min after i.v. NP injection (Figure 3g).[103] Treatment with DOX NPs significantly inhibited brain tumor growth compared to free DOX at a similar dose as assessed by *in vivo* bioluminescence imaging of brain metastases (Figure 3h).[103] To efficiently load and release the poorly water-soluble drug, DTX, while maintaining the stability of the NP system to cross the BBB, a terpolymer NP system was designed and optimized to be an amphiphilic polymer (terpolymer−lipid) nanocarrier system for DTX (DTX NP) (Figure 3i−k).[104] The DTX encapsulated within the NP was observed to cross the intact BBB of healthy mice within 15 min after i.v. injection, leading to enhanced accumulation of DTX in the brain compared to a clinically used solution formulation of DTX (taxotere) (Figure 3i). The use of PK modeling revealed that the DTX NP enhanced drug bioavailability in the brain, prolonged blood circulation with a 5.5-fold increase in blood terminal half-life, increased blood area under the curve (AUC_{0-24h}) by 1.3-fold, and caused a 29% decrease in body clearance compared to taxotere (Figure 3i,j). The DTX NP also significantly enhanced *in vivo* therapeutic efficacy as compared to the free DTX or Taxotere (Figure 3k). The above examples demonstrated that the terpolymer-based nanosystem platform exhibits versatile drug delivery capabilities and highlights the tremendous potential for the rational design of noninvasive nanomedicine-based treatments for diseases of the brain.

For the rational design of NPs, DOE helps to understand the interactions between the processing variables and their output values and obtain a final product based on mathematical and experimental techniques. For instance, synthesis of PLNs relies heavily on process optimization and components (lipids and polymers), which ultimately influences the physicochemical properties that are important for biological performance.[106,107] However, most of the NPs are prepared without having a thorough understanding of the process−property relationships which can ultimately impede the functions of final NPs in terms of their physicochemical properties and *in vivo* performances (efficacy).[107−109] The use of DOE in optimizing a processing parameter involves the use of different inputs (factors) fed into the process that generates multiple outputs (responses). During this process, the cofactors (nuisance factors) that affect outputs can be blocked from the experimental design.[110]

The poor penetration of many potential therapeutic agents to the brain impedes their potential application in therapy for glioblastoma multiforme (GBM). To overcome this problem, Ahmed et al., devised a DOX-loaded terpolymer and lipid hybrid NP (TPLN) using DOE (2^3 factorial design) methodology.[109] Of the five lipids screened, ethyl arachidate (EA) was selected due to its superior colloidal properties (particle size, shape, zeta potential, drug loading, encapsulation efficiency, and serum stability) and cytotoxicity using human GBM U87−MG−RED−FLuc cells as a target. As compared to other lipids, the superior anticancer efficacy of EA TPLNs was attributed to physicochemical properties of EA. The lower melting temperature (41.7 °C) might have helped in the formation of softer NPs with relatively weaker crystalline matrix structure. Because of this feature, the terpolymer−DOX complex could partition well in the EA matrix via hydrophobic interaction making EA TPLNs more stable in colloidal properties. These properties might ultimately enhanced DL and EE of the NPs and their intracellular DOX release. A strategically optimized EA−DOX TPLN exhibited superior cytotoxicity, endocytosis-mediated cellular uptake, and deep tumor spheroid penetration compared to free DOX *in vitro*. The interaction of TPLNs with ApoE in the circulation enabled LDLR-facilitated BBB-crossing and accumulation in the brain tumor site in an orthotopic intracranial GBM mouse model.[109]

Currently, substantial research are ongoing in mitigating the challenges of delivering therapeutics across BBB for the treatment of brain tumors[111] and CNS disorders.[112] In comparing to the passive diffusion or other invasive methods (e.g., intracranial injection and convection-enhanced delivery and temporary disruption of the BBB using ultrasound), receptor-mediated transcytosis-based BBB crossing strategies have shown great potential.[99−104] Currently, there are polymeric micelles, albumin-bound NPs, liposomes, nanogels, nanosuspensions, polymersomes, dendrimers, protein nanocapsules, and gold NPs under investigation for crossing the BBB through receptor mediated transcytosis (Table 2). Among these, the surface coating of NPs with PS 80 offers tremendous advantages in which the NPs exploits the physiological advantages in which PS 80 coated NPs upon injection can recruit ApoE from plasma and mimic LDL particles and eventually transcytose across the BBB via LDLR.[19,29,97,100,102−105,109,113,114] Nevertheless, more studies are required to further improve the NP formulation and evaluate their safety and efficacy in larger animal models. Few studies those have made it to the clinical trials will be further discussed in the "Future Perspectives" section.[115]

3.3. Multifunctional Theranostic NPs for CNS Diseases. In addition to brain tumors, neurodegenerative disorders such as AD result in synaptic dysfunction and ultimately degeneration of neurons resulting in permanent cognitive dysfunction.[19] Neurodegenerative disorders currently affect 7 million people in the USA, and this number is rising dramatically due to progressive aging of the population.[116] In Canada, over 500 000 people are currently living with different forms of dementia, and this number is estimated to increase to 912 000 by 2030.[117] Every year, 25 000 Canadians are diagnosed with dementia, on which 65% of those diagnosed are over the age of 65 costing over $12 billion annually. Unfortunately, there is at present a paucity of disease modifying therapeutic agents available to treat AD due to the complex nature of the neurodegeneration involved. One major reason suggested for this failure is a lack of sensitive early stage detection method for AD. Such a system is believed to be critical given that the neurobiological changes seen in AD appear to develop as early as 15−20 years prior to the onset of observable cognitive decline with functional symptomology in patients.[19] As a result, most patients are diagnosed at a stage in which it is believed that irreversible changes in the CNS have already occurred and when the efficacy of therapeutic intervention may be severely limited. Thus, early stage diagnosis and prevention of AD neurodegeneration is an unmet medical need. Nanomedicine has shown potential for the application of simultaneous delivery of therapeutic and diagnostic agents (theranostics) in which the aim is to assess and treat the target of injury. This section discusses the potential application of reactive NPs for theranostic application in AD.

https://doi.org/10.1021/acs.molpharmaceut.2c00038
Mol. Pharmaceutics XXXX, XXX, XXX−XXX

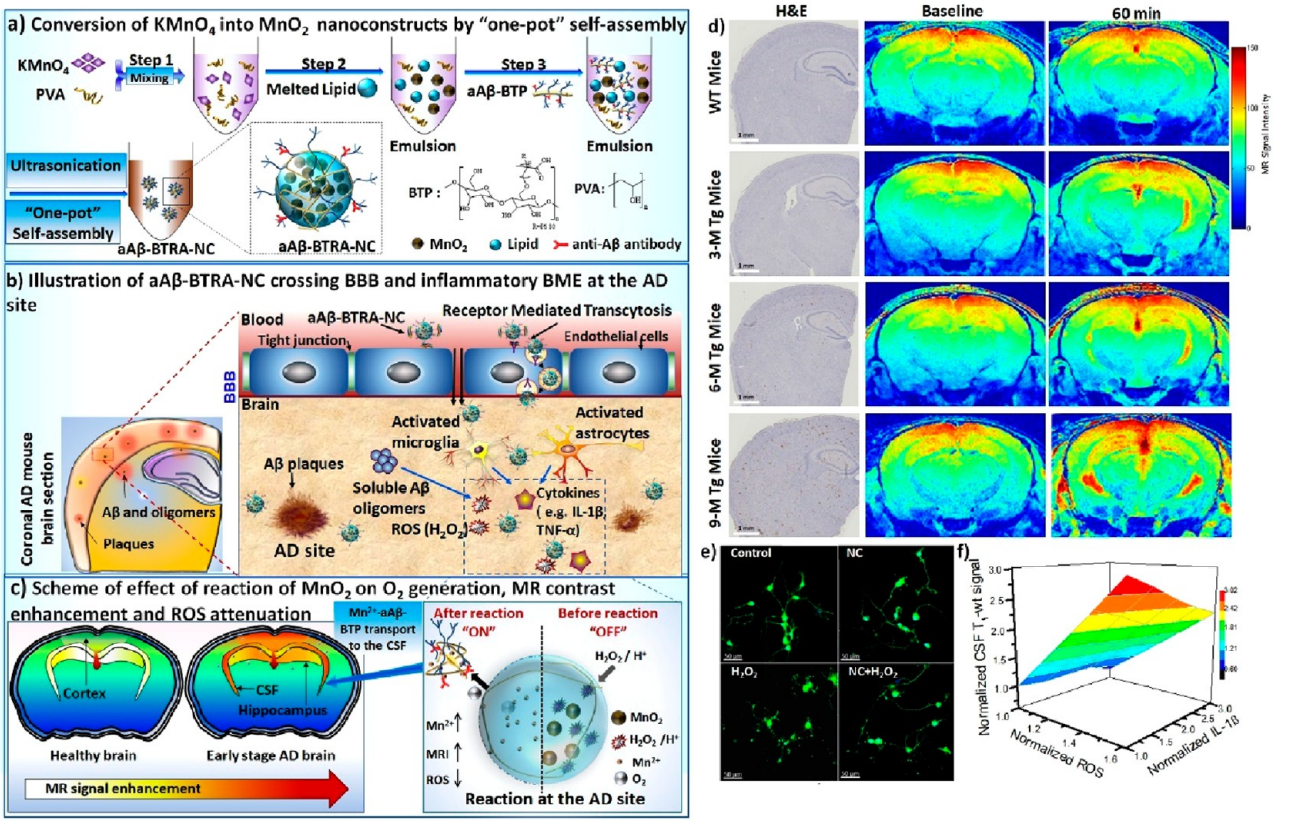

Figure 4. Hybrid aAβ-BTRA-NC for early stage diagnosis and interventions of AD. (a) Schematic illustration of synthesis of aAβ-BTRA-NC. $KMnO_4$ was converted into MnO_2 NPs using the BTP and lipids (b) BBB crossing aAβ-BTRA-NC in both healthy and AD bearing mice and targeting of inflammatory microenvironment of AD brain site. The NCs reacts at the AD site which has higher levels of ROS and inflammatory cytokines. In AD brain, the NCs crosses BBB through low density lipoprotein receptor (LDLR) mediated transcytosis and passive diffusion. (c) Mechanism of aAβ-BTRA-NC in detection of AD in CSF, cortex, and hippocampus. Upon accumulation at the AD site, NCs react with the ROS and generate Mn^{2+} ions. Then, the aAβ-BTP binds with soluble Mn^{2+} and aAβ oligomers and transports them into the CSF and enhances CSF MRI signals. (d) Hematoxylin and eosin (H&E) sections and MRI signal enhancement in different brain regions induced by of aAβ-BTRA-NC at different stages, 3, 6, and 9 months (M), of disease progression in Tg mice compared to WT mice at baseline and 60 min after i.v. injection aAβ-BTRA-NC. (e) Neuro-protective effect of NCs against ROS (H_2O_2) induced neuronal damage. Mouse primary cortical neurons (top left, control) were stressed with ROS using H_2O_2 (bottom left) and NC were coincubated (bottom right) to provide protection against it. The NCs did not show any toxicity to the neurons (top right). (f) 3D surface plot indicates the relationship between *in vivo* CSF MRI signal enhancement, *ex vivo* ROS concentration, and IL-1β concentration in brain tissue. Linear relationships were observed. BTP: brain targeted polymer (terpolymer); PVA: poly(vinyl alcohol). Adapted and reprinted in part with permission from ref 19. Copyright 2020 Elsevier, Ltd.

It has been observed that AD patients experience neurodegenerative injuries which can result in enhanced levels of reactive oxygen species (ROS), together with regional disruptions in local vasculature resulting in hypoxia and promotion of neuroinflammation. In our recent work, a novel ROS-responsive NC was devised composed of anti-Aβ antibody (aAβ), brain-targeted polymer (BTP) and ROS-activatable MnO_2 NPs (aAβ-BTRA-NC) in order to enhance sensitive, early stage detection of AD neuroinflammation (Figure 4a−c).[19] The aAβ-BTRA-NC targeted regions of AD neuroinflammation due to the presence of Aβ targeting antibody (4G8), while NP-loaded MnO_2 reacted locally with endogenous ROS and hydrogen peroxide (H_2O_2), producing paramagnetic Mn^{2+} ions and O_2, enhancing T_1-weighted MRI within affected regions of the cortex and hippocampus (Figure 4b,c). The freed Mn^{2+} interacted with terpolymer and scavenged Aβ which ultimately flowed to the CSF (Figure 4c). Such inflammation-based enhancement of the MRI signal can be seen as early as 3 months in a transgenic AD mouse model, in which CSF signals were 1.51−2.24 times higher than that seen in wild-type littermates (Figure 4d). The aAβ-BTRA-NCs were also observed to rescue ROS induced stress in primary cortical neurons; suggesting the potential for this NC to serve as a theranostic modality for AD (Figure 4e). In addition, the NC reduced pro-inflammatory cytokines (known to increase during AD) and reduce total ROS demonstrating its therapeutic potential. Consistent with this, a linear relationship of CSF MRI signal with the ROS and pro-inflammatory cytokine levels were observed in 3−9 months old transgenic (Tg) AD mouse (TgCRND8) brains (Figure 4f).

4. MULTITARGETED AND INTRACELLULARLY ACTIVATED NANOMEDICINE

Targeted therapy is widely used in the clinics to treat solid tumors.[118] In passive targeting, the therapeutic agents exploits the leaky vasculature endothelium of solid tumors through passive diffusion to accumulate in the tumor site. The impaired tumor vasculature and lymphatic systems together contribute to the EPR effects as depicted in Figure 1a. Due to the EPR effects, NPs readily passes between endothelial cells and accumulate in tumor tissues.[119] EPR also helps in enhanced retention of NPs via the tumors' inefficient lymphatic drainage

https://doi.org/10.1021/acs.molpharmaceut.2c00038
Mol. Pharmaceutics XXXX, XXX, XXX−XXX

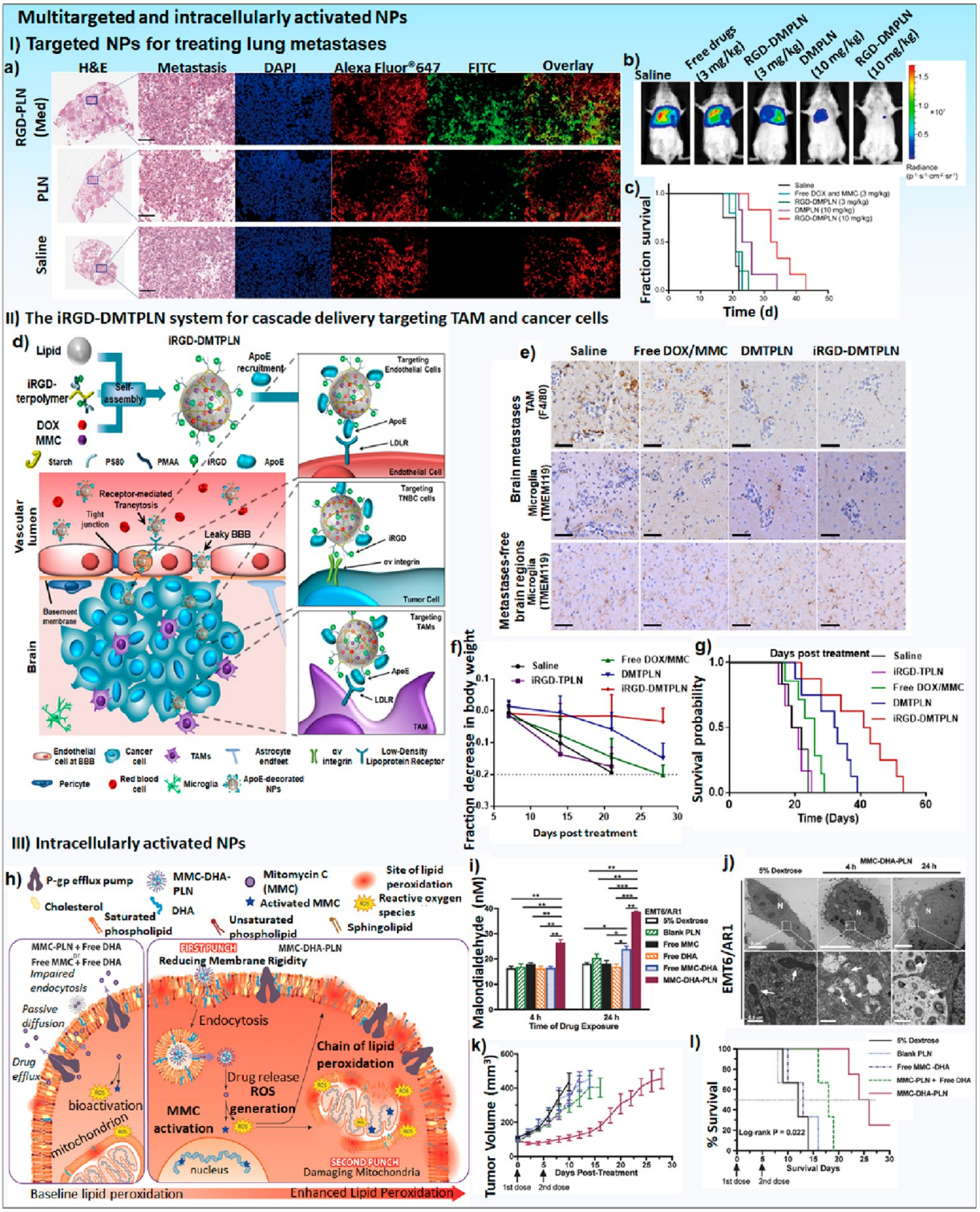

Figure 5. (I) Dual-targeted NPs for treating lung metastases. (a) Distribution of cRGD-DMPLN in the metastases-bearing lungs of mice inoculated with MDA−MB−231-luc-D3H2LN cells. Lungs were resected 4 h after i.v. treatment with FITC-labeled RGD-PLN (Med), PLN, or saline. H&E staining shows the metastatic tumor nodules. Sections were stained with DAPI for cell nuclei (blue) and Alexa Fluor647 labeled CD-31 antibody for blood vessels (red). For all zoomed images, scale bar = 200 μm. (b) *In vivo* bioluminescent images of mice from different treatment groups 28 days after tumor inoculation with MDA−MB−231-luc-D3H2LN cells. (c) Kaplan−Meier survival curve of lung metastasis-bearing mice. Panels a−c are adapted and reprinted in part with permission from ref 135. Copyright 2017 the authors, SpringerNature (http://creativecommons.org/licenses/by-nc-nd/3.0/). (II) BBB crossing of iRGD-DMTPLN via LDLR-binding. (d) Schematic diagram of self-assembly of iRGD-conjugated DOX-MMC loaded TPLN (iRGD-DMTPLN) and their cellular targeting mechanisms in αv integrin-expressing TNBC MDA−MB−231-luc-D3H2LN cells in a brain metastases mouse model. iRGD-DMTPLN binds to integrin in the tumor neovasculature. iRGD-DMTPLN targets LDLR-expressing TAMs and αv integrins expressing TNBC cells in the brain metastases. (e) Targeting tumor-associated macrophage (TAMs) with iRGD-DMTPLN *in vivo*. The iRGD-DMTPLN system reduced TAM populations and exhibited superior efficacy over DMTPLN or free drugs. (f and g) MDA−MB−231-luc-D3H2LN brain metastases-bearing NRG mouse body weight changes and Kaplan−Meier survival plot. Tumor-bearing

https://doi.org/10.1021/acs.molpharmaceut.2c00038
Mol. Pharmaceutics XXXX, XXX, XXX−XXX

Figure 5. continued

mice were treated with i.v. of saline, blank iRGD-TPLN, Free DOX/MMC (6 mg kg^{-1} DOX), DMTPLN (6 mg kg^{-1} DOX), or iRGD-DMTPLN (6 mg kg^{-1} DOX). The DOX/MMC molar ratio was 1.0:0.7 for all treatments. Panels d−g are adapted and reprinted in part with permission from ref 29. Copyright 2019 WILEY-VCH Verlag GmbH & Co. KGaA. (III) Intracellularly activated NPs. (h) Schematic diagram demonstrating two-step/one-punch strategies to deliver DHA−MMC−PLN for intracellularly activated and mitochondrial targeted therapies against MDR cancer cells. Left panel: Cellular level barriers of rigid MDR cell membrane prevent the entry of both MMC-PLN and free drug. Intracellular accumulation of drugs is further hindered by the presence of efflux pumps and lysosomal degradation during endocytosis. Right panel: First punch, MMC−DHA−PLN reduces MDR cell membrane rigidity and increases cellular uptake of PLN; second punch, mitochondrial enzymes (e.g., cytochrome b5 reductase) bioactivates MMC by generating ROS that cause peroxidation of DHA in MMC−DHA−PLN, leading to oxidative damage of mitochondria and possibly plasma membranes. (i) Level of malondialdehyde (MDA) before and after various free MMC and/or DHA formulations, blank PLN, or MMC−DHA−PLN for 4 or 24 h. (j) Transmission electron microscopy (TEM) images of drug-resistant cells treated with 5% dextrose and MMC−DHA−PLN for 4 and 24 h. Scale bar = 0.5 μm. (k) EMT6/AR1 breast tumor growth over 30 days after two sequential dose regimens. (l) Kaplan−Meyer survival curves of MMC-DHA combination in free or PLN formulations. *In vivo* studies were conducted by i.v. injecting mice on days 0 and 5 with 4.0 mg kg^{-1} MMC and 2.4 mg kg^{-1} DHA. The synergistic molar ratio of MMC: DHA= 1:0.6 were used all combinations. Panels h−l are adapted and reprinted with permission from ref 62. Copyright 2017 WILEY-VCH Verlag GmbH & Co. KGaA.

prolonging the retention of NP in tumors. The physicochemical properties of NP such as size, shape, surface charge, and polydispersity are known to have a substantial impact on the EPR effect.[13,28,119,120] However, the passive EPR effect can be limiting, for example when there is a dense solid ECM and high interstitial fluid pressure limiting NP penetration into tumors.[13,119] Most TME are heterogeneous and consist of different cells including cancer-associated fibroblasts (CAF) and TAM. The higher densities of TAMs promote tumor progression and are associated with poor patient prognosis in solid tumors.[29] Ultimately, this can limit the efficacy of chemotherapeutic and anticancer−immunomodulating drugs.[29]

In contrast, active targeting by functionalizing NPs surfaces with ligands is used to improve the specificity of drug delivery to cancer cells in the complex TME.[120] Ligands and their receptor interactions can facilitate NP diffusion into tumors through endocytosis to release their cargos in a more directed manner for a better therapeutic outcome by reducing off-target toxicities.[13,119,120] Common ligands such as antibodies (e.g., trastuzumab), small peptides (e.g., Arg−Gly−Asp, RGD), nucleic acids (aptamers), or other small molecules (e.g., vitamins, carbohydrates, and folic acid) are utilized to target different cell surface receptors such as integrins, HER2, epidermal growth factor receptor (EGFR), transferrin, LDLR, and prostate-specific membrane antigen (PSMA).[120,121] In addition to the strategy of targeting cancer cells directly, targeting nontumor stromal cells in the TME may provide therapeutic benefit due to their important roles in promoting cancer progression.[122] Due to the heterogeneity of the TME, a combination therapy can be developed that targets multiple ligands or intracellular mechanisms simultaneously on different receptors and nontumor cell types. In addition, there may be a need for multiple targeting of ligands or mechanisms to target different receptors on different cells. Multiligand functionalized NPs can target cancer and stromal cells at the same time (e.g., cancer cells and CAFs,[123,124] cancer cells and tumor-infiltrating dendritic cells (TIDCs),[125] cancer cells and tumor vasculature,[126] cancer cells and TAMs,[127,128] and cancer cells and T cells).[121,129] The above-mentioned systems ultimately help overcome tumor resistance to therapies and improve therapeutic outcomes in treating different cancers.

4.1. Functionalized PLN Targeted to Integrins, LDLR, and CD44. To maximize the efficacy of anticancer drugs, NPs can be rationally designed by careful selection of the targeting ligand to deliver imaging or therapeutic agents to more than one cellular component of TME. Table 3 summarizes commonly used targeting strategies for different cancers (namely, strategies targeting receptors highly expressed in cancer cells such as folate, transferrin, integrins, interleukin-4,13, epidermal growth factor (EGF), and HER2 receptor). For instance, Wu and co-workers devised a RGD-conjugated PLN to target tumor neovasculature and tumor cells, thus enhancing tumor penetration and efficacy of PLN-carrier drugs in various preclinical animal models. Table 1 summarizes the RGD conjugated NPs. The $\alpha v\beta 3/\beta 5$ integrin receptors are highly expressed on tumor neo-vasculature and tumor cells such as TNBC (negative for estrogen receptor (EGR), progesterone receptor (PGR) and HER2 receptor) cells and can be utilized for targeted drug delivery.[130] For instance, cyclic RGDfK (Arg−Gly−Asp-D-Phe−Lys; cRGDfK) was conjugated on to the surface of PLN to increase tumor accumulation.[131,132] However, it is challenging to find an optimal RGD density while avoiding increased liver uptake. Similar observations were reported suggesting that the RGD peptide moiety may induce a greater immunogenic response and promote liver uptake.[133,134] For the treatment of lung metastases, taking advantage of the anatomical fact that the i.v.-injected dose reaches the lungs before the liver, and the number of cRGDfK conjugated on PLN (RGD PLN) was optimized. The results showed a significant accumulation of particles in lung metastases by targeting both αv integrin-overexpressing tumor neovasculature and TNBC cells (Figure 5a).[135] Consequently, synergistic RGD−DOX−MMC PLN significantly inhibited lung metastases of TNBC in a mouse model compared to nontargeted DOX−MMC PLN (Figure 5b,c).

A new-generation iRGD (CRGDK/RGPD/EC) follows a multistep tumor-targeting mechanism; it combines targeting of the αv integrins ($\alpha v\beta 3$ and $\alpha v\beta 5$) and neuropilin-1, facilitating better deeper penetration into the tumor parenchyma compared to conventional RGD peptides.[136] A multitargeted iRGD-conjugated TPLN (iRGD TPLN) was developed that delivers synergistic drugs by first penetrating the BBB and then actively targeting the TNBC cells and TAMs in microlesions of brain metastases (Figure 5d−g).[29] For efficient drug delivery into the brain metastases, both covalently bound PS 80 and iRGD were introduced for synchronized BBB penetration via LDLR-mediated and integrin-facilitated transcytosis. Additionally, the NP surface with PS 80 helped targeting TAMs that overexpress LDLR, selectively eliminating TAMs *in vitro* and *in vivo*. Meanwhile, the conjugated iRGD peptide enhanced NP

https://doi.org/10.1021/acs.molpharmaceut.2c00038
Mol. Pharmaceutics XXXX, XXX, XXX−XXX

accumulation, cellular uptake, and drug delivery to brain metastases. The smart design of iRGD TPLN allowed for triple targeting of brain endothelial cells, cancer cells, and TAMs (Figure 5d), the iRGD−DOX−MMC TPLN demonstrated superior efficacy in reducing TAMs (Figure 5e) and inhibiting metastatic burdens than nontargeted DMTPLN or a free DOX/MMC combination (Figure 5f,g).

TNBC is known for its aggressive growth, drug resistance, and high incidence of metastasis. To target multiple pathways, Zhang et al. developed a iRGD−oHA−DOX PLN system with a synergistic ratio of DOX/oHA = 1:4.[137] The intracellular release of oHA showed antimigration and anti-invasion effects via its antagonistic effects on CD44−(HA) interaction-mediated metastasis signaling pathways, especially the interaction with the receptor for hyaluronan mediated motility (RHAAM) and downregulation of the phospho-extracellular signal-regulated kinase (p-ERK). As compared to the free DOX and oHA, the iRGD−oHA−DOX PLN substantially reduced tumor burden and prevented spontaneous metastasis to the lungs and lymph nodes in a TNBC mouse model.[137]

4.2. Intracellular Cascade Delivery and Activation of Drugs by NPs. MDR cells with a rigid plasma membrane pose a tremendous challenge to drug delivery even for most nanocarriers. Zhang et al. devised a synergistic combination of ω-3 polyunsaturated fatty acid DHA and an anticancer prodrug MMC in the same PLN (DHA−MMC PLN) to exploit the intracellular biointeraction and bioreaction of DHA and MMC to overcome P-gp and lipid-raft-mediated MDR *in vitro* and *in vivo*.[62] The DHA−MMC PLN resulted in unprecedented therapeutic efficacy in EMT6/AR 1.0 breast cancer cells and an orthotopic tumor model (Figure 5h−l).[62] Initially, DHA softened rigid plasma membrane facilitating entry of DHA−MMC PLN (Figure 5h). At the second stage (intracellular), the bioactivation of MMC produced ROS that led to a chain reaction of lipid peroxidation mediated by DHA, which destroyed mitochondria (Figure 5h−j). Intravenously administered DHA−MMC−PLN inhibited tumor growth significantly (Figure 5k,l), compared to free MMC or MMC PLN combined with free DHA without generating detectable toxicity.[62]

Overexpression of a lysosomal enzyme cathepsin-B (CathB) in invasive breast cancer was exploited to produce anticancer peptide *in situ* using a CathB-degradable acetylated rapeseed protein isolate (ARPI) polymer−DOX nanocomplex.[138] The dual responsiveness of nanocomplexes to acidic pH and CathB enzymatic degradation facilitated lysosomal escape of co-delivered anticancer drug DOX. The ARPI-derived bioactivated peptides further synergized with delivered DOX to enhance *in vitro* cytotoxicity by regulating mitochondrial apoptotic proteins (tumor suppressor protein (p53), Bcl-2 (B-cell lymphoma 2) (Bcl-2), Bcl-2-associated X protein (Bax), and pro-caspase-3). Consequently, the nanocomplex demonstrated superior therapeutic efficacy compared to free DOX solution in an orthotopic TNBC model.[138]

4.3. TME-Responsive NPs to Enhance Tumor Penetration. The presence of fibrotic stroma, higher interstitial fluid pressure, and hypovascularity impedes deep tumor penetration of drugs (large molecules) and drug-loaded NPs.[30,31] Thus, receptor-mediated active transport strategies are exploited to mitigate such challenges. In this context, the presence of overexpressed enzymes in the TME was utilized as stimuli to design a polymer−drug NPs to achieve enhanced tumor penetration and efficacy.[30−32] For instance, γ-glutamyl transpeptidase (an enzyme overexpressed at the endothelial and tumor cells)-responsive camptothecin-polymer conjugate was developed to actively infiltrate through tumor cells via transcytosis.[30] Upon contact with the endothelial cells of tumor vasculature, γ-glutamyl transpeptidase interacted with the NPs and converted the neutral NPs into a cationic one which then underwent caveolae-mediated endocytosis and transcytosis, leading to both transcellular and transendothelial transport of NPs and facilitated deep tumor penetration and antitumor efficacy against orthotopic mice pancreatic cancer. Similarly, a camptothecin−polyamidoamine (PAMAM) dendrimers were developed to achieve deep tumor penetration in ductal adenocarcinoma (PDA).[31] The charge of the dendrimers were changed by enzyme from neutral to positive, which facilitated deep tumor penetration via caveolae-mediated endocytosis and vesicle mediated transcytosis. The dendrimer-gemcitabine conjugate showed enhanced antitumor activity against patient-derived PDA and orthotopic PDA cell xenograft as compared to the free gemcitabine.[31]

5. BIOREACTIVE HYBRID NPS FOR MODULATING TME AND ENHANCING CANCER THERAPIES

As illustrated in the previous section, NPs can be designed to facilitate tumor penetration and intracellular delivery of therapeutics by responding to TME biomarkers and conditions. This section will elaborate how to fabricate NPs to modulate the undesirable TME for improving conventional cancer therapies. Bioreactive NPs can modulate TME and brain microenvironment (BME) to improve drug transport to cancer cells and intracellular targets, overcome tumor resistance to therapies, increase chemotherapy and radiation efficacy in tumor tissue, and reverse immunosuppression, thereby achieving the 3Rs in a broader sense.

5.1. TME and Hypoxia-Induced Resistance to Cancer Therapies. TME consists of cancerous and noncancerous cells embedded in an ECM with a compromised vasculature.[139] The hypoxic and chronic oxidative stress of TME upregulates hypoxia inducible factor-1α (HIF-1α, a master regulator of various genes involved in cell proliferation, survival and metabolism).[74] HIF-1α is associated with tumor progression and resistance to anticancer therapies, such as chemotherapy, radiation therapy (RT) and immunotherapy.[74] By upregulating glycolytic enzymes, hypoxic cancer cells adapt to oxidative stress and acidify the TME via efflux of glycolytic metabolites, such as lactic acid.[140] Chemo-resistance in the acidic environment can be caused by the protonation of weakly basic chemotherapeutic agents, such as DOX, which inhibits their uptake.[141] Additionally, HIF-1α upregulates drug efflux pumps, further preventing efficacious accumulation of drugs.[142] Hypoxia-associated radioresistance is due to the lack of oxygen to permanently fix oxidative DNA damage, also called the oxygen fixation hypothesis.[143] This hypothesis states that oxidative DNA damage caused by direct ionization or water radical attacks are permanently fixed into an irreparable state by oxygen molecules, resulting in enhanced DNA damage such as double-strand breaks (DSBs).[144] Thus, hypoxia mediates resistance to various anticancer therapies and modulating the TME (especially hypoxia) can overcome at least some of these resistance mechanisms.

5.2. Hypoxia-Attenuation by PLMD to Enhance RT. Wu and co-workers have pioneered the novel polymer−lipid encapsulated manganese dioxide (MnO_2) NPs (PLMD) which reacts with hydrogen peroxide and protons in the TME to

https://doi.org/10.1021/acs.molpharmaceut.2c00038
Mol. Pharmaceutics XXXX, XXX, XXX−XXX

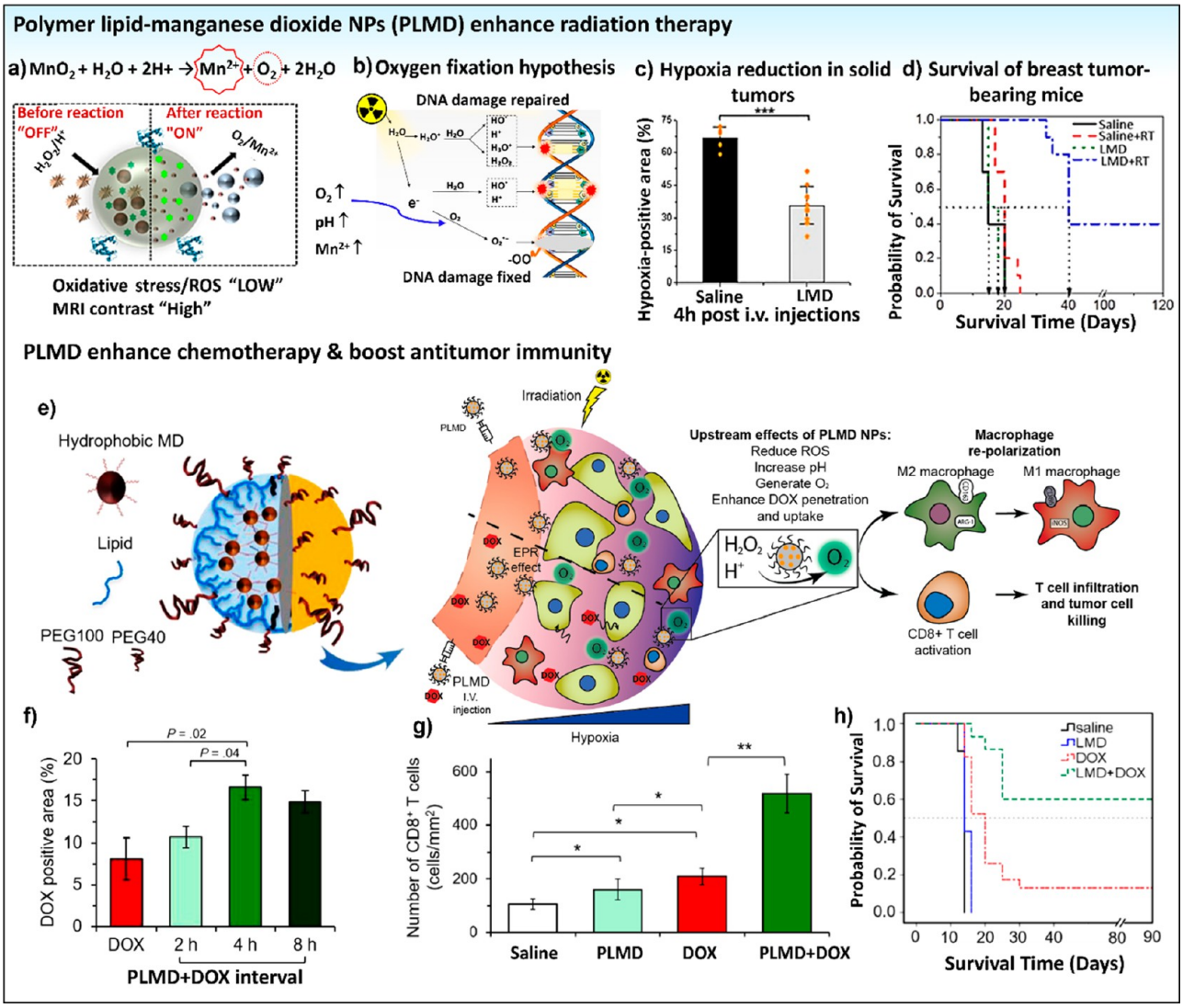

Figure 6. PLMD reacts with hydrogen peroxide to generate oxygen. (a) Reaction scheme of manganese dioxide conversion to oxygen. Adapted and reprinted in part with permission from.[145,157] Copyright 2014 American Chemical Society and 2015 WILEY-VCH Verlag GmbH & Co. KGaA. (b) The oxygen fixation hypothesis. Radiation can cause an ionization event directly on the DNA. Radiation can also indirectly damage the DNA through generation of free radical species from interactions with water molecules or macromolecules. Damaged DNA can be easily fixed in the absence of O_2. However, a peroxyl radical can form in the presence of O_2. Adapted with permission from ref 158. Copyright 2019 by the authors, Licensee MDPI, Basel, Switzerland (http://creativecommons.org/licenses/by/4.0/). (c) PLMD reduces tumor hypoxia in murine breast tumor model. (d) Kaplan−Meier survival curve of tumor-bearing mice after different RT regimen with PLMD. (e) Proposed mechanism of the PLMD +DOX combination treatment. Panels c and d are adapted and reprinted in part with permission from ref 147. Copyright 2016 American Association for Cancer Research. (f) DOX uptake in murine breast tumor model. The quantitative data obtained from the *ex vivo* fluorescence microscopic images of whole tumor tissues. The mice were treated with DOX alone or PLMD+DOX at different time intervals between PLMD and DOX treatments. For combination therapy, DOX (10 mg/kg body weight) was injected at 2, 4, and 8 h post−i.v. injection of PLMD NPs (200 μL, 1 mM MnO_2). The tumor blood vessels were stained with Alexa Flour647 anti-CD31 antibody and images were collected with an Olympus Upright microscope (Olympus, Center Valley, PA). (g) Antitumor immune cells in tumor at day 5 post-treatment. (h) Kaplan−Meier survival curve of tumor-bearing mice after different DOX regimen with PLMD. EMT6 mouse breast tumor model was treated i.v. with saline, DOX (10 mg/kg body weight), PLMD (200 μL 1 mM MnO_2 equivalent), or PLMD+DOX. The tumor growth and survival of mice was monitored up to 120 days. Panels e−h are adapted and reprinted in part with permission from ref 34. Copyright 2018 Oxford University Press.

generate oxygen molecules (examples of MnO_2 NPs are summarized in Table 1). Through this mechanism, oxidative stress, local acidosis, and hypoxia are simultaneously modified (Figure 6a,b).[145,146] The ability of PLMD to reduce tumor hypoxia and improve oxygenation rationalizes its investigation into improving RT efficacy. In murine and human orthotopic breast cancer models, PLMD achieved maximal reduction of tumor hypoxia at 4 h post-treatment (Figure 6c).[147] Using the 4 h time interval, PLMD and RT significantly improved median survival time by 2- and 1.4-fold compared to RT alone in the murine and human models, respectively (Figure 6d).[147] Additionally, 40% of the treated animals in murine model achieved complete tumor regression.[147] With the promising efficacy results, the mechanisms of PLMD enhancement were further investigated. PLMD significantly increased RT-induced DSB formation as revealed by TUNEL assay and γ-H2AX staining in tumor samples.[147] Importantly, PLMD and RT treatment significantly downregulated angiogenic markers

https://doi.org/10.1021/acs.molpharmaceut.2c00038
Mol. Pharmaceutics XXXX, XXX, XXX−XXX

vascular endothelial growth factor (VEGF) and CD31 compared to RT alone at 24 h and 5 days post-treatment, respectively.[147] Post-RT angiogenesis has been reported to promote tumor regrowth.[148] Therefore, inhibiting post-RT angiogenesis contributed to longer median survival time and in some cases, complete tumor regression. In summary, PLMD is an adjuvant therapy to increase RT efficacy.

5.3. TME-Modulation by PLMD to Enhance Chemotherapy. The capability of PLMD attenuating hypoxia and acidosis of TME was exploited to enhance chemotherapy. In an orthotopic murine breast cancer model, PLMD were able to increase tumor pH from 6.5 to 6.9 and 7.3 determined with a pH-sensitive dye and microneedle (MN) pH probe, respectively.[145] Tumor hypoxia was also significantly reduced up to 4 h as described above and in published reports.[145,147] *In vitro* experiments demonstrated that PLMD enhanced DOX uptake and cytotoxicity in murine cancer cells cultured under hypoxic conditions.[34] The translational potential of these NPs was further evaluated *in vivo*. In a murine orthotopic breast cancer model, the optimal time interval of 4 h between PLMD and DOX injection was reported to increase DOX accumulation and tumoral penetration, as measured by DOX-positive pixels on the image and the distance between DOX positivity and tumor vasculature (Figure 6f).[34] PLMD alone were also able to downregulate the expression of the TME-acidifying enzyme, carbonic anhydrase IX, and drug efflux pump, P-gp.[34] Overall, the effect of PLMD on the TME significantly improved DOX efficacy, where median survival times increased by 4.5-fold compared to DOX alone, and 60% of treated animals achieved complete tumor regression (Figure 6h).[34]

5.4. Immune Modulation by PLMD Plus Chemo-/Radiotherapy to Boost Antitumor Immunity. The hostile environment of solid tumors disrupts immune surveillance, allowing cancer cells to evade recognition and escape immune-mediated killing.[149] Hypoxia can modulate the macrophage phenotype and activity of tumor-infiltrating lymphocytes (TILs), resulting in immunosuppression and evasion of immune detection.[149] Macrophages can adopt a classical M1 phenotype or alternative M2 phenotype. The M2 phenotype in hypoxic tumors has been implicated in immunosuppression, neovascularization, metastasis, and poor responses to cancer therapies.[150] Tumor acidity can induce M2-like polarization through HIF-1α upregulation and the expression of arginase I and VEGF in macrophages.[151,152] T cells are a type of lymphocyte that develop in the thymus gland and have a central role in the adaptive immune response. After maturation, T cells differentiate into $CD4^+$ helper T cells and $CD8^+$ cytotoxic T cells. Infiltrating T cells are responsible for immune-mediated destruction of tumor cells.[153] Hypoxia-driven accumulation of metabolites, such as adenosine[154,155] and lactic acid,[156] have been demonstrated to induce T cell exhaustion, a state of T cell inactivity. Hypoxic TMEs can directly affect the tumoricidal function of $CD8^+$ T cells, leading to immunosuppression and allowing tumor cells to evade T cell-mediating killing.[149]

Thus, the ability of the PLMD in combination with DOX or RT to provide curative treatment in immunocompetent murine models was investigated for immune modulation in the TME (Figure 6e). The immunocompetent models have intact innate and adaptive immunity; therefore, the effects of the combination therapy on these areas were investigated. In preliminary studies, PLMD showed growth inhibitory effects on cancer cells cocultured with macrophages.[34] In murine orthotopic breast cancer models, PLMD and DOX increased antitumor M1 macrophages population and decreased pro-tumor M2 macrophages.[34] Correspondingly, nitric oxide (NO) produced by M1 macrophages was also increased in the tumor samples. At 5 days post-treatment, the combination treatment was able to increase T cell infiltration by 2.7-fold compared to DOX alone (Figure 6g).[34] T cells isolated from the spleen of combination-treated animals also increased cancer cell killing compared to T cells isolated from the spleen of DOX-treated animals.[34] Finally, the curative role of the adaptive immunity was demonstrated through splenocyte transfer experiments. Naïve animals receiving splenocytes from cured animals gained antitumor immunity toward the EMT6 murine cancer cells.[34] Thus, these preliminary experiments have revealed that PLMD are able to abrogate some of the immunosuppressive properties of the TME.

In the sections presented above, various NPs are discussed based on their functionality and application in mitigating the challenges of cancer therapy to achieve the goal of the 3Rs. Next, we further review the utility of stimulus-responsive nanomedicine to address the unmet need for other major chronic diseases (e.g., diabetes).

6. STIMULUS-RESPONSIVE NANOGELS AND MICROGELS FOR REGULATED DRUG DELIVERY

Stimulus-responsive nanogels and microgels have been investigated extensively for regulated drug delivery.[159] Herein, we present our recent representative research to illustrate how biocompatible polymeric nano-/microgels are designed and incorporated in various drug delivery systems for high-precision and real-time drug release. For delivering insulin at high glucose levels (hyperglycemia) or glucagon at low glucose level (hypoglycemia) at real time via subcutaneous implants and transdermal MN patches, two of the 3Rs (i.e., the *right* time and *right* dose) are the main considerations. However, precise drug release kinetics at desired segments of gastrointestinal tract can be regarded as the 3Rs.

6.1. Nanotechnology-Enabled Closed-Loop Insulin Implantable Device for Improving Diabetes Management. Diabetes mellitus (DM) is a metabolic disorder currently affecting over 460 million people worldwide,[7] projected to rise to 640 million or more in the next 20 years.[11] The cost for diabetes treatment is estimated over $300 billion USD annually in the USA alone.[160] Recent technologies, such as insulin pumps with continuous glucose monitoring (CGM), offer a safer and more convenient approach, but they are limited by the risk of infections at the catheter site, high cost, and inaccurate dosing algorithms at low blood glucose levels (BGL).[161] Ultimately, the lack of accurate dosing and convenience causes conventional strategies to fall short of fully mimicking physiological glucose regulation. To address this unmet medical need, researchers are developing novel chemically driven glucose-responsive technologies to manage diabetes more accurately and conveniently. These technologies include closed-loop insulin pump systems,[162] glucose-responsive insulin devices,[163−167] and glucose-responsive modified insulin analogues.[168,169] Some of these technologies involve the use of swellable hydrogels coupled with glucose-sensing groups to allow glucose-responsive delivery of therapeutic hormones (e.g., insulin).[170,171] Importantly, the size of the hydrogel is pivotal for accurately mimicking physiological response times with nano- or microsized hydrogels having more rapid and physiologically

https://doi.org/10.1021/acs.molpharmaceut.2c00038
Mol. Pharmaceutics XXXX, XXX, XXX−XXX

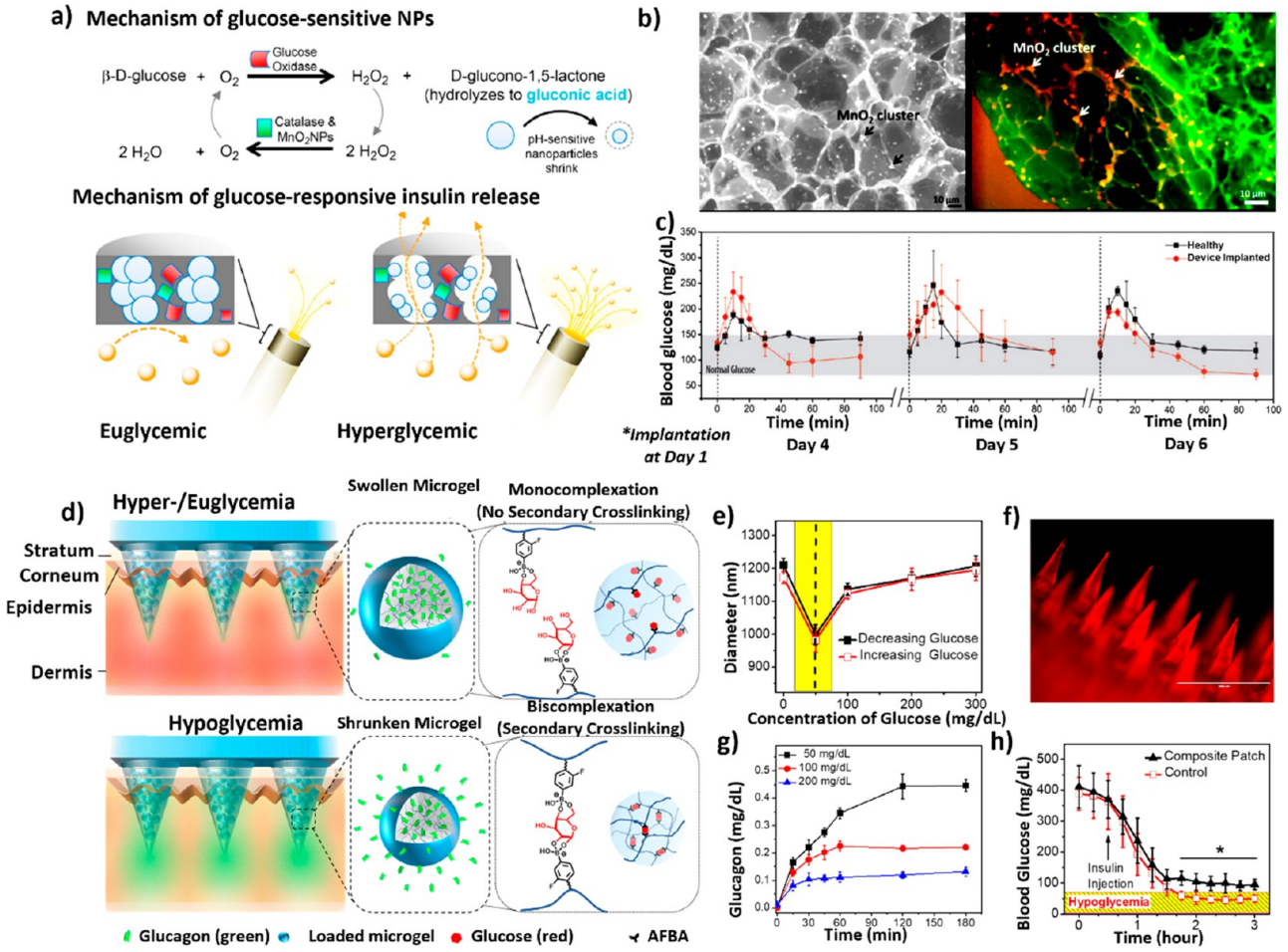

Figure 7. (a) Mechanism of glucose-responsiveness for pH-sensitive poly(NIPAM-MAA) NPs and hyperglycemia-induced insulin release from devices. Plug porosity is increased at hyperglycemic glucose levels in response to enzymatic oxidation of glucose to gluconic acid, leading to higher insulin release rates. Adapted and reprinted in part with permission from ref 163. Copyright 2015 Elsevier Ltd. (b; left) SEM image of the surface of a glucose-responsive composite membrane containing MnO_2 NPs, which were clearly visualized in the polymeric matrix due to their high contrast of electron density compared the biopolymer matrix. (b; right) Cross-sectional environmental scanning electron micrographs (ESEM) image of the composite membrane, where the base matrix shown in green and MnO_2 NPs in red and yellow. Adapted and reprinted in part with permission from ref 164. Copyright 2010 WILEY-VCH Verlag GmbH & Co. KGaA. (c) *In vivo* response of implanted diabetic rats (circles) versus healthy rats (squares) to glucose challenges on days 4, 5, and 6 after implantation. Rats were fed for 12 h in between glucose challenge cycles and fasted 1 h before glucose injection until the end of the test. Error bars represent SD (n = 3). Adapted and reprinted in part with permission from ref 166. Copyright 2015 Mary Ann Liebert, Inc. (d) Schematic of the slow glucagon release from the cMN patch during hyper-/euglycemia due to diffusion mechanism driven by swelling compared to a more rapid release during hypoglycemia driven by low glucose-induced squeezing effect. (e) DLS of microgels at varying glucose levels (critical point is shown by dashed line and hypoglycemic window is indicated by the yellow region). (f) Fluorescence microscopy image of cMN patch embedded with Rhodamine B-labeled (red) microgels (scale bar: 1000 μm). (g) *In vitro* glucose-responsive release of glucagon from microgels in various glucose media: hyperglycemic (200 mg/dL), euglycemic (100 mg/dL), or hypoglycemic (50 mg/dL). (h) Hypoglycemia prevention (efficacy) studies in T1D rats, treated with cMN patch or sham device, subjected to an overdose of insulin injection (2 IU/kg). Error bars represent SD and asterisk indicates statistical significance between groups ($p \leq 0.004$, n = 7). Panels d–h are adapted and reprinted in part with permission from ref 24. Copyright 2019 WILEY-VCH Verlag GmbH & Co. KGaA.

relevant response times for glucose-sensing and hormone delivery compared to bulk hydrogels.[14,170,172] Furthermore, there is considerable interest in developing technologies for the prevention of hypoglycemia, such as dual-hormone pump systems,[162,173] "smart" glucagon devices,[24,174] and somatostatin receptor type 2 antagonists (SSTR2A).[175−177] Our group has utilized pH-responsive nanogels and glucose-responsive microgels for self-regulated delivery of insulin or glucagon.[24,25,164,166,177−184]

An example of a nanotechnology-enabled closed-loop system for improving diabetes management was developed by Wu and co-workers. It takes the form of an implantable device comprising an enzyme/NP-coupled composite membrane for glucose-responsive delivery of insulin.[163−167] This system demonstrated a rapid response, capable of releasing insulin and reducing BGL ∼30 min after a glucose challenge *in vivo*.[163,166] The glucose-responsive composite membrane consisted of GOX, catalase (CAT), manganese dioxide NPs (MnO_2 NPs), and pH-responsive poly(*N*-isopropylacrylamide-*co*-methyl acrylic acid) NPs (PNIPAm-MAA NPs)[185] cross-linked within a matrix of bovine serum albumin (Figure 7a). GOX is an enzyme that binds specifically to glucose, and in the presence of oxygen (O_2), converts glucose into gluconic acid and H_2O_2. Catalase is an enzyme that catalyzes H_2O_2 decomposition, and MnO_2 NPs (Figure 7b) convert H_2O_2 to O_2,[164,165] both mitigating the problem of oxygen limitation in

https://doi.org/10.1021/acs.molpharmaceut.2c00038
Mol. Pharmaceutics XXXX, XXX, XXX−XXX

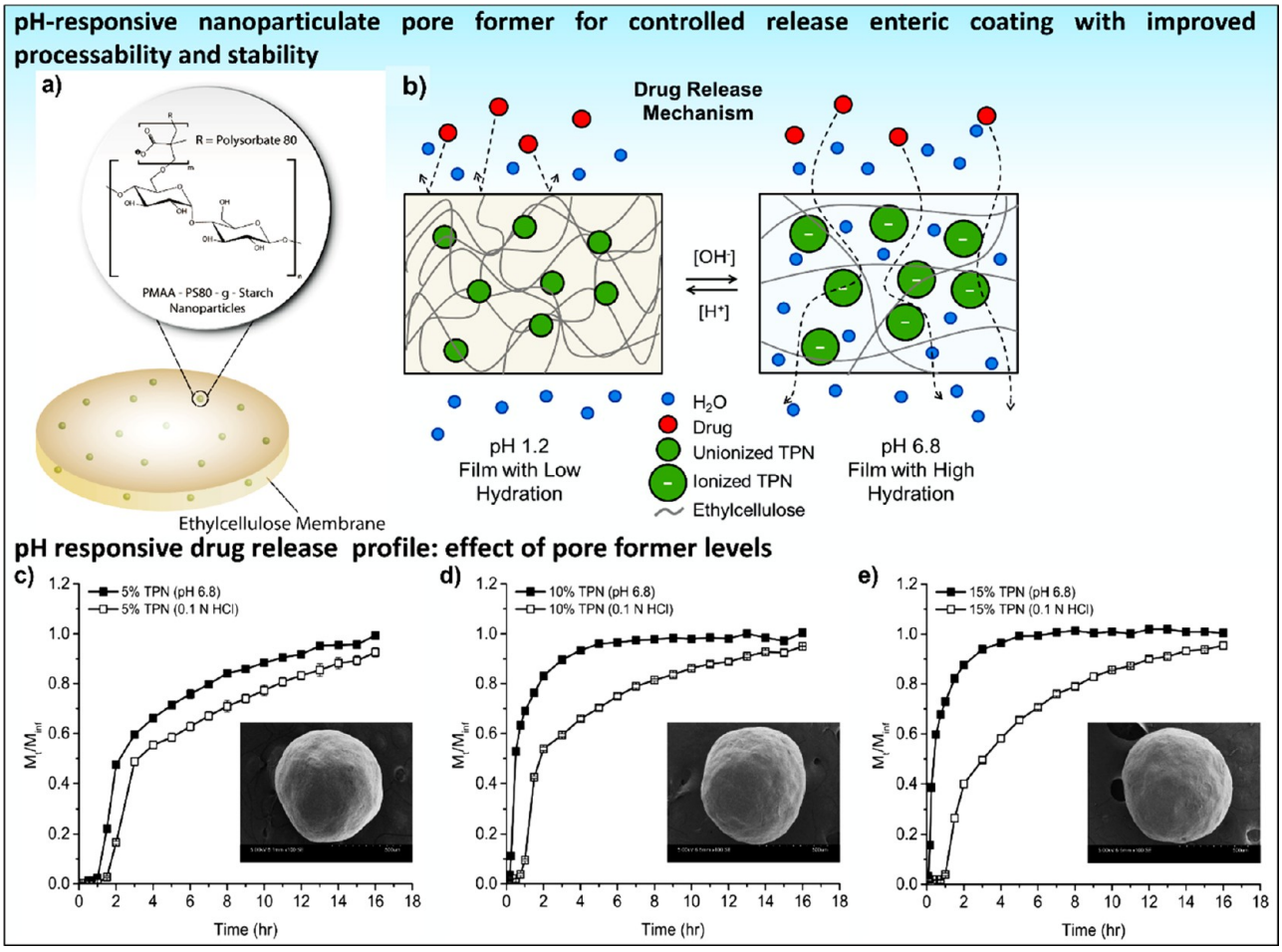

Figure 8. Controlled release dosage form design. Mechanism of drug release through a terpolymer NP (TPN)-embedded ethylcellulose (EC) membrane. (a) Structure of terpolymer NP (TPN) and diagram of TPN-EC film. (b) Drug release mechanism of the TPN-EC film as a function of pH. Drug release profiles at pH 1.2 and 6.8 of TPN-EC coated diltiazem HCl layered- microcrystalline cellulose (MCC) beads with pore former levels of TPN: (c) 5%; (d) 10%; and (e) 15%. The inserts are representative scanning electron microscope (SEM) photographs of the bead surface. Adapted and reprinted in part with permission from ref 201. Copyright 2017 Elsevier B.V.

glucose oxidation and enzyme stability. The mechanism of glucose-responsive insulin release involves gluconic acid driven pore formation within the membrane embedded with percolated pH-responsive PNIPAm-MAA NPs (Figure 7a).[163−167,178,186,187] Specifically, at high BGL, the membrane becomes acidic due to the elevated conversion of glucose into gluconic acid causing the percolated pH-responsive PNIPAm-MAA NPs to collapse (due to charge neutralization),[188,189] leading to the formation of porous channels across the membrane to promote insulin release. Glucose-responsiveness was confirmed *in vivo* where the device's response to glucose challenges in T1D rats was virtually superimposable with that of healthy rats over multiple days of testing, restoring normal BGL within 20−40 min of glucose challenge (Figure 7c). This physiologically mimicking response is attributable to the small size of the PNIPAm-MAA NPs (~150−300 nm) allowing for rapid shrinking/swelling.[14,165] Moreover, the matrix of the bioinorganic membrane provided a basal release of insulin throughout the implant period, which is comparable to long-acting insulin used in conventional pharmacotherapy. More recently, surface polyethylene glycol (PEG), PEGylation,[166] a microporous polydimethylsiloxane (PDMS) outer membrane,[163] and a month-long thermostable insulin F-127 gel formulation[183] were implemented to improve device biocompatibility and functional longevity. In summary, the closed-loop implantable insulin delivery technology highlights the potential of nanotechnology-enabled glucose-responsive systems for tighter glycemic control in people with T1D.

6.2. Glucose-Responsive Microgel-Containing Composite Microneedle Patch for Fully Autonomous Prevention of Hypoglycemia. An often-overlooked area of concern with diabetes management is hypoglycemia (low BGL, ≤70 mg/dL); it is the most serious acute complication associated with intensive insulin therapy and can lead to seizures, unconsciousness, and death.[181,182,190,191] The only treatments available for severe hypoglycemia are emergency glucagon kits and a nasal spray powder.[192] However, the use of glucagon can be challenging as it is highly unstable.[193] Furthermore, emergency kits require patients to recognize the signs of hypoglycemia, and this is not always possible as an estimated 20% of individuals with T1D suffer from hypoglycemia unawareness or asymptomatic hypoglycemia.[194] Thus, there is a clear demand for more effective solutions to address this largely unmet medical need. Recently, transdermal delivery via MNs has emerged as an attractive delivery platform due to its ease of self-administration, painlessness, and ability to deliver biomolecules transcutaneously.[195−199]

https://doi.org/10.1021/acs.molpharmaceut.2c00038
Mol. Pharmaceutics XXXX, XXX, XXX−XXX

A "smart" composite MN (cMN) patch capable of delivering native glucagon in response to hypoglycemia was recently reported by the Wu group.[24,25] The system was composed of photopolymerized methacrylated HA (MeHA) embedded with novel glucagon-loaded glucose-responsive microgels synthesized by dispersion polymerization of zwitterionic comonomers with a phenylboronic acid (PBA)-derivative comonomer, 4-acrylamido-3-fluorophenylboronic acid (AFBA).[24] Zwitterionic comonomers stabilized the peptide hormone and release was triggered at hypoglycemia-induced by the squeezing of the microgels due to secondary cross-linking formation (biscomplexation) between AFBA residues and glucose molecules (Figure 7d). To achieve a system with linear and rapid glucose-responsiveness, various microgel compositions were investigated. Microgels containing 15 mol % AFBA provided desirable volumetric responses with maximum shrinking at hypoglycemic glucose levels (Figure 7e). The microgels were combined with the MeHA and cast into MN molds to produce a cMN patch featuring 800 μm pyramidal, sharp tips (Figure 7f). The microgels (and cMN) demonstrated a glucose-concentration-dependent glucagon delivery profile, with higher release at hypoglycemia compared to eu-/hyperglycemia (Figure 7g). In response to an insulin overdose challenge in a T1D rat model, the "smart" cMN patch effectively restored counter-regulation and prevented hypoglycemia (Figure 7h). A related development was also reported by the same group demonstrating the innate ability of the glucose-responsive microgel to regulate BGL via subcutaneous depot injection.[184] Even more recently, the Wu group successfully designed an MN for the delivery of an SSTR2A (PRL-2903) to prevent insulin-induced hypoglycemia *in vivo*.[177] The development of these technologies aims to address the potential life-threatening complication of hypoglycemia associated with intensive insulin therapy that is largely an unsolved problem for people with insulin-dependent diabetes. Taken together, these nanotechnology-enabled approaches can be useful for the design of stimuli-responsive technologies with physiologically relevant features, such as glucose-responsive hormone delivery devices and MNs for management of diabetic complications.

6.3. Stimuli-Responsive NPs for Controlled Drug Release. Owing to the submicrometer dimension, NP hydrogels have been applied to regulate drug release in rapid response to external stimuli (i.e., magnetic force, light, and ultrasound) or specific internal stimuli such as pH or temperature.[200] Chen et al. has introduced pH-sensitive poly(MAA-*g*-starch-PS80) terpolymer NPs as a new pore former to a pharmaceutical coating material, ethylcellulose (EC), and achieved pH-dependent release of the antihypertensive drug diltiazem HCl (Figure 8). The terpolymer NPs incorporated in the EC membrane ionized at a higher pH, forming water pores that allowed faster drug release. Higher contents of terpolymer reduced drug release in a low-pH environment, leading to pH-responsive drug release from the coated beads.[201]

7. COMPUTATIONAL ANALYSES FOR THE RATIONAL DESIGN OF DDSS

Computational analyses have found important applications for optimizing the design of DDSs with desired properties, release profiles, and bioactivity of loaded therapeutics to achieve the goal of the 3Rs. Molecular dynamics (MD) simulation has been implemented for rational selection of polymeric materials to stabilize biomacromolecular therapeutics.[177,183] Various mathematical methods, including thermodynamic modeling,[202] ANN,[203,204] factorial DOE,[109] and empirical regression[205,206] have been applied to optimize the composition of drug carriers for given drug candidates to maximize drug loading, optimize drug release profile, and increase drug efficacy. mechanistic modeling, numerical analysis,

Numerical analysis of controlled drug release can be processed based on two different types of mathematical models: (1) mechanistic models and (2) statistical models. The mechanistic modeling requires a clear understanding of the release mechanism, the structure of DDS, the material properties, and well-defined initial and boundary conditions. Once the model parameters are validated by experimental results, mechanistic model based numerical analysis can aid the design and optimization of the given DDS. In contrast, statistical model based numerical analysis does not need a well-defined mechanism and system, but it requires a large set of experimental data to build correlations between the input and output.[205] Several examples are presented below to illustrate how different mathematical methods can be utilized to predict and optimize microparticle/NP DDS.

In a study of formulation factors on the bioactivity and anticancer efficacy of a glucose oxidase encapsulated chitosan−alginate MS (GOX−MS), a mathematical model was developed to describe the release kinetics of H_2O_2 produced by enzymatic oxidation of glucose inside the MS. This model included simultaneous diffusion of reactants (oxygen and glucose), products (H_2O_2 and gluconic acid), and enzymatic reaction. In the model, the effect of pH decrease due to production of gluconic acid on the solute diffusivity inside MS hydrogel was computed spatiotemporally based on the internal pH, Donnan equilibrium, and MS swelling profiles. The numerical analysis successfully predicted the influence of formulations factors (e.g., GOX loading and particle size) and external conditions (e.g., glucose concentration) on the release of H_2O_2.[66]

Abdekhodaie and Wu established a mathematical model for coupled diffusion and ion exchange process with inclusion of external counterion concentration.[207] The numerical results, first confirmed with experimental data, predicted the kinetics of cationic verapamil HCl released from a sulfopropyl dextran based ion-exchange MS as a function of initial drug loading, MS loading capacity, and counterion concentration.[207] This was the first report on the counterion in the release medium as a rate limiting factor. A similar approach was applied to a study by Chen et al. on membranes containing different ratios of Eudragit RS and RL enteric coatings, with statistical modeling of experimental data and acknowledgment of known drug loading mechanisms of polymer membranes.[208]

In the above examples and other studies of complex DDSs, variable boundary conditions, space- and time-dependent parameters, and multiple release mechanisms, numerical methods, such as FEM and finite difference method based computer programs are required to solve the governing equations of the mathematical models.[209−217] For instance, FEM-based computer simulations were carried out to study the release kinetics in relation with different polymeric matrix compositions,[210] 3D anisotropic shapes,[211] matrix DDSs with variable size and concentration distributions with drug loading higher than its drug solubility,[212,213] or even for moving boundary conditions from changes in fluid viscosity, solute drug accumulation, or progressive tablet erosion.[214−217] To analyze the influence of drug accumulation in a finite release

https://doi.org/10.1021/acs.molpharmaceut.2c00038
Mol. Pharmaceutics XXXX, XXX, XXX−XXX

medium, Zhou and Wu predicted the release kinetics of the antiviral drug azidothmidine (AZT) from preswollen poly(methyl methacrylate-*co*-methacrylic acid) MS in a monolayer or multilayer using FEM.[213] In another study, Huang et al. modeled a biphasic release profile of AZT from a composite matrix DDS containing pH-responsive MS sandwiched between two layers of a pH-insensitive polymer in a release medium that mimicked the condition in a GI tract.[217,218]

Although mechanistic model based numerical analysis can provide more insights into direct correlation between independent and dependent variables, it is difficult to make predictions for complex systems involving multiple variables and unclear mechanistic relationships. In these cases, other numerical methods are needed to extract possible correlation from empirical data. In one example, for determining actual kinetic profiles of drug release from NP or MS, a numerical deconvolution method was used to extract the information from the release profiles of free drug solution and NP/MS encased in a dialysis bag.[219] These models can, therefore, be used to forecast future output responses through robust estimation of residual error and subsequent curve-fitting of data, even if not all underlying principles are fully elucidated or understood. However, statistical models generally require a very large volume of data and can become labor-intensive to construct, though what construes a "suitable" quantity of data is debatable.

Many disciplines utilize the coveted DOE in some fashion.[109] Factorial designs, a type of DOE, which construct multivariate linear regressions with experimental observations in relation to multiple equidistantly coded factors. This provides information on correlations between not only one response and its factors but also the interaction among the factors being studied to eradicate any spurious correlations that would have been obscured in one-factor-at-a-time (OFAT) experiments. For relationships not adequately described with linear functions, response surface methodologies (RSM) can be used to augment these factorial designs by simply adding a few more data points at calculated input variables to construct quadratic regression models.[220] For example, Li et al. constructed a 2^3 composite response surface model by studying the effect of drug-to-lipid ratios, Tween 80 content, and Pluronic F68 content on drug-loading efficiency and mean particle size in a verapamil-loaded PLN, with experimental confirmation of a predicted optimized formulation.[203] For progressively complex DDS, a "living" model such as ANN can provide an empirical computational model capable of making robust predictions based on defined inputs. For instance, in the same study by Li et al. mentioned previously, ANNs were fitted with 2 hidden nodes for drug loading efficiency and three nodes for mean particle size to predict values that were similar to the values determined through RSM.[203] Likewise, in another system, the same authors predicted drug release kinetics of DOX from a sulfopropyl dextran-based ion-exchange MS by constructing four independent models for four different time points. This study predicted quantitatively the influence of drug loading level, concentration and valence of electrolytes in the release medium, the fractional release profiles of DOX with computational extendibility for future data.[204]

8. SUMMARY

This review discusses how multidisciplinary strategies are developed and exploited to design advanced nanomedicines and nanotechnology-enabled intelligent DDS using examples from our firsthand experience. The works highlight key innovative approaches to achieving the 3Rs of drug delivery which are integral parts for addressing today's ever-growing unmet medical needs. The multidisciplinary approaches include: (1) molecular pharmacology-based selection of new synergistic drug−drug or drug-nanomaterial combinations and codelivery by nanocarriers to (intra)cellular targets for overcoming multiple drug resistance mechanisms in cancer cells and reducing cancer metastasis; (2) harnessing nanomaterial−biology interplay to prepare BBB-penetrating smart nanoplatform for imaging and treating brain tumor/metastasis and CNS diseases; (3) design of multitargeted NPs able to target multiple intratumoral cell populations (e.g., cancer cells and tumor vessel endothelial cells that overexpress integrin receptors) and TAM that overexpress LDLR; (4) exploiting differential water-solubility of polymer and lipid to formulate transformable PLN for enhancing tumor penetration, cascade drug delivery, and enabling FABP-mediated intracellular transport; (5) engineering bioreactive hybrid MDNPs to modulate TME and BME for enhancing cancer therapies and MRI; (6) utilizing stimulus-responsive polymeric materials and nanotechnology for self-regulated drug delivery on demand in real-time; and (7) applying mathematical modeling and computational analysis to design and optimize novel controlled drug delivery systems for high precision drug delivery to improve therapeutic efficacy and safety. Our examples and other groups' studies demonstrated that these approaches can be employed rationally to mitigate the challenges of macro-/microscopic and cellular level barriers thereby providing precise drug delivery spatiotemporally.

8.1. Future Perspectives. In general, nanomedicines and nanotechnology-incorporated DDS can be designed to alter the PK, pharmacodynamics, and toxicity profiles of the delivered therapeutics toward higher treatment benefits. However, to successfully develop effective and safe medication for clinical use, a thorough understanding of the specific roles and potential bioactivities of components of the nanocarrier is critical. Use of materials generally regarded as safe (GRAS) is an essential consideration for easy approval by the healthcare regulatory authorities. For this reason, widely used pharmaceutical excipients and their rational combinations are of advantageous for manufacturing the NPs. Nonetheless, GRAS ingredients may produce positive or negative pharmacological effects under disease conditions and/or in the presence of active ingredients. Depending on the spatiotemporal occurrence, pharmaceutically inactive ingredients may be utilized to synergize with anticancer agents, like the DHA−MMC or oHA−DOX presented in this review, or generating unwanted adverse side effects.[221]

In addition, the acute toxicity of the NP components needs to be studied thoroughly, which is required for developing nanomedicine. The most important aspect of clinical phase I studies is the safety of the formulations. If the preclinical studies on animal models do not include a focus on evaluating such toxicities, then the clinical application of such nanoformulations will be substantially hindered. Another barrier to the translation of nanoformulations from "bench to bedside" is the complex structure and use of numerous components (e.g., multitargeting ligands, multiple lipids, polymers, and drugs), which makes it difficult to reproduce and scale-up some types of NPs.

Over the last 30 years, substantial progress has been made in the approval of new nanomedicines by both the US Food and

https://doi.org/10.1021/acs.molpharmaceut.2c00038
Mol. Pharmaceutics XXXX, XXX, XXX−XXX

Table 4. Partial List of Recent Clinical Trials (Updated since 2019) of Different NPs for Treating Breast Cancer and Brain Cancer[a]

particle type	therapeutic agent	application/indication	ClinicalTrials.gov identifiers (phase)	status
Different NP-Based Formulations for Treating Breast Cancer				
topical fluorescent NPs-conjugated somatostatin analog	quantum dots coated with veldoreotide	breast cancer, skin cancer, skin diseases	NCT04138342 recruitment status: recruiting first posted: October 24, 2019 last update posted: October 24, 2019 sponsor: Al-Azhar University	phase 1
NP albumin-bound (NAB)-paclitaxel and carboplatin with combination of other drugs	chemotherapeutic agent: paclitaxel and carboplatin; epirubicin in combination with cyclophosphamide as neoadjuvant chemotherapy	TNBC	NCT03799679 recruitment status: unknown verified January 2019 by Zhimin Shao, Fudan University. recruitment status was: recruiting first posted: January 10, 2019 last update posted: January 10, 2019 sponsor: Fudan University	phase 4
paclitaxel albumin-stabilized NP formulation	paclitaxel	metastatic breast cancer	NCT00609791 recruitment status: active, not recruiting first posted: February 7, 2008 last update posted: March 18, 2022 sponsor: City of Hope Medical Center	phase 2
albumin-bound paclitaxel combined with carboplatin	paclitaxel and carboplatin combined with carboplatin as neoadjuvant chemotherapy	luminal B/HER-2 negative breast cancer	NCT03799692 recruitment status: unknown verified January 2019 by Zhimin Shao, Fudan University. recruitment status was: recruiting first posted: January 10, 2019 last update posted: January 10, 2019	phase 4
carbon NP	carbon NP suspension injection to be injected into or around the cortex of the clinically assessed positive lymph nodes	location and biopsy of axillary lymph nodes	NCT04482803 recruitment status: recruiting first posted: July 23, 2020 last update posted: March 10, 2022 sponsor: Fudan University	not applicable
NAB-paclitaxel/cyclophosphamide	paclitaxel, cyclophosphamide, trastuzumab	early-stage breast cancer	NCT00629499 recruitment status: completed first posted: March 6, 2008 results first posted: December 20, 2012 last update posted: November 24, 2021 sponsor: SCRI Development Innovations, LLC	phase 2
albumin-stabilized NP formulation along with combination of other drugs	pertuzumab, trastuzumab, paclitaxel albumin-stabilized NP formulation	HER2-positive breast cancer, recurrent breast cancer stage IIA or IIB, breast cancer stage IIIA or IIIB, breast cancer stage IIIC or IV, adenocarcinoma inflammatory	NCT01730833 recruitment status: active, not recruiting first posted: November 21, 2012 last update posted: March 18, 2022 sponsor: City of Hope Medical Center	phase 2
NAB-paclitaxel	NAB-paclitaxel, phenelzine sulfate	metastatic or advanced breast cancer	NCT03505528 recruitment status: completed	phase 1

https://doi.org/10.1021/acs.molpharmaceut.2c00038
Mol. Pharmaceutics XXXX, XXX, XXX−XXX

Table 4. continued

particle type	therapeutic agent	application/indication	ClinicalTrials.gov identifiers (phase)	status
Different NP-Based Formulations for Treating Breast Cancer				
paclitaxel albumin-stabilized NP formulation in combination with other regimens	carboplatin, paclitaxel albumin-stabilized NP formulation, vorinostat, placebo	newly diagnosed operable breast cancer	first posted: April 23, 2018 last update posted: November 13, 2019 sponsor: EpiAxis Therapeutics NCT00616967 recruitment status: active, not recruiting first posted: February 15, 2008 results first posted: July 16, 2014 last update posted: February 3, 2022 sponsor: Sidney Kimmel Comprehensive Cancer Center at Johns Hopkins NCT01525966	phase 2
carboplatin and paclitaxel albumin-stabilized NP formulation	carboplatin, paclitaxel albumin-stabilized NP formulation	inflammatory breast cancer stage IIA; breast cancer stage IIIA; breast cancer stage IIIB, IIIC, or IIB; breast cancer triple-negative; breast cancer estrogen receptor negative, progesterone receptor negative, HER2/Neu negative	recruitment status: active, not recruiting first posted: February 3, 2012 last update posted: July 13, 2021 sponsor: City of Hope Medical Center NCT00785291	phase 2
paclitaxel albumin-stabilized NP formulation (NAB-paclitaxel) along with combination of other therapeutic agents.	bevacizumab, ixabepilone, NAB-paclitaxel, paclitaxel	estrogen receptor negative, estrogen receptor positive, HER2/Neu negative, HER2/Neu positive, progesterone receptor negative, progesterone receptor positive, recurrent breast carcinoma stage IIIC, breast cancer AJCC v6, stage IV breast cancer AJCC v6 and v7	recruitment status: active, not recruiting first posted: November 5, 2008 results first posted: July 2, 2015 last update posted: March 2, 2022 sponsor: National Cancer Institute (NCI) NCT00093145	phase 3
albumin-bound NP paclitaxel (ABI-007)	paclitaxel, carboplatin, herceptin	advanced breast cancer	recruitment status: completed first posted: October 5, 2004 results first posted: July 17, 2013 last update posted: November 25, 2019 sponsor: Celgene NCT02788981	phase 2
NAB-paclitaxel (abraxane)	mifepristone, placebo, NAB-paclitaxel	TNBC	recruitment status: active, not recruiting first posted: June 2, 2016 last update posted: March 16, 2022 sponsor: University of Chicago NCT00331630	phase 2
paclitaxel albumin-stabilized NP formulation	lapatinib ditosylate, paclitaxel	stage I, II, or III breast cancer	recruitment status: completed first posted: May 31, 2006 results first posted: March 6, 2020 last update posted: March 6, 2020 sponsor: Northwestern University NCT00709761	early phase 1
NAB-Paclitaxel (or ABRAXANE)	lapatinib/NAB-paclitaxel	HER2+ metastatic breast cancer	recruitment status: completed first posted: July 3, 2008 results first posted: November 22, 2011 last update posted: March 26, 2019	phase 2

https://doi.org/10.1021/acs.molpharmaceut.2c00038
Mol. Pharmaceutics XXXX, XXX, XXX−XXX

Table 4. continued

particle type	therapeutic agent	application/indication	ClinicalTrials.gov identifiers (phase)	status
Different NP-Based Formulations for Treating Breast Cancer				
carboplatin and paclitaxel albumin-stabilized NP formulation along with other therapeutic agents.	carboplatin; paclitaxel; bevacizumab; trastuzumab; magnetic resonance imaging and therapeutic conventional surgery	breast cancer HER2-negative, breast cancer HER2-positive, recurrent breast cancer breast cancer stages IA, IB, II, IIIA, IIIB, and IIIC	sponsor: Novartis Pharmaceuticals NCT00618657 recruitment status: active, not recruiting first posted: February 20, 2008 last update posted: April 19, 2021	phase 2
paclitaxel-incorporating micellar NP	NK105 and paclitaxel	breast cancer nonmetastatic recurrent	sponsor: University of California, Irvine NCT01644890 recruitment status: completed first posted: July 19, 2012 results first posted: July 29, 2019 last update posted: July 29, 2019	phase 3
NAB-paclitaxel along with other therapeutic agents	pembrolizumab, NAB-paclitaxel, epirubicin, cyclophosphamide	TNBC, malignant neoplasm of breast	sponsor: Nippon Kayaku Co., Ltd. NCT03289819 recruitment status: completed first posted: September 21, 2017 last update posted: April 8, 2021	phase 2
NAB-rapamycin	rapamycin; other: quality-of-life assessment, and laboratory biomarker assessment	patients with advanced cancer with mechanistic target of rapamycin (mTOR) mutations	sponsor: Institut fuer Frauengesundheit NCT02646319 recruitment status: completed first posted: January 5, 2016 last update posted: June 6, 2019	early phase 1
albumin-bound paclitaxel NP and other combination therapy	NAB-paclitaxel + carboplatin; paclitaxel + carboplatin	TNBC	sponsor: Mayo Clinic NCT04137653 recruitment status: recruiting first posted: October 24, 2019 last update posted: July 20, 2021	phase 3
NP-based paclitaxel with solvent-based paclitaxel	paclitaxel	early breast cancer: tubular breast cancer stage II; mucinous breast cancer stage II; breast cancer female NOS; invasive ductal breast cancer; tubular breast cancer stage III; HER-2 positive breast cancer; inflammatory breast cancer stage IV; inflammatory breast cancer	sponsor: Shengjing Hospital NCT01583426 recruitment status: completed first posted: April 24, 2012 last update posted: August 6, 2020	phase 3
NAB-paclitaxel (NAB-pac, abraxane) for stomach, pancreas, breast, and ovarian cancer (PIPAC−NAB−pac)	PIPAC with abraxane	peritoneal carcinomatosis, ovarian cancer stages IIIB, IIIC, and IV; breast cancer stages IIIB, IIIc, and IV; stomach cancer stage III, IV-metastases; pancreas cancer, stages III and IV	sponsor: German Breast Group NCT03304210 recruitment status: completed first posted: October 6, 2017 last update posted: August 4, 2020	phase 1
NAB-paclitaxel (abraxane)	NAB-paclitaxel	locally advanced or metastatic breast cancer	sponsor: University Hospital, Ghent NCT01463072 recruitment status: active, not recruiting first posted: November 1, 2011 last update posted: August 16, 2021 sponsor: City of Hope Medical Center	phase 2

https://doi.org/10.1021/acs.molpharmaceut.2c00038
Mol. Pharmaceutics XXXX, XXX, XXX−XXX

Table 4. continued

particle type	therapeutic agent	application/indication	ClinicalTrials.gov identifiers (phase)	status
Different NP-Based Formulations for Treating Breast Cancer				
NAB-paclitaxel with combination of other therapeutic agents	etrumadenant (AB928) IPI-549, PEGylated liposomal DOX (PLD), paclitaxel	TNBC, ovarian cancer	NCT03719326 recruitment status: completed first posted: October 25, 2018 last update posted: April 7, 2022 sponsor: Arcus Biosciences, Inc.	phase 1
NAB-taxane, NAB-paclitaxel (abraxane)	NAB-paclitaxel	metastatic breast cancer	NCT01746225 recruitment status: active, not recruiting first posted: December 10, 2012 results first posted: March 27, 2020 last update posted: March 2, 2021 sponsor: International breast cancer Study Group	phase 2
mRNA-2752, a lipid NP encapsulating mRNAs encoding human OX40L, IL-23, and IL-36γ	mRNA-2752, durvalumab	dose escalation: relapsed/refractory solid tumor malignancies or lymphoma dose expansion: TNBC, HNSCC, non-Hodgkins, urothelial cancer, immune checkpoint refractory melanoma, and non-small-cell lung cancer (NSCLC) lymphoma	NCT03739931 recruitment status: recruiting first posted: November 14, 2018 last update posted: March 11, 2022 sponsor: ModernaTX, Inc.	phase 1
superparamagnetic iron oxide (SPIO) NPs	diagnostic test: delayed SLND; diagnostic test: late SLND	ductal cancer *in situ* of the breast (DCIS), breast cancer, breast neoplasms, sentinel lymph node	NCT04722692 recruitment status: recruiting first posted: January 25, 2021 last update posted: March 29, 2022 sponsor: Uppsala University	phase 3
neoadjuvant treatment	DOX, cyclophosphamide, carboplatin, albumin-stabilized NP formulation of paclitaxel, NAB-paclitaxel, GM-CSF, trastuzumab and bevacizumab	large or inflammatory breast cancer	NCT00254592 recruitment status: completed first posted: November 16, 2005 results first posted: November 11, 2013 last update posted: February 28, 2019 sponsor: University of California, Irvine	phase 2
albumin-stabilized NP paclitaxel along with another drug	alpelisib, NAB-paclitaxel	anthracycline refractory TNBC with PIK3CA or PTEN alterations	NCT04216472 recruitment status: unknown verified February 2020 by M.D. Anderson Cancer Center. recruitment status was: recruiting first posted: January 2, 2020 last update posted: February 13, 2020 sponsor: M.D. Anderson Cancer Center	phase 2
combination therapy	IPI-549 (eganelisib), atezolizumab, NAB-paclitaxel, bevacizumab,	TNBC, renal cell carcinoma	NCT03961698 recruitment status: active, not recruiting first posted: May 23, 2019 last update posted: April 4, 2022 sponsor: Infinity Pharmaceuticals, Inc.	phase 2
albumin-stabilized nanoparticle paclitaxel with another drug	atezolizumab, NAB-paclitaxel	breast adenocarcinoma, invasive breast carcinoma, TNBC	NCT02530489 recruitment status: active, not recruiting first posted: August 21, 2015	phase 2

https://doi.org/10.1021/acs.molpharmaceut.2c00038
Mol. Pharmaceutics XXXX, XXX, XXX−XXX

Table 4. continued

particle type	therapeutic agent	application/indication	ClinicalTrials.gov identifiers (phase)	status
Different NP-Based Formulations for Treating Breast Cancer				
ELU001 (drug-conjugate)	ELU001	patients with advanced, recurrent, or refractory folate receptor alpha (FRα)-overexpressing tumors	last update posted: April 8, 2021 sponsor: M.D. Anderson Cancer Center NCT05001282 recruitment status: recruiting first posted: August 11, 2021 last update posted: March 22, 2022 sponsor: Elucida Oncology	phase 1 phase 2
combination therapy	docetaxel, lumpectomy, mastectomy, NAB-paclitaxel, paclitaxel, pertuzumab, radiation therapy, trastuzumab, emtansine	breast cancer patients after presurgery chemo and targeted therapy	NCT04266249 recruitment status: recruiting first posted: February 12, 2020 last update posted: January 11, 2022 sponsor: ECOG-ACRIN Cancer Research Group	phase 2
combination therapy	atezolizumab, cabozantinib *S*-malate, NAB-paclitaxel, tumor-treating Fields therapy	advanced/metastatic solid tumors involving the abdomen or thorax	NCT05092373 recruitment status: not yet recruiting first posted: October 25, 2021 last update posted: March 21, 2022 sponsor: M.D. Anderson Cancer Center	phase 1
9-ING-41, a glycogen synthase kinase-3 beta (GSK-3γ) inhibitor along with other therapeutic agents	9-ING-41, gemcitabine (21 day cycle), DOX, lomustine, carboplatin, NAB-paclitaxel, paclitaxel, gemcitabine (28 day cycle), irinotecan	patients with refractory hematologic malignancies or solid tumors	NCT03678883 recruitment status: recruiting first posted: September 20, 2018 last update posted: February 17, 2022 sponsor: Actuate Therapeutics Inc.	phase 1, phase 2
combination therapy	carboplatin, durvalumab, gemcitabine hydrochloride, NAB-paclitaxel, personalized synthetic long peptide vaccine, poly ICLC, tremelimumab	patients with metastatic TNBC, anatomic stage IV-breast cancer AJCC v8, invasive breast carcinoma, metastatic triple-negative breast carcinoma, prognostic stage IV breast cancer AJCC v8	NCT03606967 recruitment status: recruiting first posted: July 31, 2018 last update posted: March 8, 2022 sponsor: National Cancer Institute (NCI)	phase 2
serial measurements of molecular and architectural responses to therapy (SMMART) adaptive clinical treatment (ACT) trial	19 different small molecule drugs including NAB-paclitaxel and 4 different biologics; quality-of-life assessment	metastatic or locally advanced solid tumors	NCT05238831 recruitment status: not yet recruiting first posted: February 14, 2022 last update posted: February 25, 2022 sponsor: OHSU Knight Cancer Institute	phase 2
SMMART PRIME trial	47 different drugs, 7 biological agents.	advanced solid tumor and hematological malignancies	NCT03878524 recruitment status: recruiting first posted: March 18, 2019 last update posted: February 17, 2022 sponsor: OHSU Knight Cancer Institute	phase 1
Nanoparticle-Based Clinical Trials for Brain Tumor Treatment				
stereotactic radiation plus activation and guidance of irradiation by X-ray (AGuIX) gadolinium-based nanoparticles	radiation: stereotactic radiation; AGuIX, gadolinium-based NPs, placebo	brain cancer, brain metastases, melanoma, lung cancer, breast cancer, HER2-positive breast cancer, colorectal cancer, gastrointestinal cancer, SRSSRT,	NCT04899908 recruitment status: recruiting	phase 2

https://doi.org/10.1021/acs.molpharmaceut.2c00038
Mol. Pharmaceutics XXXX, XXX, XXX−XXX

Table 4. continued

particle type	therapeutic agent	application/indication	ClinicalTrials.gov identifiers (phase)	status
Nanoparticle-Based Clinical Trials for Brain Tumor Treatment				
		whole brain radiation, stereotactic radiation, AGuIX, nanoparticle, cystic, brain tumor	first posted: May 25, 2021 last update posted: October 21, 2021 sponsor: Dana-Farber Cancer Institute NCT04094077	
AGuIX NPs in combination with stereotactic radiation	AGuIX	brain metastases	recruitment status: terminated (study stopped after a negative result delivered by the CPP for a substantial modification of the protocol) first posted: September 18, 2019 last update posted: June 8, 2021 sponsor: Centre Leon Berard NCT02820454	phase 2
NANO-RAD	AGuIX; radiation: whole brain radiation therapy	brain metastases	recruitment status: completed first posted: July 1, 2016 last update posted: June 7, 2019 sponsor: University Hospital, Grenoble NCT03818386	phase 1
AGuIX (NANORAD2)	AGuIX; radiation: whole brain radiation therapy	brain metastases, adult radiotherapy	recruitment status: recruiting first posted: January 28, 2019 last update posted: March 16, 2022 sponsor: University Hospital, Grenoble NCT04964960	phase 2
pembrolizumab and chemotherapy	pembrolizumab, NAB-paclitaxel, paclitaxel, pemetrexed, carboplatin	brain metastasis from NSCLC, lung cancer, lung cancer metastatic, brain cancer, cancer	recruitment status: recruiting first posted: July 16, 2021 last update posted: January 19, 2022 sponsor: John L. Villano, M.D., Ph.D. NCT04899908	phase 2
AGuIX gadolinium-based NPs	radiation: stereotactic radiation; drug: AGuIX gadolinium-based NPs; other: placebo	brain metastases, brain cancer	recruitment status: recruiting first posted: May 25, 2021 last update posted: October 21, 2021 sponsor: Dana-Farber Cancer Institute NCT04999618	phase 2
hemoblock (NPs of silver)	hemoblock, other: placebo	vascular diseases, vascular malformation, capillary malformation-arteriovenous malformation, port-wine stain, Sturge–Weber syndrome, vascular tumor	recruitment status: completed first posted: August 11, 2021 last update posted: November 4, 2021 sponsor: Center for Vascular Pathology, Moscow NCT03566199	phase 4
nanoparticle formulation MTX110 (MTX110)	panobinostat nanoparticle formulation, MTX110, convection-enhanced delivery (CED)	newly-diagnosed, diffuse intrinsic pontine glioma	recruitment status: completed first posted: June 25, 2018 results first posted: February 25, 2022 last update posted: February 25, 2022 sponsor: Sabine Mueller, M.D., Ph.D.	phase 1, phase 2

https://doi.org/10.1021/acs.molpharmaceut.2c00038
Mol. Pharmaceutics XXXX, XXX, XXX−XXX

Table 4. continued

particle type	therapeutic agent	application/indication	ClinicalTrials.gov identifiers (phase)	status
Nanoparticle-Based Clinical Trials for Brain Tumor Treatment				
MTX110 (a water-soluble panobinostat NP formulation)	infusate with MTX110 and gadolinium; device: convection-enhanced delivery (CED)	diffuse intrinsic pontine glioma, diffuse pontine and thalamic gliomas, diffuse midline glioma	NCT04264143 recruitment status: recruiting first posted: February 11, 2020 last update posted: March 10, 2022 sponsor: Luca Szalontay	phase 1
EGFR (vectibix sequence)-targeted EnGeneIC dream vectors (EDV) containing DOX (EGFR (V)−EDV−DOX)	EGFR(V)−EDV−DOX, payload-packaged EDV nanocells	glioblastoma, astrocytoma, grade IV	NCT02766699 recruitment status: unknown verified August 2019 by Engeneic Pty Limited. recruitment status was: recruiting first posted: May 10, 2016 last update posted: August 29, 2019 sponsor: Engeneic Pty Limited	phase 1
ABI-009 (NAB-rapamycin), NAB-rapamycin	ABI-009, bevacizumab, temozolomide, lomustine, marizomib, radiation: radiation	high-grade recurrent glioma and newly diagnosed glioblastoma	NCT03463265 recruitment status: active, not recruiting first posted: March 13, 2018 last update posted: June 4, 2021 sponsor: Aadi, LLC	phase 2
AGuIX NPs (polysiloxane Gd-chelates based NPs)	polysiloxane Gd-chelates based NPs (AGuIX); radiation: radiotherapy; drug: temozolomide	glioblastoma	NCT04881032 recruitment status: recruiting first posted: May 11, 2021 last update posted: December 13, 2021 sponsor: Centre Jean Perrin	phase 1, phase 2
NU-0129: a spherical nucleic acid (SNA) gold nanoparticle targeting BCL2L12	other: laboratory biomarker analysis; other: pharmacological study; drug: targeted molecular therapy	gliosarcoma, recurrent glioblastoma	NCT03020017 recruitment status: completed first posted: January 13, 2017 last update posted: October 27, 2020 sponsor: Northwestern University	early phase 1
temozolomide and SGT-53 nanocomplex (targeted P53 gene therapy (SGT-53)	genetic: SGT-53; drug: temozolomide	recurrent glioblastoma	NCT02340156 recruitment status: terminated first posted: January 16, 2015 results first posted: March 3, 2021 last update posted: March 3, 2021 sponsor: SynerGene Therapeutics, Inc.	phase 2
Lipid NPs in Clinical Trials for Anticancer Therapy				
WGI-0301: lipid nanoparticle suspension of Akt-1 antisense oligonucleotide	WGI-0301	advanced solid tumors	NCT05267899 recruitment status: not yet recruiting first posted: March 7, 2022 last update posted: March 21, 2022 sponsor: Zhejiang Haichang Biotech Co., Ltd.	phase 1
mRNA-2416, a lipid nanoparticle encapsulated mRNA encoding human OX40L	mRNA-2416, durvalumab	relapsed/refractory solid tumor malignancies or lymphoma, ovarian cancer	NCT03323398 recruitment status: active, not recruiting first posted: October 27, 2017	phase 1, phase 2

https://doi.org/10.1021/acs.molpharmaceut.2c00338
Mol. Pharmaceutics XXXX, XXX, XXX−XXX

Table 4. continued

particle type	therapeutic agent	application/indication	ClinicalTrials.gov identifiers (phase)	status
		Lipid NPs in Clinical Trials for Anticancer Therapy		
mRNA-2752, a lipid nanoparticle encapsulating mRNAs encoding human OX40L, IL-23, and IL-36γ	mRNA-2752, durvalumab	dose escalation: relapsed/refractory solid tumor malignancies or lymphoma dose expansion: TNBC, HNSCC, non-Hodgkins, urothelial cancer, immune checkpoint refractory melanoma, and NSCLC lymphoma	last update posted: December 20, 2021 sponsor: ModernaTX, Inc. NCT03739931 recruitment status: recruiting first posted: November 14, 2018 last update posted: March 11, 2022 sponsor: ModernaTX, Inc. NCT05062980	phase 1
reqorsa (quaratusugene ozeplasmid, formerly known as GPX-001): comprises nonviral lipid NPs which encapsulate a DNA plasmid with the TUSC2 tumor suppressor gene	quaratusugene, ozeplasmid, pembrolizumab, docetaxel, and ramucirumab	NSCLC	recruitment status: not yet recruiting first posted: September 30, 2021 last update posted: March 3, 2022 sponsor: Genprex, Inc. NCT04675996	phase 1 phase 2
INT-1B3	INT-1B3: lipid-nanoparticle-formulated microRNA (miR-193a-3p)	advanced solid tumors	recruitment status: recruiting first posted: December 19, 2020 last update posted: February 7, 2022 sponsor: InteRNA NCT04486833	phase 1
reqorsa (quaratusugene ozeplasmid, formerly known as GPX-001)	biological: quaratusugene, ozeplasmid, and osimertinib	carcinoma, NSCLC	recruitment status: recruiting first posted: July 27, 2020 last update posted: April 8, 2022 sponsor: Genprex, Inc.	phase 2

[a]Information obtained from https://clinicaltrials.gov/ct2/home (accessed on April 12, 2022).

https://doi.org/10.1021/acs.molpharmaceut.2c00338
Mol. Pharmaceutics XXXX, XXX, XXX−XXX

Drug Administration (FDA) and the European Medicines Agency (EMA). Up to date, there are about 100 approved nanomedicines[115,222] and ∼663 nanomedicine-including clinical trials of various stages.[115] The approved and ongoing nanomedicines in clinical trials are extensively reviewed elsewhere.[115,222−225] As showcased in a partial list of recent clinical trials (Table 4), combination therapy has gained an increasing momentum in clinical translation. For the treatment of breast cancer, most studies are focused on using paclitaxel or its NPs formulation (Abraxane) in combination with other biologics and small-molecule cancer drugs.[115] Few studies have reached phase 4, demonstrating the success of such combination therapy for breast cancers.[115] On the basis of the current development of nanomedicine, we anticipate that there will be more clinically effective nanomedicines moving to treatment of breast cancer and other types of cancer. Further advancement in the understanding of synergies of drug combination therapy and spatiotemporal codelivery by rationally designed nanoformulations will drive more drug combination nanomedicines into clinical trials and their approval for clinical use.

The global market of nanomedicine reached ∼$112 billion USD in 2016 and is anticipated to reach $350.8 billion USD in 2025.[226,227] This significant growth in the nanomedicine market confirms the potential of such DDS to target different diseases and improve treatment outcomes. Advanced protein, nucleic acid, and small molecule based nanopharmaceuticals are all key technologies currently under development.[223,227] Nevertheless, nanomedicine must overcome various challenges for commercialization and regulatory body approval. These challenges include: the production challenges (scale-up), reproducibility (batch to batch consistency), and regulatory agency (lack of robust FDA guidelines for proper characterization of NPs).

Nanomedicine continues to exhibit a huge potential with respect to modern DDSs and show promise to meet clinical challenges of unmet medical needs.[228−230] With regards to future applications, NP-based mRNA delivery strategies have been poised to offer even more effective vaccines.[6] Likewise, nanomedicines based on CRISPR/Cas9 will likely open new dimensions of molecular repair in the near term for treating various unmet medical needs.[231] Over the past decade, nanomedicine has primarily focused on the development of nanocarriers for treating cancer.[1] Also, the majority of the research focused on the material science aspects in which novel polymers, lipids, targeting ligands, and other components are incorporated into the NPs to facilitate their therapeutic efficacy. With a thorough understanding of nanomaterials, the overall scope of nanomedicine can be expanded to other unmet medical needs (e.g., antibiotic resistance, infectious disease, vaccine developments, and diagnostics).

AUTHOR INFORMATION

Corresponding Author

Xiao Yu Wu − *Advanced Pharmaceutics and Drug Delivery Laboratory, Leslie Dan Faculty of Pharmacy, University of Toronto, Toronto, Ontario M5S 3M2, Canada;* orcid.org/0000-0002-5333-8115; Phone: +(416) 978-5272; Email: sxy.wu@utoronto.ca; Fax: +(416) 978-8511

Authors

Taksim Ahmed − *Advanced Pharmaceutics and Drug Delivery Laboratory, Leslie Dan Faculty of Pharmacy, University of Toronto, Toronto, Ontario M5S 3M2, Canada*

Fuh-Ching Franky Liu − *Advanced Pharmaceutics and Drug Delivery Laboratory, Leslie Dan Faculty of Pharmacy, University of Toronto, Toronto, Ontario M5S 3M2, Canada*

Brian Lu − *Advanced Pharmaceutics and Drug Delivery Laboratory, Leslie Dan Faculty of Pharmacy, University of Toronto, Toronto, Ontario M5S 3M2, Canada*

HoYin Lip − *Advanced Pharmaceutics and Drug Delivery Laboratory, Leslie Dan Faculty of Pharmacy, University of Toronto, Toronto, Ontario M5S 3M2, Canada*

Elliya Park − *Advanced Pharmaceutics and Drug Delivery Laboratory, Leslie Dan Faculty of Pharmacy, University of Toronto, Toronto, Ontario M5S 3M2, Canada*

Ibrahim Alradwan − *Advanced Pharmaceutics and Drug Delivery Laboratory, Leslie Dan Faculty of Pharmacy, University of Toronto, Toronto, Ontario M5S 3M2, Canada*

Jackie Fule Liu − *Advanced Pharmaceutics and Drug Delivery Laboratory, Leslie Dan Faculty of Pharmacy, University of Toronto, Toronto, Ontario M5S 3M2, Canada*

Chunsheng He − *Advanced Pharmaceutics and Drug Delivery Laboratory, Leslie Dan Faculty of Pharmacy, University of Toronto, Toronto, Ontario M5S 3M2, Canada*

Abdulmottaleb Zetrini − *Advanced Pharmaceutics and Drug Delivery Laboratory, Leslie Dan Faculty of Pharmacy, University of Toronto, Toronto, Ontario M5S 3M2, Canada*

Tian Zhang − *Advanced Pharmaceutics and Drug Delivery Laboratory, Leslie Dan Faculty of Pharmacy, University of Toronto, Toronto, Ontario M5S 3M2, Canada;* orcid.org/0000-0003-0254-9817

Amin Ghavaminejad − *Advanced Pharmaceutics and Drug Delivery Laboratory, Leslie Dan Faculty of Pharmacy, University of Toronto, Toronto, Ontario M5S 3M2, Canada*

Andrew M. Rauth − *Departments of Medical Biophysics and Radiation Oncology, University of Toronto, Princess Margaret Cancer Centre, Toronto, Ontario M5G 2M9, Canada*

Jeffrey T. Henderson − *Advanced Pharmaceutics and Drug Delivery Laboratory, Leslie Dan Faculty of Pharmacy, University of Toronto, Toronto, Ontario M5S 3M2, Canada*

Complete contact information is available at: https://pubs.acs.org/10.1021/acs.molpharmaceut.2c00038

Author Contributions

The manuscript was written through contributions of all authors. X.Y.W. and T.A. generated the idea and wrote the manuscript. T.A. drafted and finalized the manuscript along with the subsection of PLN system. T.A., C.H., and E.P. wrote the CNS drug delivery section. B.L., F.J.L., A.GN., and T.A. wrote the diabetes section. H.Y.L., A.Z., and T.A. wrote the T.M.E. modulating cancer therapies section. T.Z., T.A., and I.A. wrote the targeted therapies section. F.F.L, T.A., E.P., and X.Y.W wrote the controlled release dosage form section. T.A., F.F.L., B.L., H.Y.L., J.T.H., A.M.R., and X.Y.W. edited the manuscript. All authors have given approval to the final version of the manuscript.

Notes

The authors declare no competing financial interest.

https://doi.org/10.1021/acs.molpharmaceut.2c00038
Mol. Pharmaceutics XXXX, XXX, XXX−XXX

■ ACKNOWLEDGMENTS

This work is supported in part by the Weston Brain Institute Transformational Grant, University of Toronto Connaught Innovation Award, Killam Research Fellowship by the Canada Council for the Arts, Project Grants from the Canadian Institutes of Health Research, Discovery and Equipment Grants from the Natural Sciences and Engineering Research Council of Canada, JDRF International, and Hemsley Charitable Trust Grants to X.Y.W. The authors also acknowledge the University of Toronto Connaught International Scholarship for Doctoral Students and the Pfizer Canada Graduate Fellowship in Pharmaceutical Sciences to T.A., the Centre for Collaborative Drug Research Graduate Student Incentive Fund to X.Y.W., the Ontario Graduate Scholarship (OGS) to B.L. and T.Z., the Queen Elizabeth Award to B.L. and H.Y.L., the Pharmaceutical Sciences Graduate Student Association Fellowship to E.P., King Abdulaziz City for Science and Technology (KACST) for the scholarship to I.A., Libyan Ministry of Higher Education scholarship to A.Z., Mitacs Accelerate Intership to F.J.L., the BBDC Seller Fellowship to A.GN., and the Mitacs Accelerate Fellowship to K.C.

■ REFERENCES

(1) Kirtane, A. R.; Verma, M.; Karandikar, P.; Furin, J.; Langer, R.; Traverso, G. Nanotechnology approaches for global infectious diseases. *Nat. Nanotechnol* **2021**, *16* (4), 369−384.

(2) Lozano, R.; Fullman, N.; Abate, D.; Abay, S. M.; Abbafati, C.; Abbasi, N.; Abbastabar, H.; Abd-Allah, F.; Abdela, J.; Abdelalim, A. Measuring progress from 1990 to 2017 and projecting attainment to 2030 of the health-related Sustainable Development Goals for 195 countries and territories: a systematic analysis for the Global Burden of Disease Study 2017. *Lancet* **2018**, *392* (10159), 2091−2138.

(3) Murray, C. J. L.; Lopez, A. D. Measuring the Global Burden of Disease. *N. Engl. J. Med.* **2013**, *369* (5), 448−457.

(4) Vollset, S. E.; Goren, E.; Yuan, C. W.; Cao, J.; Smith, A. E.; Hsiao, T.; Bisignano, C.; Azhar, G. S.; Castro, E.; Chalek, J. Fertility, mortality, migration, and population scenarios for 195 countries and territories from 2017 to 2100: a forecasting analysis for the Global Burden of Disease Study. *Lancet* **2020**, *396*, 1285−1306.

(5) Institute for Health Metrics and Evaluation (IHME). *Findings from the Global Burden of Disease Study 2017*; IHME: Seattle, WA, 2018.

(6) Mitchell, M. J.; Billingsley, M. M.; Haley, R. M.; Wechsler, M. E.; Peppas, N. A.; Langer, R. Engineering precision nanoparticles for drug delivery. *Nat. Rev. Drug Discovery* **2021**, *20* (2), 101−124.

(7) Saeedi, P.; Petersohn, I.; Salpea, P.; Malanda, B.; Karuranga, S.; Unwin, N.; Colagiuri, S.; Guariguata, L.; Motala, A. A.; Ogurtsova, K.; Shaw, J. E.; Bright, D.; Williams, R. Global and regional diabetes prevalence estimates for 2019 and projections for 2030 and 2045: Results from the International Diabetes Federation Diabetes Atlas, 9(th) edition. *Diabetes Res. Clin. Pract.* **2019**, *157*, 107843.

(8) World Health Organization. Diabetes, 2020. https://www.who.int/news-room/fact-sheets/detail/diabetes (accessed on September 17, 2020).

(9) Roser, M.; Ritchie, H. Burden of Disease, 2016 https://ourworldindata.org/burden-of-disease.

(10) The IQVIA Institute for Human Data Science. Global Medicine Spending and Usage Trends, Outlook to 2024, Mar 05, 2020. https://www.iqvia.com/insights/the-iqvia-institute/reports/global-medicine-spending-and-usage-trends (accessed on Nov 27, 2021).

(11) Reusch, J. E. B.; Manson, J. E. Management of Type 2 Diabetes in 2017: Getting to Goal. *JAMA* **2017**, *317* (10), 1015−1016.

(12) Xu, X.; Ho, W.; Zhang, X.; Bertrand, N.; Farokhzad, O. Cancer nanomedicine: from targeted delivery to combination therapy. *Trends Mol. Med.* **2015**, *21* (4), 223−32.

(13) Zhang, R. X.; Ahmed, T.; Li, L. Y.; Li, J.; Abbasi, A. Z.; Wu, X. Y. Design of nanocarriers for nanoscale drug delivery to enhance cancer treatment using hybrid polymer and lipid building blocks. *Nanoscale* **2017**, *9* (4), 1334−1355.

(14) Zhang, R. X.; Li, J.; Zhang, T.; Amini, M. A.; He, C.; Lu, B.; Ahmed, T.; Lip, H.; Rauth, A. M.; Wu, X. Y. Importance of integrating nanotechnology with pharmacology and physiology for innovative drug delivery and therapy - an illustration with firsthand examples. *Acta Pharmacol. Sin.* **2018**, *39* (5), 825−844.

(15) Zhang, R. X.; Wong, H. L.; Xue, H. Y.; Eoh, J. Y.; Wu, X. Y. Nanomedicine of synergistic drug combinations for cancer therapy - Strategies and perspectives. *J. Controlled Release* **2016**, *240*, 489−503.

(16) Fouad, Y. A.; Aanei, C. Revisiting the hallmarks of cancer. *Am. J. Cancer Res.* **2017**, *7* (5), 1016−1036.

(17) Panza, F.; Lozupone, M.; Logroscino, G.; Imbimbo, B. P. A critical appraisal of amyloid-beta-targeting therapies for Alzheimer disease. *Nat. Rev. Neurol.* **2019**, *15* (2), 73−88.

(18) Chapter 2: Global Burden of Neurological Disorders Estimates and Projections. In *Neurological Disorders: Public Health Challenges*; The World Health Organization: Geneva, Switzerland, 2006; pp 27−39.

(19) He, C.; Ahmed, T.; Abbasi, A. Z.; Li, L. Y.; Foltz, W. D.; Cai, P.; Knock, E.; Fraser, P. E.; Rauth, A. M.; Henderson, J. T.; Wu, X. Y. Multifunctional bioreactive-nanoconstructs for sensitive and accurate MRI of cerebrospinal fluid pathology and intervention of Alzheimer's disease. *Nano Today* **2020**, *35*, 100965.

(20) Wong, H. L.; Wu, X. Y.; Bendayan, R. Nanotechnological advances for the delivery of CNS therapeutics. *Adv. Drug Deliv Rev.* **2012**, *64* (7), 686−700.

(21) Arvanitis, C. D.; Ferraro, G. B.; Jain, R. K. The blood-brain barrier and blood-tumour barrier in brain tumours and metastases. *Nat. Rev. Cancer* **2020**, *20* (1), 26−41.

(22) Martín-Timón, I.; Del Cañizo-Gómez, F. J. Mechanisms of hypoglycemia unawareness and implications in diabetic patients. *World J. Diabetes* **2015**, *6* (7), 912−926.

(23) Veiseh, O.; Tang, B. C.; Whitehead, K. A.; Anderson, D. G.; Langer, R. Managing diabetes with nanomedicine: challenges and opportunities. *Nat. Rev. Drug Discovery* **2015**, *14* (1), 45−57.

(24) GhavamiNejad, A.; Li, J.; Lu, B.; Zhou, L.; Lam, L.; Giacca, A.; Wu, X. Y. Glucose-Responsive Composite Microneedle Patch for Hypoglycemia-Triggered Delivery of Native Glucagon. *Adv. Mater.* **2019**, *31* (30), No. e1901051.

(25) Lu, B.; GhavamiNejad, A.; Liu, J. F.; Li, J.; Mirzaie, S.; Giacca, A.; Wu, X. Y. "Smart" Composite Microneedle Patch Stabilizes Glucagon and Prevents Nocturnal Hypoglycemia: Experimental Studies and Molecular Dynamics Simulation. *ACS Appl. Mater. Interfaces* **2022**, *14*, 20576−20590.

(26) Ahmed, T.; Kamel, A. O.; Wettig, S. D. Interactions between DNA and Gemini surfactant: impact on gene therapy: part I. *Nanomedicine (London, England)* **2016**, *11* (3), 289−306.

(27) Ahmed, T.; Kamel, A. O.; Wettig, S. D. Interactions between DNA and gemini surfactant: impact on gene therapy: part II. *Nanomedicine (London, England)* **2016**, *11* (4), 403−20.

(28) Sindhwani, S.; Syed, A. M.; Ngai, J.; Kingston, B. R.; Maiorino, L.; Rothschild, J.; MacMillan, P.; Zhang, Y.; Rajesh, N. U.; Hoang, T.; Wu, J. L. Y.; Wilhelm, S.; Zilman, A.; Gadde, S.; Sulaiman, A.; Ouyang, B.; Lin, Z.; Wang, L.; Egeblad, M.; Chan, W. C. W. The entry of nanoparticles into solid tumours. *Nat. Mater.* **2020**, *19* (5), 566−575.

(29) Zhang, T.; Lip, H.; He, C.; Cai, P.; Wang, Z.; Henderson, J. T.; Rauth, A. M.; Wu, X. Y. Multitargeted Nanoparticles Deliver Synergistic Drugs across the Blood-Brain Barrier to Brain Metastases of Triple Negative Breast Cancer Cells and Tumor-Associated Macrophages. *Adv. Healthcare Mater.* **2019**, *8* (18), No. 1900543.

(30) Zhou, Q.; Shao, S.; Wang, J.; Xu, C.; Xiang, J.; Piao, Y.; Zhou, Z.; Yu, Q.; Tang, J.; Liu, X.; Gan, Z.; Mo, R.; Gu, Z.; Shen, Y. Enzyme-activatable polymer-drug conjugate augments tumour penetration and treatment efficacy. *Nat. Nanotechnol* **2019**, *14* (8), 799−809.

(31) Wang, G.; Zhou, Z.; Zhao, Z.; Li, Q.; Wu, Y.; Yan, S.; Shen, Y.; Huang, P. Enzyme-Triggered Transcytosis of Dendrimer-Drug Conjugate for Deep Penetration into Pancreatic Tumors. *ACS Nano* **2020**, *14* (4), 4890−4904.
(32) Zou, T.; Lu, W.; Mezhuev, Y.; Lan, M.; Li, L.; Liu, F.; Cai, T.; Wu, X.; Cai, Y. A review of nanoparticle drug delivery systems responsive to endogenous breast cancer microenvironment. *Eur. J. Pharm. Biopharm.* **2021**, *166*, 30−43.
(33) Amini, M. A.; Ahmed, T.; Liu, F. F.; Abbasi, A. Z.; Soeandy, C. D.; Zhang, R. X.; Prashad, P.; Cummins, C. L.; Rauth, A. M.; Henderson, J. T.; Wu, X. Y. Exploring the transformability of polymer-lipid hybrid nanoparticles and nanomaterial-biology interplay to facilitate tumor penetration, cellular uptake and intracellular targeting of anticancer drugs. *Expert opinion on drug delivery* **2021**, *18* (7), 991−1004.
(34) Amini, M. A.; Abbasi, A. Z.; Cai, P.; Lip, H.; Gordijo, C. R.; Li, J.; Chen, B.; Zhang, L.; Rauth, A. M.; Wu, X. Y. Combining Tumor Microenvironment Modulating Nanoparticles with Doxorubicin to Enhance Chemotherapeutic Efficacy and Boost Antitumor Immunity. *J. Natl. Cancer Inst.* **2019**, *111* (4), 399−408.
(35) Wilhelm, S.; Tavares, A. J.; Dai, Q.; Ohta, S.; Audet, J.; Dvorak, H. F.; Chan, W. C. W. Analysis of nanoparticle delivery to tumours. *Nat. Rev. Mater.* **2016**, *1* (5), 16014.
(36) Zhang, R. X.; Liu, F. F.; Lip, H.; Liu, J.; Zhang, Q.; Wu, X. Y. Pharmaceutical nanoformulation strategies to spatiotemporally manipulate oxidative stress for improving cancer therapies - exemplified by polyunsaturated fatty acids and other ROS-modulating agents. *Drug Deliv. and Transl. Res.* **2022** DOI: 10.1007/s13346-021-01104-3.
(37) World Health Organization. Cancer, 2020. https://www.who.int/news-room/fact-sheets/detail/cancer (accessed on September 17, 2020).
(38) Bray, F.; Ferlay, J.; Soerjomataram, I.; Siegel, R. L.; Torre, L. A.; Jemal, A. Global cancer statistics 2018: GLOBOCAN estimates of incidence and mortality worldwide for 36 cancers in 185 countries. *CA Cancer J. Clin.* **2018**, *68* (6), 394−424.
(39) Canadian Cancer Society. Cancer statistics at a glance, 2022. https://cancer.ca/en/research/cancer-statistics/cancer-statistics-at-a-glance (accessed on Feb 25, 2022).
(40) Mariotto, A. B.; Yabroff, K. R.; Shao, Y.; Feuer, E. J.; Brown, M. L. Projections of the cost of cancer care in the United States: 2010−2020. *J. Natl. Cancer Inst.* **2011**, *103* (2), 117−128.
(41) Wong, H. L.; Wu, X. Y.; Bendayan, R. Multidrug Resistance in Solid Tumor and Its Reversal. In *Pharmaceutical Perspectives of Cancer Therapeutics*; Lu, Y., Mahato, R. I., Eds.; Springer US: New York, 2009; pp 121−148.
(42) Vasan, N.; Baselga, J.; Hyman, D. M. A view on drug resistance in cancer. *Nature* **2019**, *575* (7782), 299−309.
(43) Holohan, C.; Van Schaeybroeck, S.; Longley, D. B.; Johnston, P. G. Cancer drug resistance: an evolving paradigm. *Nat. Rev. Cancer* **2013**, *13* (10), 714−26.
(44) Lai, J. I.; Tseng, Y. J.; Chen, M. H.; Huang, C. F.; Chang, P. M. Clinical Perspective of FDA Approved Drugs With P-Glycoprotein Inhibition Activities for Potential Cancer Therapeutics. *Front. Oncol.* **2020**, *10*, 561936.
(45) Wong, H. L.; Bendayan, R.; Rauth, A. M.; Wu, X. Y. Simultaneous delivery of doxorubicin and GG918 (Elacridar) by new polymer-lipid hybrid nanoparticles (PLN) for enhanced treatment of multidrug-resistant breast cancer. *J. Controlled Release* **2006**, *116* (3), 275−84.
(46) Liu, Z.; Ballinger, J. R.; Rauth, A. M.; Bendayan, R.; Wu, X. Y. Delivery of an anticancer drug and a chemosensitizer to murine breast sarcoma by intratumoral injection of sulfopropyl dextran microspheres. *J. Pharm. Pharmacol.* **2010**, *55* (8), 1063−73.
(47) Liu, Z.; Wu, X. Y.; Bendayan, R. In vitro investigation of ionic polysaccharide microspheres for simultaneous delivery of chemosensitizer and antineoplastic agent to multidrug-resistant cells. *J. Pharm. Sci.* **1999**, *88* (4), 412−8.
(48) Liu, Z.; Cheung, R.; Wu, X. Y.; Ballinger, J. R.; Bendayan, R.; Rauth, A. M. A study of doxorubicin loading onto and release from sulfopropyl dextran ion-exchange microspheres. *J. Controlled Release* **2001**, *77* (3), 213−24.
(49) Cheung, R. Y.; Rauth, A. M.; Yu Wu, X. In vivo efficacy and toxicity of intratumorally delivered mitomycin C and its combination with doxorubicin using microsphere formulations. *Anticancer Drugs* **2005**, *16* (4), 423−33.
(50) Cheung, R. Y.; Rauth, A. M.; Ronaldson, P. T.; Bendayan, R.; Wu, X. Y. In vitro toxicity to breast cancer cells of microsphere-delivered mitomycin C and its combination with doxorubicin. *Eur. J. Pharm. Biopharm.* **2006**, *62* (3), 321−31.
(51) Wong, H. L.; Bendayan, R.; Rauth, A. M.; Wu, X. Y. Development of solid lipid nanoparticles containing ionically complexed chemotherapeutic drugs and chemosensitizers. *J. Pharm. Sci.* **2004**, *93* (8), 1993−2008.
(52) Wong, H. L.; Bendayan, R.; Rauth, A. M.; Wu, X. Y. Development of solid lipid nanoparticles carrying ionic-linked anticancer drugs for the treatment of lymphatic metastasis. *J. Pharm. Sci.* **2004**, *93*, 1993−2008.
(53) Wong, H. L.; Bendayan, R.; Rauth, A. M.; Xue, H. Y.; Babakhanian, K.; Wu, X. Y. A mechanistic study of enhanced doxorubicin uptake and retention in multidrug resistant breast cancer cells using a polymer-lipid hybrid nanoparticle system. *J. Pharmacol. Exp. Ther.* **2006**, *317* (3), 1372−81.
(54) Wong, H. L.; Rauth, A. M.; Bendayan, R.; Manias, J. L.; Ramaswamy, M.; Liu, Z.; Erhan, S. Z.; Wu, X. Y. A new polymer-lipid hybrid nanoparticle system increases cytotoxicity of doxorubicin against multidrug-resistant human breast cancer cells. *Pharm. Res.* **2006**, *23* (7), 1574−85.
(55) Wong, H. L.; Rauth, A. M.; Bendayan, R.; Wu, X. Y. In vivo evaluation of a new polymer-lipid hybrid nanoparticle (PLN) formulation of doxorubicin in a murine solid tumor model. *Eur. J. Pharm. Biopharm.* **2007**, *65* (3), 300−8.
(56) Shuhendler, A. J.; O'Brien, P. J.; Rauth, A. M.; Wu, X. Y. On the synergistic effect of doxorubicin and mitomycin C against breast cancer cells. *Drug Metabol. Drug Interact.* **2007**, *22* (4), 201−33.
(57) Shuhendler, A. J.; Cheung, R. Y.; Manias, J.; Connor, A.; Rauth, A. M.; Wu, X. Y. A novel doxorubicin-mitomycin C co-encapsulated nanoparticle formulation exhibits anti-cancer synergy in multidrug resistant human breast cancer cells. *Breast Cancer Res. Treat.* **2010**, *119* (2), 255−69.
(58) Prasad, P.; Cheng, J.; Shuhendler, A.; Rauth, A. M.; Wu, X. Y. A novel nanoparticle formulation overcomes multiple types of membrane efflux pumps in human breast cancer cells. *Drug delivery and translational research* **2012**, *2* (2), 95−105.
(59) Prasad, P.; Shuhendler, A.; Cai, P.; Rauth, A. M.; Wu, X. Y. Doxorubicin and mitomycin C co-loaded polymer-lipid hybrid nanoparticles inhibit growth of sensitive and multidrug resistant human mammary tumor xenografts. *Cancer Lett.* **2013**, *334* (2), 263−73.
(60) Shuhendler, A. J.; Prasad, P.; Zhang, R. X.; Amini, M. A.; Sun, M.; Liu, P. P.; Bristow, R. G.; Rauth, A. M.; Wu, X. Y. Synergistic nanoparticulate drug combination overcomes multidrug resistance, increases efficacy, and reduces cardiotoxicity in a nonimmunocompromised breast tumor model. *Mol. Pharmaceutics* **2014**, *11* (8), 2659−74.
(61) Zhang, R. X.; Cai, P.; Zhang, T.; Chen, K.; Li, J.; Cheng, J.; Pang, K. S.; Adissu, H. A.; Rauth, A. M.; Wu, X. Y. Polymer-lipid hybrid nanoparticles synchronize pharmacokinetics of co-encapsulated doxorubicin-mitomycin C and enable their spatiotemporal co-delivery and local bioavailability in breast tumor. *Nanomedicine* **2016**, *12* (5), 1279−90.
(62) Zhang, R. X.; Li, L. Y.; Li, J.; Xu, Z.; Abbasi, A. Z.; Lin, L.; Amini, M. A.; Weng, W. Y.; Sun, Y.; Rauth, A. M.; Wu, X. Y. Coordinating Biointeraction and Bioreaction of a Nanocarrier Material and an Anticancer Drug to Overcome Membrane Rigidity and Target Mitochondria in Multidrug-Resistant Cancer Cells. *Adv. Funct. Mater.* **2017**, *27* (39), 1700804.

https://doi.org/10.1021/acs.molpharmaceut.2c00038
Mol. Pharmaceutics XXXX, XXX, XXX−XXX

(63) Liu, Q.; Rauth, A. M.; Wu, X. Y. Immobilization and bioactivity of glucose oxidase in hydrogel microspheres formulated by an emulsification-internal gelation-adsorption-polyelectrolyte coating method. *Int. J. Pharm.* **2007**, *339* (1−2), 148−56.
(64) Liu, Q.; Rauth, A. M.; Liu, J.; Babakhanian, K.; Wang, X.; Bendayan, R.; Wu, X. Y. Characterization of a microsphere formulation containing glucose oxidase and its in vivo efficacy in a murine solid tumor model. *Pharm. Res.* **2009**, *26* (10), 2343−57.
(65) Liu, Q.; Shuhendler, A.; Cheng, J.; Rauth, A. M.; O'Brien, P.; Wu, X. Y. Cytotoxicity and mechanism of action of a new ROS-generating microsphere formulation for circumventing multidrug resistance in breast cancer cells. *Breast Cancer Res. Treat.* **2010**, *121* (2), 323−33.
(66) Abdekhodaie, M. J.; Cheng, J.; Wu, X. Y. Effect of formulation factors on the bioactivity of glucose oxidase encapsulated chitosan-alginate microspheres: In vitro investigation and mathematical model prediction. *Chem. Eng. Sci.* **2015**, *125*, 4−12.
(67) Cheng, J.; Liu, Q.; Shuhendler, A. J.; Rauth, A. M.; Wu, X. Y. Optimizing the design and in vitro evaluation of bioreactive glucose oxidase-microspheres for enhanced cytotoxicity against multidrug resistant breast cancer cells. *Colloids Surf. B. Biointerfaces* **2015**, *130*, 164−72.
(68) Wu, X. Y. Strategies for optimizing polymer-lipid hybrid nanoparticle-mediated drug delivery. *Expert opinion on drug delivery* **2016**, *13* (5), 609−12.
(69) Wong, H. L.; Bendayan, R.; Rauth, A. M.; Li, Y.; Wu, X. Y. Chemotherapy with anticancer drugs encapsulated in solid lipid nanoparticles. *Adv. Drug Deliv Rev.* **2007**, *59* (6), 491−504.
(70) Xiong, X. B.; Lavasanifar, A. Traceable multifunctional micellar nanocarriers for cancer-targeted co-delivery of MDR-1 siRNA and doxorubicin. *ACS Nano* **2011**, *5* (6), 5202−13.
(71) Lou, S.; Zhao, Z.; Dezort, M.; Lohneis, T.; Zhang, C. Multifunctional Nanosystem for Targeted and Controlled Delivery of Multiple Chemotherapeutic Agents for the Treatment of Drug-Resistant Breast Cancer. *ACS Omega* **2018**, *3* (8), 9210−9219.
(72) Roy, A.; Murakami, M.; Ernsting, M. J.; Hoang, B.; Undzys, E.; Li, S.-D. Carboxymethylcellulose-based and docetaxel-loaded nanoparticles circumvent P-glycoprotein-mediated multidrug resistance. *Mol. Pharmaceutics* **2014**, *11* (8), 2592−2599.
(73) Roy, A.; Ernsting, M. J.; Undzys, E.; Li, S. D. A highly tumor-targeted nanoparticle of podophyllotoxin penetrated tumor core and regressed multidrug resistant tumors. *Biomaterials* **2015**, *52*, 335−46.
(74) Wigerup, C.; Påhlman, S.; Bexell, D. Therapeutic targeting of hypoxia and hypoxia-inducible factors in cancer. *Pharmacol. Ther.* **2016**, *164*, 152−69.
(75) Burden, D. A.; Osheroff, N. Mechanism of action of eukaryotic topoisomerase II and drugs targeted to the enzyme. *Biochim. Biophys. Acta* **1998**, *1400* (1−3), 139−54.
(76) Tewey, K. M.; Rowe, T. C.; Yang, L.; Halligan, B. D.; Liu, L. F. Adriamycin-induced DNA damage mediated by mammalian DNA topoisomerase II. *Science* **1984**, *226* (4673), 466−8.
(77) Wang, P.; Song, Y.; Zhang, L.; He, H.; Zhou, X. Quinone methide derivatives: important intermediates to DNA alkylating and DNA cross-linking actions. *Curr. Med. Chem.* **2005**, *12* (24), 2893−913.
(78) Hortobagyi, G. N. Mitomycin: its evolving role in the treatment of breast cancer. *Oncology* **2004**, *50*, 1−8.
(79) Andersson, M.; Daugaard, S.; von der Maase, H.; Mouridsen, H. T. Doxorubicin versus mitomycin versus doxorubicin plus mitomycin in advanced breast cancer: a randomized study. *Cancer Treat. Rep.* **1986**, *70* (10), 1181−1186.
(80) Zhang, R. X.; Zhang, T.; Chen, K.; Cheng, J.; Lai, P.; Rauth, A. M.; Pang, K. S.; Wu, X. Y. Sample Extraction and Simultaneous Chromatographic Quantitation of Doxorubicin and Mitomycin C Following Drug Combination Delivery in Nanoparticles to Tumor-bearing Mice. *J. Vis. Exp.* **2017**, No. 128, 56159.
(81) Date, T.; Nimbalkar, V.; Kamat, J.; Mittal, A.; Mahato, R. I.; Chitkara, D. Lipid-polymer hybrid nanocarriers for delivering cancer therapeutics. *J. Controlled Release* **2018**, *271*, 60−73.
(82) Zhang, C.; Zhou, X.; Zhang, H.; Han, X.; Li, B.; Yang, R.; Zhou, X. Recent Progress of Novel Nanotechnology Challenging the Multidrug Resistance of Cancer. *Front. Pharmacol.* **2022**, *13*, 776895.
(83) Majidinia, M.; Mirza-Aghazadeh-Attari, M.; Rahimi, M.; Mihanfar, A.; Karimian, A.; Safa, A.; Yousefi, B. Overcoming multidrug resistance in cancer: Recent progress in nanotechnology and new horizons. *IUBMB life* **2020**, *72* (5), 855−871.
(84) Park, J. H.; Ban, S. J.; Ahmed, T.; Choi, H. S.; Yoon, H. E.; Yoon, J. H.; Choi, H. K. Development of DH-I-180−3 loaded lipid nanoparticle for photodynamic therapy. *Int. J. Pharm.* **2015**, *491* (1−2), 393−401.
(85) Li, Y.; Taulier, N.; Rauth, A. M.; Wu, X. Y. Screening of lipid carriers and characterization of drug-polymer-lipid interactions for the rational design of polymer-lipid hybrid nanoparticles (PLN). *Pharm. Res.* **2006**, *23* (8), 1877−87.
(86) Li, Y.; Wong, H. L.; Shuhendler, A. J.; Rauth, A. M.; Wu, X. Y. Molecular interactions, internal structure and drug release kinetics of rationally developed polymer-lipid hybrid nanoparticles. *J. Controlled Release* **2008**, *128* (1), 60−70.
(87) Li, Y.; Abbaspour, M. R.; Grootendorst, P. V.; Rauth, A. M.; Wu, X. Y. Optimization of controlled release nanoparticle formulation of verapamil hydrochloride using artificial neural networks with genetic algorithm and response surface methodology. *Eur. J. Pharm. Biopharm.* **2015**, *94*, 170−179.
(88) Wong, H.-L.; Rauth, A. M.; Bendayan, R.; Wu, X. Y. Novel solid lipid nanoparticles formulations increase the cytotoxicity and prolong the cellular accumulation of doxorubicin in human multidrug-resistant breast cancer cells. *Cancer Res.* **2005**, *65*, 336.
(89) Wang, H.; Huang, Y. Combination therapy based on nano codelivery for overcoming cancer drug resistance. *Medicine in Drug Discovery* **2020**, *6*, 100024.
(90) Brain Tumor Foundation of Canada. Facts About Brain Tumours, 2021. https://www.braintumour.ca/facing-a-brain-tumour/facts-about-brain-tumours/ (accessed on Nov 4, 2021).
(91) Global Cancer Observatory, International Agency for Research on Cancer, World Health Organization. Brain, Central nervous system, 2020. https://gco.iarc.fr/today/home (accessed on Nov 27, 2021).
(92) Brosnan, E. M.; Anders, C. K. Understanding patterns of brain metastasis in breast cancer and designing rational therapeutic strategies. *Annals of translational medicine* **2018**, *6* (9), 163−163.
(93) Witzel, I.; Oliveira-Ferrer, L.; Pantel, K.; Muller, V.; Wikman, H. Breast cancer brain metastases: biology and new clinical perspectives. *Breast Cancer Res.* **2016**, *18* (1), 8.
(94) Bailleux, C.; Eberst, L.; Bachelot, T. Treatment strategies for breast cancer brain metastases. *Br. J. Cancer* **2021**, *124* (1), 142−155.
(95) Pandit, R.; Chen, L.; Götz, J. The blood-brain barrier: Physiology and strategies for drug delivery. *Adv. Drug Deliv Rev.* **2020**, *165−166*, 1−14.
(96) Hajal, C.; Le Roi, B.; Kamm, R. D.; Maoz, B. M. Biology and Models of the Blood-Brain Barrier. *Annu. Rev. Biomed. Eng.* **2021**, *23* (1), 359−384.
(97) Wohlfart, S.; Gelperina, S.; Kreuter, J. Transport of drugs across the blood-brain barrier by nanoparticles. *J. Controlled Release* **2012**, *161* (2), 264−73.
(98) Maier-Hauff, K.; Ulrich, F.; Nestler, D.; Niehoff, H.; Wust, P.; Thiesen, B.; Orawa, H.; Budach, V.; Jordan, A. Efficacy and safety of intratumoral thermotherapy using magnetic iron-oxide nanoparticles combined with external beam radiotherapy on patients with recurrent glioblastoma multiforme. *J. Neurooncol.* **2011**, *103* (2), 317−24.
(99) Shalviri, A.; Chan, H. K.; Raval, G.; Abdekhodaie, M. J.; Liu, Q.; Heerklotz, H.; Wu, X. Y. Design of pH-responsive nanoparticles of terpolymer of poly(methacrylic acid), polysorbate 80 and starch for delivery of doxorubicin. *Colloids Surf. B. Biointerfaces* **2013**, *101*, 405−13.
(100) Shalviri, A.; Raval, G.; Prasad, P.; Chan, C.; Liu, Q.; Heerklotz, H.; Rauth, A. M.; Wu, X. Y. pH-Dependent doxorubicin release from terpolymer of starch, polymethacrylic acid and polysorbate 80 nanoparticles for overcoming multi-drug resistance

https://doi.org/10.1021/acs.molpharmaceut.2c00038
Mol. Pharmaceutics XXXX, XXX, XXX−XXX

in human breast cancer cells. *Eur. J. Pharm. Biopharm.* **2012**, *82* (3), 587−97.
(101) Shalviri, A.; Foltz, W. D.; Cai, P.; Rauth, A. M.; Wu, X. Y. Multifunctional terpolymeric MRI contrast agent with superior signal enhancement in blood and tumor. *J. Controlled Release* **2013**, *167* (1), 11−20.
(102) Shalviri, A.; Cai, P.; Rauth, A. M.; Henderson, J. T.; Wu, X. Y. Evaluation of new bi-functional terpolymeric nanoparticles for simultaneous in vivo optical imaging and chemotherapy of breast cancer. *Drug delivery and translational research* **2012**, *2* (6), 437−53.
(103) Li, J.; Cai, P.; Shalviri, A.; Henderson, J. T.; He, C.; Foltz, W. D.; Prasad, P.; Brodersen, P. M.; Chen, Y.; DaCosta, R.; Rauth, A. M.; Wu, X. Y. A multifunctional polymeric nanotheranostic system delivers doxorubicin and imaging agents across the blood-brain barrier targeting brain metastases of breast cancer. *ACS Nano* **2014**, *8* (10), 9925−40.
(104) He, C.; Cai, P.; Li, J.; Zhang, T.; Lin, L.; Abbasi, A. Z.; Henderson, J. T.; Rauth, A. M.; Wu, X. Y. Blood-brain barrier-penetrating amphiphilic polymer nanoparticles deliver docetaxel for the treatment of brain metastases of triple negative breast cancer. *J. Controlled Release* **2017**, *246*, 98−109.
(105) He, C.; Li, J.; Cai, P.; Ahmed, T.; Henderson, J. T.; Foltz, W. D.; Bendayan, R.; Rauth, A. M.; Wu, X. Y. Two-Step Targeted Hybrid Nanoconstructs Increase Brain Penetration and Efficacy of the Therapeutic Antibody Trastuzumab against Brain Metastasis of HER2-Positive Breast Cancer. *Adv. Funct. Mater.* **2018**, *28* (9), 1705668.
(106) Tyner, K. M.; Zou, P.; Yang, X.; Zhang, H.; Cruz, C. N.; Lee, S. L. Product quality for nanomaterials: current U.S. experience and perspective. *Wiley Interdiscip Rev. Nanomed* **2015**, *7* (5), 640−54.
(107) Paliwal, R.; Babu, R. J.; Palakurthi, S. Nanomedicine scale-up technologies: feasibilities and challenges. *AAPS PharmSciTech* **2014**, *15* (6), 1527−34.
(108) Yu, L. X. Pharmaceutical quality by design: product and process development, understanding, and control. *Pharm. Res.* **2008**, *25* (4), 781−91.
(109) Ahmed, T.; Liu, F. F.; He, C.; Abbasi, A. Z.; Cai, P.; Rauth, A. M.; Henderson, J. T.; Wu, X. Y. Optimizing the Design of Blood-Brain Barrier-Penetrating Polymer-Lipid-Hybrid Nanoparticles for Delivering Anticancer Drugs to Glioblastoma. *Pharm. Res.* **2021**, *38* (11), 1897−1914.
(110) Liu, F.-C. F. Involvement of Lipids in the Physicochemical and In Vitro Characteristics of Polymer-lipid Nanoparticles in Cancer Cell Models. M.S. thesis, University of Toronto, Toronto, Ontario Canada, 2019.
(111) Quader, S.; Kataoka, K.; Cabral, H. Nanomedicine for brain cancer. *Adv. Drug Deliv Rev.* **2022**, *182*, 114115.
(112) Nguyen, T. T.; Dung Nguyen, T. T.; Vo, T. K.; Tran, N. M.; Nguyen, M. K.; Van Vo, T.; Van Vo, G. Nanotechnology-based drug delivery for central nervous system disorders. *Biomed. Pharmacother.* **2021**, *143*, 112117.
(113) Alves, S. R.; Colquhoun, A.; Wu, X. Y.; de Oliveira Silva, D. Synthesis of terpolymer-lipid encapsulated diruthenium(II,III)-anti-inflammatory metallodrug nanoparticles to enhance activity against glioblastoma cancer cells. *J. Inorg. Biochem.* **2020**, *205*, 110984.
(114) He, C. C.; Cai, P.; Li, J.; Henderson, J. T.; Rauth, A. M.; Wu, X. Y. Blood-brain barrier-penetrating terpolymer nanoparticles deliver docetaxel and trastuzumab to brain metastases of breast cancer (Abstract LB-096). In *Proceedings of the 106th Annual Meeting of the AACR*, Philadelphia, PA, April 18−22, 2015; AACR: Philadelphia, PA, 2015. *Cancer Res.* **2015**, *75*, LB-096.
(115) Shan, X.; Gong, X.; Li, J.; Wen, J.; Li, Y.; Zhang, Z. Current approaches of nanomedicines in the market and various stage of clinical translation. *Acta Pharm. Sin. B* **2022** DOI: 10.1016/j.apsb.2022.02.025.
(116) Hebert, L. E.; Weuve, J.; Scherr, P. A.; Evans, D. A. Alzheimer disease in the United States (2010−2050) estimated using the 2010 census. *Neurology* **2013**, *80* (19), 1778−1783.
(117) Dementia numbers in Canada, 2021. https://alzheimer.ca/en/about-dementia/what-dementia/dementia-numbers-canada (accessed on Nov 14, 2021).
(118) Shi, J.; Kantoff, P. W.; Wooster, R.; Farokhzad, O. C. Cancer nanomedicine: progress, challenges and opportunities. *Nat. Rev. Cancer* **2017**, *17* (1), 20−37.
(119) Behzadi, S.; Serpooshan, V.; Tao, W.; Hamaly, M. A.; Alkawareek, M. Y.; Dreaden, E. C.; Brown, D.; Alkilany, A. M.; Farokhzad, O. C.; Mahmoudi, M. Cellular uptake of nanoparticles: journey inside the cell. *Chem. Soc. Rev.* **2017**, *46* (14), 4218−4244.
(120) Bertrand, N.; Wu, J.; Xu, X.; Kamaly, N.; Farokhzad, O. C. Cancer nanotechnology: the impact of passive and active targeting in the era of modern cancer biology. *Adv. Drug Deliv Rev.* **2014**, *66*, 2−25.
(121) Fernandes, C.; Suares, D.; Yergeri, M. C. Tumor Microenvironment Targeted Nanotherapy. *Front. Pharmacol.* **2018**, *9*, 1230.
(122) Hanahan, D.; Coussens, L. M. Accessories to the crime: functions of cells recruited to the tumor microenvironment. *Cancer Cell* **2012**, *21* (3), 309−22.
(123) Miao, L.; Huang, L. Exploring the tumor microenvironment with nanoparticles. *Cancer Treat. Res.* **2015**, *166*, 193−226.
(124) Ernsting, M. J.; Hoang, B.; Lohse, I.; Undzys, E.; Cao, P.; Do, T.; Gill, B.; Pintilie, M.; Hedley, D.; Li, S. D. Targeting of metastasis-promoting tumor-associated fibroblasts and modulation of pancreatic tumor-associated stroma with a carboxymethylcellulose-docetaxel nanoparticle. *J. Controlled Release* **2015**, *206*, 122−30.
(125) Dominguez, A. L.; Lustgarten, J. Targeting the tumor microenvironment with anti-neu/anti-CD40 conjugated nanoparticles for the induction of antitumor immune responses. *Vaccine* **2010**, *28* (5), 1383−90.
(126) Sun, Z.; Zhang, Y.; Cao, D.; Wang, X.; Yan, X.; Li, H.; Huang, L.; Qu, X.; Kong, C.; Qin, H.; Wang, M.; Xu, W.; Liang, L. PD-1/PD-L1 pathway and angiogenesis dual recognizable nanoparticles for enhancing chemotherapy of malignant cancer. *Drug Delivery* **2018**, *25* (1), 1746−1755.
(127) Shen, S.; Li, H. J.; Chen, K. G.; Wang, Y. C.; Yang, X. Z.; Lian, Z. X.; Du, J. Z.; Wang, J. Spatial Targeting of Tumor-Associated Macrophages and Tumor Cells with a pH-Sensitive Cluster Nanocarrier for Cancer Chemoimmunotherapy. *Nano Lett.* **2017**, *17* (6), 3822−3829.
(128) Zhao, P. F.; Yin, W. M.; Wu, A. H.; Tang, Y. S.; Wang, J. Y.; Pan, Z. Z.; Lin, T. T.; Zhang, M.; Chen, B. F.; Duan, Y. F.; Huang, Y. Z. Dual-Targeting to Cancer Cells and M2Macrophages via Biomimetic Delivery of Mannosylated Albumin Nanoparticles for Drug-Resistant Cancer Therapy. *Adv. Funct. Mater.* **2017**, *27* (44), 1700403.
(129) Kosmides, A. K.; Sidhom, J. W.; Fraser, A.; Bessell, C. A.; Schneck, J. P. Dual Targeting Nanoparticle Stimulates the Immune System To Inhibit Tumor Growth. *ACS Nano* **2017**, *11* (6), 5417−5429.
(130) Hamidi, H.; Ivaska, J. Every step of the way: integrins in cancer progression and metastasis. *Nat. Rev. Cancer* **2018**, *18* (9), 533−548.
(131) Shuhendler, A. J.; Prasad, P.; Leung, M.; Rauth, A. M.; Dacosta, R. S.; Wu, X. Y. A novel solid lipid nanoparticle formulation for active targeting to tumor α(v) β(3) integrin receptors reveals cyclic RGD as a double-edged sword. *Adv. Healthcare Mater.* **2012**, *1* (5), 600−8.
(132) Shan, D.; Li, J.; Cai, P.; Prasad, P.; Liu, F.; Rauth, A. M.; Wu, X. Y. RGD-conjugated solid lipid nanoparticles inhibit adhesion and invasion of α v β 3 integrin-overexpressing breast cancer cells. *Drug delivery and translational research* **2015**, *5* (1), 15−26.
(133) Nie, S. Understanding and overcoming major barriers in cancer nanomedicine. *Nanomedicine (London, England)* **2010**, *5* (4), 523−8.
(134) Shokeen, M.; Pressly, E. D.; Hagooly, A.; Zheleznyak, A.; Ramos, N.; Fiamengo, A. L.; Welch, M. J.; Hawker, C. J.; Anderson, C. J. Evaluation of multivalent, functional polymeric nanoparticles for imaging applications. *ACS Nano* **2011**, *5* (2), 738−47.

(135) Zhang, T.; Prasad, P.; Cai, P.; He, C.; Shan, D.; Rauth, A. M.; Wu, X. Y. Dual-targeted hybrid nanoparticles of synergistic drugs for treating lung metastases of triple negative breast cancer in mice. *Acta Pharmacol. Sin.* **2017**, *38* (6), 835−847.
(136) Desgrosellier, J. S.; Cheresh, D. A. Integrins in cancer: biological implications and therapeutic opportunities. *Nature Reviews Cancer* **2010**, *10* (1), 9−22.
(137) Zhang, T.; Fu, C.; Alradwan, I.; Yen, T.; Lip, H.; Cai, P.; Rauth, A. M.; Zhang, L.; Wu, X. Y. Targeting Signaling Pathways of Hyaluronic Acid and Integrin Receptors by Synergistic Combination Nanocomposites Inhibits Systemic Metastases and Primary Triple Negative Breast Cancer. *Adv. Ther (Weinh)* **2021**, *4* (6), 2100022.
(138) Wang, Z.; Zhang, R. X.; Zhang, T.; He, C.; He, R.; Ju, X.; Wu, X. Y. In Situ Proapoptotic Peptide-Generating Rapeseed Protein-Based Nanocomplexes Synergize Chemotherapy for Cathepsin-B Overexpressing Breast Cancer. *ACS Appl. Mater. Interfaces* **2018**, *10*, 41056−41069.
(139) McMillin, D. W.; Negri, J. M.; Mitsiades, C. S. The role of tumour-stromal interactions in modifying drug response: challenges and opportunities. *Nat. Rev. Drug Discovery* **2013**, *12* (3), 217−228.
(140) Gatenby, R. A.; Gillies, R. J. A microenvironmental model of carcinogenesis. *Nature Reviews Cancer* **2008**, *8* (1), 56−61.
(141) Li, H.; Fan, X.; Houghton, J. Tumor microenvironment: the role of the tumor stroma in cancer. *J. Cell. Biochem.* **2007**, *101* (4), 805−815.
(142) Jing, X.; Yang, F.; Shao, C.; Wei, K.; Xie, M.; Shen, H.; Shu, Y. Role of hypoxia in cancer therapy by regulating the tumor microenvironment. *Mol. Cancer* **2019**, *18* (1), 157.
(143) Graham, K.; Unger, E. Overcoming tumor hypoxia as a barrier to radiotherapy, chemotherapy and immunotherapy in cancer treatment. *Int. J. Nanomedicine* **2018**, *13*, 6049−6058.
(144) Cadet, J.; Davies, K. J. A. Oxidative DNA damage & repair: An introduction. *Free Radic. Biol. Med.* **2017**, *107*, 2−12.
(145) Prasad, P.; Gordijo, C. R.; Abbasi, A. Z.; Maeda, A.; Ip, A.; Rauth, A. M.; DaCosta, R. S.; Wu, X. Y. Multifunctional Albumin-MnO2 Nanoparticles Modulate Solid Tumor Microenvironment by Attenuating Hypoxia, Acidosis, Vascular Endothelial Growth Factor and Enhance Radiation Response. *ACS Nano* **2014**, *8* (4), 3202−3212.
(146) Freitas, C.; Müller, R. H. Correlation between long-term stability of solid lipid nanoparticles (SLN) and crystallinity of the lipid phase. *Eur. J. Pharm. Biopharm.* **1999**, *47* (2), 125−132.
(147) Abbasi, A. Z.; Gordijo, C. R.; Amini, M. A.; Maeda, A.; Rauth, A. M.; DaCosta, R. S.; Wu, X. Y. Hybrid manganese dioxide nanoparticles potentiate radiation therapy by modulating tumor hypoxia. *Cancer Res.* **2016**, *76* (22), 6643−6656.
(148) Shaked, Y. Balancing efficacy of and host immune responses to cancer therapy: the yin and yang effects. *Nature Reviews Clinical Oncology* **2016**, *13* (10), 611.
(149) Vito, A.; El-Sayes, N.; Mossman, K. Hypoxia-Driven Immune Escape in the Tumor Microenvironment. *Cells* **2020**, *9* (4), 992.
(150) Hughes, R.; Qian, B. Z.; Rowan, C.; Muthana, M.; Keklikoglou, I.; Olson, O. C.; Tazzyman, S.; Danson, S.; Addison, C.; Clemons, M.; Gonzalez-Angulo, A. M.; Joyce, J. A.; De Palma, M.; Pollard, J. W.; Lewis, C. E. Perivascular M2Macrophages Stimulate Tumor Relapse after Chemotherapy. *Cancer Res.* **2015**, *75* (17), 3479−91.
(151) Selleri, S.; Bifsha, P.; Civini, S.; Pacelli, C.; Dieng, M. M.; Lemieux, W.; Jin, P.; Bazin, R.; Patey, N.; Marincola, F. M.; Moldovan, F.; Zaouter, C.; Trudeau, L.-E.; Benabdhalla, B.; Louis, I.; Beauséjour, C.; Stroncek, D.; Le Deist, F.; Haddad, E. Human mesenchymal stromal cell-secreted lactate induces M2-macrophage differentiation by metabolic reprogramming. *Oncotarget* **2016**, *7* (21), 30193−30210.
(152) Colegio, O. R.; Chu, N. Q.; Szabo, A. L.; Chu, T.; Rhebergen, A. M.; Jairam, V.; Cyrus, N.; Brokowski, C. E.; Eisenbarth, S. C.; Phillips, G. M.; Cline, G. W.; Phillips, A. J.; Medzhitov, R. Functional polarization of tumour-associated macrophages by tumour-derived lactic acid. *Nature* **2014**, *513* (7519), 559−63.
(153) Anderson, K. G.; Stromnes, I. M.; Greenberg, P. D. Obstacles Posed by the Tumor Microenvironment to T cell Activity: A Case for Synergistic Therapies. *Cancer Cell* **2017**, *31* (3), 311−325.
(154) Maj, T.; Wang, W.; Crespo, J.; Zhang, H.; Wang, W.; Wei, S.; Zhao, L.; Vatan, L.; Shao, I.; Szeliga, W.; Lyssiotis, C.; Liu, J. R.; Kryczek, I.; Zou, W. Oxidative stress controls regulatory T cell apoptosis and suppressor activity and PD-L1-blockade resistance in tumor. *Nat. Immunol.* **2017**, *18* (12), 1332−1341.
(155) Kjaergaard, J.; Hatfield, S.; Jones, G.; Ohta, A.; Sitkovsky, M. A(2A) Adenosine Receptor Gene Deletion or Synthetic A(2A) Antagonist Liberate Tumor-Reactive CD8(+) T Cells from Tumor-Induced Immunosuppression. *J. Immunol.* **2018**, *201* (2), 782−791.
(156) Haas, R.; Smith, J.; Rocher-Ros, V.; Nadkarni, S.; Montero-Melendez, T.; D'Acquisto, F.; Bland, E. J.; Bombardieri, M.; Pitzalis, C.; Perretti, M.; Marelli-Berg, F. M.; Mauro, C. Lactate Regulates Metabolic and Pro-inflammatory Circuits in Control of T Cell Migration and Effector Functions. *PLoS Biol.* **2015**, *13* (7), No. e1002202.
(157) Gordijo, C. R.; Abbasi, A. Z.; Amini, M. A.; Lip, H. Y.; Maeda, A.; Cai, P.; O'Brien, P. J.; DaCosta, R. S.; Rauth, A. M.; Wu, X. Y. Design of Hybrid MnO2-Polymer-Lipid Nanoparticles with Tunable Oxygen Generation Rates and Tumor Accumulation for Cancer Treatment. *Adv. Funct. Mater.* **2015**, *25* (12), 1858−1872.
(158) Wang, H.; Jiang, H.; Van De Gucht, M.; De Ridder, M. Hypoxic Radioresistance: Can ROS Be the Key to Overcome It? *Cancers (Basel)* **2019**, *11* (1), 112.
(159) GhavamiNejad, A.; Ashammakhi, N.; Wu, X. Y.; Khademhosseini, A. Crosslinking Strategies for 3D Bioprinting of Polymeric Hydrogels. *Small* **2020**, *16* (35), 2002931.
(160) Wu, M.; Zhang, Y.; Huang, H.; Li, J.; Liu, H.; Guo, Z.; Xue, L.; Liu, S.; Lei, Y. Assisted 3D printing of microneedle patches for minimally invasive glucose control in diabetes. *Mater. Sci. Eng., C* **2020**, *117*, 111299−111299.
(161) Berget, C.; Messer, L. H.; Forlenza, G. P. A Clinical Overview of Insulin Pump Therapy for the Management of Diabetes: Past, Present, and Future of Intensive Therapy. *Diabetes spectrum: a publication of the American Diabetes Association* **2019**, *32* (3), 194−204.
(162) Haidar, A.; Legault, L.; Dallaire, M.; Alkhateeb, A.; Coriati, A.; Messier, V.; Cheng, P.; Millette, M.; Boulet, B.; Rabasa-Lhoret, R. Glucose-responsive insulin and glucagon delivery (dual-hormone artificial pancreas) in adults with type 1 diabetes: a randomized crossover controlled trial. *Can. Med. Assoc. J.* **2013**, *185* (4), 297.
(163) Li, J.; Chu, M. K.; Gordijo, C. R.; Abbasi, A. Z.; Chen, K.; Adissu, H. A.; Lohn, M.; Giacca, A.; Plettenburg, O.; Wu, X. Y. Microfabricated microporous membranes reduce the host immune response and prolong the functional lifetime of a closed-loop insulin delivery implant in a type 1 diabetic rat model. *Biomaterials* **2015**, *47*, 51−61.
(164) Gordijo, C. R.; Shuhendler, A. J.; Wu, X. Y. Glucose-Responsive Bioinorganic Nanohybrid Membrane for Self-Regulated Insulin Release. *Adv. Funct. Mater.* **2010**, *20* (9), 1404−1412.
(165) Gordijo, C. R.; Koulajian, K.; Shuhendler, A. J.; Bonifacio, L. D.; Huang, H. Y.; Chiang, S.; Ozin, G. A.; Giacca, A.; Wu, X. Y. Nanotechnology-Enabled Closed Loop Insulin Delivery Device: In Vitro and In Vivo Evaluation of Glucose-Regulated Insulin Release for Diabetes Control. *Adv. Funct. Mater.* **2011**, *21* (1), 73−82.
(166) Chu, M. K.; Gordijo, C. R.; Li, J.; Abbasi, A. Z.; Giacca, A.; Plettenburg, O.; Wu, X. Y. In vivo performance and biocompatibility of a subcutaneous implant for real-time glucose-responsive insulin delivery. *Diabetes Technol. Ther.* **2015**, *17* (4), 255−67.
(167) Chu, M. K.; Chen, J.; Gordijo, C. R.; Chiang, S.; Ivovic, A.; Koulajian, K.; Giacca, A.; Wu, X. Y.; Sun, Y. In vitro and in vivo testing of glucose-responsive insulin-delivery microdevices in diabetic rats. *Lab Chip* **2012**, *12* (14), 2533−9.
(168) Bakh, N. A.; Cortinas, A. B.; Weiss, M. A.; Langer, R. S.; Anderson, D. G.; Gu, Z.; Dutta, S.; Strano, M. S. Glucose-responsive insulin by molecular and physical design. *Nat. Chem.* **2017**, *9* (10), 937−943.

https://doi.org/10.1021/acs.molpharmaceut.2c00038
Mol. Pharmaceutics XXXX, XXX, XXX−XXX

(169) Chou, D. H.; Webber, M. J.; Tang, B. C.; Lin, A. B.; Thapa, L. S.; Deng, D.; Truong, J. V.; Cortinas, A. B.; Langer, R.; Anderson, D. G. Glucose-responsive insulin activity by covalent modification with aliphatic phenylboronic acid conjugates. *Proc. Natl. Acad. Sci. U. S. A.* **2015**, *112* (8), 2401−6.
(170) Ravaine, V.; Ancla, C.; Catargi, B. Chemically controlled closed-loop insulin delivery. *J. Controlled Release* **2008**, *132* (1), 2−11.
(171) Zhao, L.; Xiao, C.; wang, L.; Gai, G.; Ding, J. Glucose-sensitive polymer nanoparticles for self-regulated drug delivery. *Chem. Commun.* **2016**, *52* (49), 7633−7652.
(172) Podual, K.; Doyle, F. J., 3rd; Peppas, N. A. Dynamic behavior of glucose oxidase-containing microparticles of poly(ethylene glycol)-grafted cationic hydrogels in an environment of changing pH. *Biomaterials* **2000**, *21* (14), 1439−50.
(173) Haidar, A.; Rabasa-Lhoret, R.; Legault, L.; Lovblom, L. E.; Rakheja, R.; Messier, V.; D'Aoust, É.; Falappa, C. M.; Justice, T.; Orszag, A.; Tschirhart, H.; Dallaire, M.; Ladouceur, M.; Perkins, B. A. Single- and Dual-Hormone Artificial Pancreas for Overnight Glucose Control in Type 1 Diabetes. *Journal of Clinical Endocrinology & Metabolism* **2016**, *101* (1), 214−223.
(174) Wen, X.; Wang, K.; Zhao, Z.; Zhang, Y.; Sun, T.; Zhang, F.; Wu, J.; Fu, Y.; Du, Y.; Zhang, L.; Sun, Y.; Liu, Y.; Ma, K.; Liu, H.; Song, Y. Brain-targeted delivery of trans-activating transcriptor-conjugated magnetic PLGA/lipid nanoparticles. *PLoS One* **2014**, *9* (9), No. e106652.
(175) Yue, J. T. Y.; Burdett, E.; Coy, D. H.; Giacca, A.; Efendic, S.; Vranic, M. Somatostatin Receptor Type 2 Antagonism Improves Glucagon and Corticosterone Counterregulatory Responses to Hypoglycemia in Streptozotocin-Induced Diabetic Rats. *Diabetes* **2012**, *61* (1), 197−207.
(176) Leclair, E.; Liggins, R. T.; Peckett, A. J.; Teich, T.; Coy, D. H.; Vranic, M.; Riddell, M. C. Glucagon responses to exercise-induced hypoglycaemia are improved by somatostatin receptor type 2 antagonism in a rat model of diabetes. *Diabetologia* **2016**, *59* (8), 1724−1731.
(177) GhavamiNejad, A.; Lu, B.; Samarikhalaj, M.; Liu, J. F.; Mirzaie, S.; Pereira, S.; Zhou, L.; Giacca, A.; Wu, X. Y. Transdermal delivery of a somatostatin receptor type 2 antagonist using microneedle patch technology for hypoglycemia prevention. *Drug delivery and translational research* **2022**, *12* (4), 792−804.
(178) Zhang, K.; Wu, X. Y. Modulated insulin permeation across a glucose-sensitive polymeric composite membrane. *J. Controlled Release* **2002**, *80* (1−3), 169−78.
(179) Zhang, K.; Quan, C.; Huang, H.; Taulier, N.; Wu, X. Y. On the stability of insulin delivered through a new glucose-responsive polymeric composite membrane. *J. Pharm. Pharmacol* **2010**, *56* (5), 611−20.
(180) Huang, H. Y.; Shaw, J.; Yip, C.; Wu, X. Y. Microdomain pH gradient and kinetics inside composite polymeric membranes of pH and glucose sensitivity. *Pharm. Res-Dordr* **2008**, *25* (5), 1150−1157.
(181) Gordijo, C. R.; Koulajian, K.; Shuhendler, A. J.; Bonifacio, L. D.; Huang, H. Y.; Chiang, S.; Ozin, G. A.; Giacca, A.; Wu, X. Y. Nanotechnology-Enabled Closed Loop Insulin Delivery Device: In Vitro and In Vivo Evaluation of Glucose-Regulated Insulin Release for Diabetes Control. *Adv. Funct. Mater.* **2011**, *21* (1), 73−82.
(182) Chu, M. K. L.; Chen, J.; Gordijo, C. R.; Chiang, S.; Ivovic, A.; Koulajian, K.; Giacca, A.; Wu, X. Y.; Sun, Y. In vitro and in vivo testing of glucose-responsive insulin-delivery microdevices in diabetic rats. *Lab Chip* **2012**, *12* (14), 2533−2539.
(183) Li, J.; Chu, M. K.; Lu, B.; Mirzaie, S.; Chen, K.; Gordijo, C. R.; Plettenburg, O.; Giacca, A.; Wu, X. Y. Enhancing thermal stability of a highly concentrated insulin formulation with Pluronic F-127 for long-term use in microfabricated implantable devices. *Drug delivery and translational research* **2017**, *7* (4), 529−543.
(184) GhavamiNejad, A.; Lu, B.; Giacca, A.; Wu, X. Y. Glucose regulation by modified boronic acid-sulfobetaine zwitterionic nano-gels - a non-hormonal strategy for the potential treatment of hyperglycemia. *Nanoscale* **2019**, *11* (21), 10167−10171.
(185) Wu, X. Y.; Lee, P. I. Preparation and characterization of thermal- and pH-sensitive nanospheres. *Pharm. Res.* **1993**, *10* (10), 1544−7.
(186) Zhang, K.; Huang, H.; Yang, G.; Shaw, J.; Yip, C.; Wu, X. Y. Characterization of Nanostructure of Stimuli-Responsive Polymeric Composite Membranes. *Biomacromolecules* **2004**, *5* (4), 1248−1255.
(187) Zhang, K.; Quan, C.; Huang, H.; Taulier, N.; Wu, X. Y. On the stability of Insulin delivered through a new glucose-responsive polymeric composite membrane. *J. Pharm. Pharmacol.* **2010**, *56* (5), 611−620.
(188) Yam, F.; Wu, X. Y.; Zhang, Q. A Novel Composite Membrane for Temperature- and pH-Responsive Permeation. *ACS Symp. Ser.* **2000**, *752*, 263−272.
(189) Zhang, K.; Wu, X. Y. Temperature and pH-responsive polymeric composite membranes for controlled delivery of proteins and peptides. *Biomaterials* **2004**, *25*, 5281−5291.
(190) Swinnen, S. G.; Hoekstra, J. B.; DeVries, J. H. Insulin Therapy for Type 2 Diabetes. *Diabetes Care* **2009**, *32*, S253−S259.
(191) Wang, M. Q.; Wang, Q.; Whim, M. D. Fasting induces a form of autonomic synaptic plasticity that prevents hypoglycemia. *Proc. Natl. Acad. Sci. U. S. A.* **2016**, *113* (21), E3029−E3038.
(192) Jackson, M. A.; Caputo, N.; Castle, J. R.; David, L. L.; Roberts, C. T.; Ward, W. K. Stable Liquid Glucagon Formulations for Rescue Treatment and Bi-Hormonal Closed-Loop Pancreas. *Curr. Diab. Rep.* **2012**, *12* (6), 705−710.
(193) Day, J. W.; Ottaway, N.; Patterson, J. T.; Gelfanov, V.; Smiley, D.; Gidda, J.; Findeisen, H.; Bruemmer, D.; Drucker, D. J.; Chaudhary, N.; Holland, J.; Hembree, J.; Abplanalp, W.; Grant, E.; Ruehl, J.; Wilson, H.; Kirchner, H.; Lockie, S. H.; Hofmann, S.; Woods, S. C.; Nogueiras, R.; Pfluger, P. T.; Perez-Tilve, D.; DiMarchi, R.; Tschop, M. H. A new glucagon and GLP-1 co-agonist eliminates obesity in rodents. *Nat. Chem. Biol.* **2009**, *5* (10), 749−757.
(194) Abitbol, A.; Rabasa-Lhoret, R.; Messier, V.; Legault, L.; Smaoui, M.; Cohen, N.; Haidar, A. Overnight Glucose Control with Dual- and Single-Hormone Artificial Pancreas in Type 1 Diabetes with Hypoglycemia Unawareness: A Randomized Controlled Trial. *Diabetes Technol. Ther.* **2018**, *20*, 189−196.
(195) Tuan-Mahmood, T. M.; McCrudden, M. T. C.; Torrisi, B. M.; McAlister, E.; Garland, M. J.; Singh, T. R. R.; Donnelly, R. F. Microneedles for intradermal and transdermal drug delivery. *Eur. J. Pharm. Sci.* **2013**, *50* (5), 623−637.
(196) Morteza Amjadi, S. S.; Bradley, J.; Nelson, B. J.; Sitti, M. Recent Advances in Wearable Transdermal Delivery Systems. *Adv. Mater.* **2018**, *30*, 201704530.
(197) Kim, Y. C.; Park, J. H.; Prausnitz, M. R. Microneedles for drug and vaccine delivery. *Adv. Drug Delivery Rev.* **2012**, *64* (14), 1547−1568.
(198) Veiseh, O.; Langer, R. DIABETES A smart insulin patch. *Nature* **2015**, *524* (7563), 39−40.
(199) Gupta, J.; Felner, E. I.; Prausnitz, M. R. Minimally Invasive Insulin Delivery in Subjects with Type 1 Diabetes Using Hollow Microneedles (vol 11, pg 329, 2009). *Diabetes Technol. Ther.* **2009**, *11* (7), 471.
(200) Mura, S.; Nicolas, J.; Couvreur, P. Stimuli-responsive nanocarriers for drug delivery. *Nat. Mater.* **2013**, *12* (11), 991−1003.
(201) Chen, K.; Chang, H. H. R.; Shalviri, A.; Li, J.; Lugtu-Pe, J. A.; Kane, A.; Wu, X. Y. Investigation of a new pH-responsive nanoparticulate pore former for controlled release enteric coating with improved processability and stability. *Eur. J. Pharm. Biopharm.* **2017**, *120*, 116−125.
(202) Fan, H. Y.; Raval, G.; Shalviri, A.; May, S.; Wu, X. Y.; Heerklotz, H. Coupled equilibria of a self-associating drug loaded into polymeric nanoparticles. *Methods* **2015**, *76*, 162−170.
(203) Li, Y.; Abbaspour, M. R.; Grootendorst, P. V.; Rauth, A. M.; Wu, X. Y. Optimization of controlled release nanoparticle formulation of verapamil hydrochloride using artificial neural networks with genetic algorithm and response surface methodology. *Eur. J. Pharm. Biopharm.* **2015**, *94*, 170−9.

https://doi.org/10.1021/acs.molpharmaceut.2c00038
Mol. Pharmaceutics XXXX, XXX, XXX−XXX

(204) Li, Y.; Rauth, A. M.; Wu, X. Y. Prediction of kinetics of doxorubicin release from sulfopropyl dextran ion-exchange microspheres using artificial neural networks. *Eur. J. Pharm. Sci.* **2005**, *24* (5), 401−10.
(205) Wu, X. Y.; Zhou, Y. Mechanistic modeling and computer software for quality by design in formulation of modified release dosage forms. *AIChE Annu. Meet., Conf. Proc.*, **2012**, 89−96.
(206) Thombre, A. G.; Wu, X. Y.; am Ende, M. T. Controlled release technology and design of oral controlled release dosage forms. In *Chemical Engineering in the Pharmaceutical Industry: Drug Product Design, Development, and Modeling*, 2nd ed.; am Ende, M. T., am Ende, D. J., Eds.; Wiley/AIChe: Hoboken, NJ, 2019; pp 381−407.
(207) Abdekhodaie, M.; Wu, X. Y. Drug release from ion-exchange microspheres: mathematical modeling and experimental verification. *Biomaterials* **2008**, *29* (11), 1654−63.
(208) Chen, K.; Li, L. Y.; Li, J.; Zhou, Y.; Kane, A.; Wu, X. Y. Modeling, numerical simulation, and experimental investigation of ion-exchange-diffusion coupled drug transport in controlled release dosage forms. I. Pharmaceutical membranes of cationic polyacrylates. **2020**.
(209) Zhou, Y.; Wu, X. Y. Finite element analysis of diffusional drug release from complex matrix systems. I.: Complex geometries and composite structures1Presented in part at the Conference on Advances in Controlled Delivery, Controlled Release Society, Inc. Proceedings, p. 169−170 (August, 1996, Baltimore, USA), and at the Annual Meeting of the American Association of Pharmaceutical Scientists (October, 1996, Seattle, USA).1. *J. Controlled Release* **1997**, *49* (2), 277−288.
(210) Wu, X. Y.; Zhou, Y. Studies of diffusional release of a dispersed solute from polymeric matrixes by finite element method. *J. Pharm. Sci.* **1999**, *88* (10), 1050−7.
(211) Zhou, Y.; Chu, J. S.; Zhou, T.; Wu, X. Y. Modeling of dispersed-drug release from two-dimensional matrix tablets. *Biomaterials* **2005**, *26* (8), 945−52.
(212) Zhou, Y.; Chu, J. S.; Wu, X. Y. Theoretical analysis of drug release into a finite medium from sphere ensembles with various size and concentration distributions. *Eur. J. Pharm. Sci.* **2004**, *22* (4), 251−9.
(213) Wu, X. Y.; Zhou, Y. Kinetics of drug release from solid dosage forms with drug loading higher than the solubility. *AAPS Annual Meeting, Pharm. Sci.* **1998**, *1*, S420.
(214) Balaji, V. K. Mechanism of Drug Release from Matrix Tablets Involving Moving Boundaries. M.S. Thesis, University of Toronto, Toronto, Ontario, Canada, 2001.
(215) Wu, X. Y.; Zhou, Y. Numerical simulation of controlled drug release from matrix tablets involving swelling, erosion and diffusion. *Pharm. Res.* **1997**, *14*, S716.
(216) Wu, X. Y.; Zhou, Y. Computational analysis and design of matrix systems involving moving boundaries. *Proc. Int. Symp. Control. Rel. Bioact. Mater.* **2001**, *28*, 828−829.
(217) Huang, J.; Kao, H.; Wu, X. Y. The pH-dependent biphasic release of azidothymidine from a layered composite of PVA disks and P(MMA/MAA) spheres. *J. Controlled Release* **2000**, *67* (1), 45−54.
(218) Wu, X. Y.; Ly, J.; Zhou, Y. Modeling of bimodal release from composite polymeric beads. *Proc. Int. Symp. Control. Release Bioact. Mater.* **1998**, *25*, 447−448.
(219) Zhou, Y.; He, C.; Chen, K.; Ni, J.; Cai, Y.; Guo, X.; Wu, X. Y. A New Method for Evaluating Actual Drug Release Kinetics of Nanoparticles inside Dialysis Devices via Numerical Deconvolution. *J. Controlled Release* **2016**, *243*, 11−20.
(220) Box, G. E. P.; Hunter, J. S.; Hunter, W. G. *Statistics for Experimenters: Design, Innovation and Discovery*, 2nd ed.; Wiley-Interscience: Hoboken, NJ, 2005.
(221) Zhang, R. X.; Liu, F. F.-C.; Lip, H.; Liu, J.; Zhang, Q.; Wu, X. Y. Pharmaceutical Nanoformulation Strategies to Spatiotemporally Manipulate Oxidative Stress for Improving Cancer Therapy - Exemplified by Polyunsaturated Fatty Acids and Other ROS-Modulating Agents. *Drug Delivery Transl. Res.* **2022** DOI: 10.1007/s13346-021-01104-3
(222) Anselmo, A. C.; Mitragotri, S. Nanoparticles in the clinic. *Bioengineering & translational medicine* **2016**, *1* (1), 10−29.
(223) Anselmo, A. C.; Mitragotri, S. Nanoparticles in the clinic: An update. *Bioeng. Transl. Med.* **2019**, *4* (3), No. e10143.
(224) Farjadian, F.; Ghasemi, A.; Gohari, O.; Roointan, A.; Karimi, M.; Hamblin, M. R. Nanopharmaceuticals and nanomedicines currently on the market: challenges and opportunities. *Nanomedicine (London)* **2019**, *14* (1), 93−126.
(225) Van Norman, G. A. Drugs, Devices, and the FDA: Part 1: An Overview of Approval Processes for Drugs. *JACC Bas. Transl. Sci.* **2016**, *1* (3), 170−179.
(226) Nanomedicine Market Size, 2021. https://www.grandviewresearch.com/press-release/global-nanomedicine-market (accessed Nov 21, 2021).
(227) Farjadian, F.; Ghasemi, A.; Gohari, O.; Roointan, A.; Karimi, M.; Hamblin, M. R. Nanopharmaceuticals and nanomedicines currently on the market: challenges and opportunities. *Nanomedicine (Lond)* **2019**, *14* (1), 93−126.
(228) Park, K. The beginning of the end of the nanomedicine hype. *J. Controlled Release* **2019**, *305*, 221−222.
(229) Hua, S.; de Matos, M. B. C.; Metselaar, J. M.; Storm, G. Current Trends and Challenges in the Clinical Translation of Nanoparticulate Nanomedicines: Pathways for Translational Development and Commercialization. *Front. Pharmacol.* **2018**, *9*, 790.
(230) Salvioni, L.; Rizzuto, M. A.; Bertolini, J. A.; Pandolfi, L.; Colombo, M.; Prosperi, D. Thirty Years of Cancer Nanomedicine: Success, Frustration, and Hope. *Cancers (Basel)* **2019**, *11* (12), 1855.
(231) Xu, X.; Liu, C.; Wang, Y.; Koivisto, O.; Zhou, J.; Shu, Y.; Zhang, H. Nanotechnology-based delivery of CRISPR/Cas9 for cancer treatment. *Adv. Drug Delivery Rev.* **2021**, *176*, 113891.
(232) Cheung, R.; Ying, Y.; Wu, X. Y.; Rauth, A.; Marcon, N. Microsphere-delivered mitomycin C (MMC) and the effects on cancer cells of combining mitomycin C and doxorubicin. *J. Controlled Release* **2003**, *91* (1−2), 233−266.
(233) Wang, Z.; Zhang, R. X.; Zhang, T.; He, C.; He, R.; Ju, X.; Wu, X. Y. In Situ Proapoptotic Peptide-Generating Rapeseed Protein-Based Nanocomplexes Synergize Chemotherapy for Cathepsin-B Overexpressing Breast Cancer. *ACS Appl. Mater. Interfaces* **2018**, *10* (48), 41056−41069.
(234) Alves Rico, S. R.; Abbasi, A. Z.; Ribeiro, G.; Ahmed, T.; Wu, X. Y.; de Oliveira Silva, D. Diruthenium(ii,iii) metallodrugs of ibuprofen and naproxen encapsulated in intravenously injectable polymer-lipid nanoparticles exhibit enhanced activity against breast and prostate cancer cells. *Nanoscale* **2017**, *9* (30), 10701−10714.
(235) Shuhendler, A. J.; Staruch, R.; Oakden, W.; Gordijo, C. R.; Rauth, A. M.; Stanisz, G. J.; Chopra, R.; Wu, X. Y. Thermally-triggered 'off-on-off' response of gadolinium-hydrogel-lipid hybrid nanoparticles defines a customizable temperature window for non-invasive magnetic resonance imaging thermometry. *J. Controlled Release* **2012**, *157* (3), 478−84.
(236) Shan, D.; Cai, P.; Prasad, P.; Rauth, A. M.; Wu, X. Y. Abstract 4339: RGD-conjugated nanoparticles for targeted inhibition of adhesion and migration of integrin $\alpha v\beta 3$-overexpressing breast cancer cells. *Cancer Res.* **2013**, *73*, 4339.
(237) Shan, D.; Li, J.; Cai, P.; Prasad, P.; Liu, F.; Rauth, A. M.; Wu, X. Y. RGD-conjugated solid lipid nanoparticles inhibit adhesion and invasion of $\alpha v\beta 3$ integrin-overexpressing breast cancer cells. *Drug delivery and translational research* **2015**, *5* (1), 15−26.
(238) Gordijo, C. R.; Abbasi, A. Z.; Amini, M. A.; Lip, H. Y.; Maeda, A.; Cai, P.; O'Brien, P. J.; DaCosta, R. S.; Rauth, A. M.; Wu, X. Y. Hybrid Nanoparticles: Design of Hybrid MnO2-Polymer-Lipid Nanoparticles with Tunable Oxygen Generation Rates and Tumor Accumulation for Cancer Treatment. *Adv. Funct. Mater.* **2015**, *25* (12), 1857−1587.
(239) Abbasi, A. Z.; Prasad, P.; Cai, P.; He, C.; Foltz, W. D.; Amini, M. A.; Gordijo, C. R.; Rauth, A. M.; Wu, X. Y. Manganese oxide and docetaxel co-loaded fluorescent polymer nanoparticles for dual modal imaging and chemotherapy of breast cancer. *J. Controlled Release* **2015**, *209*, 186−96.

https://doi.org/10.1021/acs.molpharmaceut.2c00038
Mol. Pharmaceutics XXXX, XXX, XXX−XXX

(240) Amini, M. A.; Abbasi, A.; Cai, P.; Lip, H.; Li, J.; Gordijo, C.; Zhang, L.; Rauth, M.; Wu, X. Y. Abstract 5218: Boosting doxorubicin-induced immunogenic cell death by using tumor microenvironment modulating nanoparticles. *Cancer Res.* **2018**, *78*, 5218.
(241) Michaelis, K.; Hoffmann, M. M.; Dreis, S.; Herbert, E.; Alyautdin, R. N.; Michaelis, M.; Kreuter, J.; Langer, K. Covalent linkage of apolipoprotein e to albumin nanoparticles strongly enhances drug transport into the brain. *J. Pharmacol. Exp. Ther.* **2006**, *317* (3), 1246−53.
(242) Panova, I. G.; Spiridonov, V. V.; Kaplan, I. B.; Trubinov, S. S.; Elizova, N. V.; Melnichenko, A. A.; Orekhov, A. N.; Yaroslavov, A. A. Inhibitory effect of polyethylene oxide and polypropylene oxide triblock copolymers on aggregation and fusion of atherogenic low density lipoproteins. *Biochemistry (Moscow)* **2015**, *80* (8), 1057−1064.
(243) Soni, S.; Babbar, A. K.; Sharma, R. K.; Maitra, A. Delivery of hydrophobised 5-fluorouracil derivative to brain tissue through intravenous route using surface modified nanogels. *J. Drug Target.* **2006**, *14* (2), 87−95.
(244) Shubar, H. M.; Dunay, I. R.; Lachenmaier, S.; Dathe, M.; Bushrab, F. N.; Mauludin, R.; Müller, R. H.; Fitzner, R.; Borner, K.; Liesenfeld, O. The role of apolipoprotein E in uptake of atovaquone into the brain in murine acute and reactivated toxoplasmosis. *J. Drug Target.* **2009**, *17* (4), 257−267.
(245) Li, W.; Qiu, J.; Li, X. L.; Aday, S.; Zhang, J.; Conley, G.; Xu, J.; Joseph, J.; Lan, H.; Langer, R. BBB pathophysiology-independent delivery of siRNA in traumatic brain injury. *Sci. Adv.* **2021**, *7* (1), eabd6889.
(246) Gao, K.; Jiang, X. Influence of particle size on transport of methotrexate across blood brain barrier by polysorbate 80-coated polybutylcyanoacrylate nanoparticles. *Int. J. Pharm.* **2006**, *310* (1−2), 213−9.
(247) Kuo, Y. C.; Chen, H. H. Effect of nanoparticulate polybutylcyanoacrylate and methylmethacrylate-sulfopropylmethacrylate on the permeability of zidovudine and lamivudine across the in vitro blood-brain barrier. *Int. J. Pharm.* **2006**, *327* (1−2), 160−9.
(248) Wei, Y.; Sun, Y.; Wei, J.; Qiu, X.; Meng, F.; Storm, G.; Zhong, Z. Selective transferrin coating as a facile strategy to fabricate BBB-permeable and targeted vesicles for potent RNAi therapy of brain metastatic breast cancer in vivo. *J. Controlled Release* **2021**, *337*, 521−529.
(249) Liu, W.; Lin, Q.; Fu, Y.; Huang, S.; Guo, C.; Li, L.; Wang, L.; Zhang, Z.; Zhang, L. Target delivering paclitaxel by ferritin heavy chain nanocages for glioma treatment. *J. Controlled Release* **2020**, *323*, 191−202.
(250) Pang, Z.; Gao, H.; Yu, Y.; Guo, L.; Chen, J.; Pan, S.; Ren, J.; Wen, Z.; Jiang, X. Enhanced Intracellular Delivery and Chemotherapy for Glioma Rats by Transferrin-Conjugated Biodegradable Polymersomes Loaded with Doxorubicin. *Bioconjugate Chem.* **2011**, *22* (6), 1171−1180.
(251) He, H.; Li, Y.; Jia, X. R.; Du, J.; Ying, X.; Lu, W. L.; Lou, J. N.; Wei, Y. PEGylated Poly(amidoamine) dendrimer-based dual-targeting carrier for treating brain tumors. *Biomaterials* **2011**, *32* (2), 478−87.
(252) Laine, A.-L.; Huynh, N. T.; Clavreul, A.; Balzeau, J.; Béjaud, J.; Vessieres, A.; Benoit, J.-P.; Eyer, J.; Passirani, C. Brain tumour targeting strategies via coated ferrociphenol lipid nanocapsules. *European journal of pharmaceutics and biopharmaceutics: official journal of Arbeitsgemeinschaft fur Pharmazeutische Verfahrenstechnik e.V* **2012**, *81* (3), 690−693.
(253) Zhang, Y.; Pardridge, W. M. Near complete rescue of experimental Parkinson's disease with intravenous, non-viral GDNF gene therapy. *Pharm. Res.* **2009**, *26* (5), 1059−63.
(254) Wu, D.; Qin, M.; Xu, D.; Wang, L.; Liu, C.; Ren, J.; Zhou, G.; Chen, C.; Yang, F.; Li, Y.; Zhao, Y.; Huang, R.; Pourtaheri, S.; Kang, C.; Kamata, M.; Chen, I. S. Y.; He, Z.; Wen, J.; Chen, W.; Lu, Y. A Bioinspired Platform for Effective Delivery of Protein Therapeutics to the Central Nervous System. *Adv. Mater.* **2019**, *31* (18), 1807557.
(255) Wu, H.; Lu, H.; Xiao, W.; Yang, J.; Du, H.; Shen, Y.; Qu, H.; Jia, B.; Manna, S. K.; Ramachandran, M.; Xue, X.; Ma, Z.; Xu, X.; Wang, Z.; He, Y.; Lam, K. S.; Zawadzki, R. J.; Li, Y.; Lin, T.-Y. Sequential Targeting in Crosslinking Nanotheranostics for Tackling the Multibarriers of Brain Tumors. *Adv. Mater.* **2020**, *32* (14), 1903759.
(256) Dhanikula, R. S.; Argaw, A.; Bouchard, J. F.; Hildgen, P. Methotrexate loaded polyether-copolyester dendrimers for the treatment of gliomas: enhanced efficacy and intratumoral transport capability. *Mol. Pharmaceutics* **2008**, *5* (1), 105−16.
(257) Vinogradov, S. V.; Batrakova, E. V.; Kabanov, A. V. Nanogels for oligonucleotide delivery to the brain. *Bioconjugate Chem.* **2004**, *15* (1), 50−60.
(258) Dou, H.; Grotepas, C. B.; McMillan, J. M.; Destache, C. J.; Chaubal, M.; Werling, J.; Kipp, J.; Rabinow, B.; Gendelman, H. E. Macrophage delivery of nanoformulated antiretroviral drug to the brain in a murine model of neuroAIDS. *J. Immunol.* **2009**, *183* (1), 661−9.
(259) Cheng, Y.; Dai, Q.; Morshed, R. A.; Fan, X.; Wegscheid, M. L.; Wainwright, D. A.; Han, Y.; Zhang, L.; Auffinger, B.; Tobias, A. L.; et al. Blood-brain barrier permeable gold nanoparticles: an efficient delivery platform for enhanced malignant glioma therapy and imaging. *Small* **2014**, *10* (24), 5137−5150.
(260) Lee, C.; Hwang, H. S.; Lee, S.; Kim, B.; Kim, J. O.; Oh, K. T.; Lee, E. S.; Choi, H. G.; Youn, Y. S. Rabies Virus-Inspired Silica-Coated Gold Nanorods as a Photothermal Therapeutic Platform for Treating Brain Tumors. *Adv. Mater.* **2017**, *29* (13), 201605563.
(261) Gao, H.; Zhang, S.; Yang, Z.; Cao, S.; Jiang, X.; Pang, Z. In vitro and in vivo intracellular distribution and anti-glioblastoma effects of docetaxel-loaded nanoparticles functioned with IL-13 peptide. *Int. J. Pharm.* **2014**, *466* (1), 8−17.
(262) Babu, A.; Amreddy, N.; Muralidharan, R.; Pathuri, G.; Gali, H.; Chen, A.; Zhao, Y. D.; Munshi, A.; Ramesh, R. Chemodrug delivery using integrin-targeted PLGA-Chitosan nanoparticle for lung cancer therapy. *Sci. Rep.* **2017**, *7* (1), 14674.
(263) Goren, D.; Horowitz, A. T.; Tzemach, D.; Tarshish, M.; Zalipsky, S.; Gabizon, A. Nuclear Delivery of Doxorubicin via Folate-targeted Liposomes with Bypass of Multidrug-resistance Efflux Pump. *Clin. Cancer Res.* **2000**, *6* (5), 1949−1957.
(264) Namgung, R.; Mi Lee, Y.; Kim, J.; Jang, Y.; Lee, B.-H.; Kim, I.-S.; Sokkar, P.; Rhee, Y. M.; Hoffman, A. S.; Kim, W. J. Poly-cyclodextrin and poly-paclitaxel nano-assembly for anticancer therapy. *Nat. Commun.* **2014**, *5* (1), 3702.
(265) Hu, G.; Chun, X.; Wang, Y.; He, Q.; Gao, H. Peptide mediated active targeting and intelligent particle size reduction-mediated enhanced penetrating of fabricated nanoparticles for triple-negative breast cancer treatment. *Oncotarget* **2015**, *6* (38), 41258−74.
(266) Zhong, Y.; Zhang, J.; Cheng, R.; Deng, C.; Meng, F.; Xie, F.; Zhong, Z. Reversibly crosslinked hyaluronic acid nanoparticles for active targeting and intelligent delivery of doxorubicin to drug resistant CD44+ human breast tumor xenografts. *J. Controlled Release* **2015**, *205*, 144−54.
(267) Zhang, C.; Wang, W.; Liu, T.; Wu, Y.; Guo, H.; Wang, P.; Tian, Q.; Wang, Y.; Yuan, Z. Doxorubicin-loaded glycyrrhetinic acid-modified alginate nanoparticles for liver tumor chemotherapy. *Biomaterials* **2012**, *33* (7), 2187−2196.
(268) Singh, B.; Jang, Y.; Maharjan, S.; Kim, H.-J.; Lee, A. Y.; Kim, S.; Gankhuyag, N.; Yang, M.-S.; Choi, Y.-J.; Cho, M.-H.; Cho, C.-S. Combination therapy with doxorubicin-loaded galactosylated poly-(ethyleneglycol)-lithocholic acid to suppress the tumor growth in an orthotopic mouse model of liver cancer. *Biomaterials* **2017**, *116*, 130−144.
(269) Patra, C. R.; Bhattacharya, R.; Wang, E.; Katarya, A.; Lau, J. S.; Dutta, S.; Muders, M.; Wang, S.; Buhrow, S. A.; Safgren, S. L.; Yaszemski, M. J.; Reid, J. M.; Ames, M. M.; Mukherjee, P.; Mukhopadhyay, D. Targeted Delivery of Gemcitabine to Pancreatic Adenocarcinoma Using Cetuximab as a Targeting Agent. *Cancer Res.* **2008**, *68* (6), 1970−1978.
(270) Mishra, P. K.; Gulbake, A.; Jain, A.; Vyas, S. P.; Jain, S. K. Targeted delivery of an anti-cancer agent via steroid coupled liposomes. *Drug Delivery* **2009**, *16* (8), 437−447.

AQ

(271) Dhar, S.; Gu, F. X.; Langer, R.; Farokhzad, O. C.; Lippard, S. J. Targeted delivery of cisplatin to prostate cancer cells by aptamer functionalized Pt(IV) prodrug-PLGA-PEG nanoparticles. *Proc. Natl. Acad. Sci. U. S. A.* **2008**, *105* (45), 17356−17361.
(272) Liu, C. W.; Lin, W. J. Polymeric nanoparticles conjugate a novel heptapeptide as an epidermal growth factor receptor-active targeting ligand for doxorubicin. *Int. J. Nanomedicine* **2012**, *7*, 4749−4767.
(273) Dubey, R. D.; Alam, N.; Saneja, A.; Khare, V.; Kumar, A.; Vaidh, S.; Mahajan, G.; Sharma, P. R.; Singh, S. K.; Mondhe, D. M.; Gupta, P. N. Development and evaluation of folate functionalized albumin nanoparticles for targeted delivery of gemcitabine. *Int. J. Pharm.* **2015**, *492* (1), 80−91.

https://doi.org/10.1021/acs.molpharmaceut.2c00038
Mol. Pharmaceutics XXXX, XXX, XXX−XXX